Charles University in Prague

1ˢᵗ Faculty of Medicine

Program: Parasitology

Mgr. Klára Jiráková

Cell cycle and differentiation

in

Giardia intestinalis

Ph.D. Thesis

Supervisor: RNDr. Eva Nohýnková, Ph.D.

Prague, 2012

Prohlášení:

Prohlašuji, že jsem závěrečnou práci zpracovala samostatně a že jsem řádně uvedla a citovala všechny použité prameny a literaturu. Současně prohlašuji, že práce nebyla využita k získání jiného nebo stejného titulu.

Souhlasím s trvalým uložením elektronické verze mé práce v databázi systému meziuniverzitního projektu Theses.cz za účelem soustavné kontroly podobnosti kvalifikačních prací.

V Praze, 25.3.2012

Klára Jiráková

Podpis:

Identifikační záznam:

JIRÁKOVÁ, Klára, Mgr. *Buněčný cyklus a diferenciace Giardia intestinalis. [Cell cycle and differentiation in Giardia intestinalis]*. Praha, 2012. 58 s., 4 příl. Dizertační práce. Univerzita Karlova v Praze, 1. lékařská fakulta, Oddělení Tropické Medicíny. Vedoucí práce, RNDr. Eva Nohýnková, PhD.

ABSTRACT

Giardia is a unicellular parasitic organism; it is a worldwide cause of human diarrhea. It has minimalistic genome equipment and simplified molecular and metabolic pathways. In this respect, it is a suitable model organism for studying cell cycle regulation and to define the minimal genetic and protein equipment required for the functional reproduction of the eukaryotic cell. Its life cycle comprises of two stages; a pathogenic trophozoite and an infective cyst, which can survive in outer environment. New knowledge about encystation can be therapeutically important because this process is a target for vaccine and drug development. Since cell cycle analysis requires a synchronized population, we studied the effect of the synchronization drug aphidicolin on individual cell characteristics during the cell cycle of *Giardia* trophozoites. Our results showed that aphidicolin caused inhibition of DNA synthesis and trophozoites were aligned according to their DNA content in G1/S border. Subsequent inhibition of entry into mitosis and cytokinesis indicates, that *Giardia* has functioning DNA damage checkpoint. Extensive treatment with aphidicolin causes side effects. We detected positive signals for phosphorylated histone H2A which, in mammalian cells, is involved in a signaling pathway triggered as a reaction to double stranded DNA breaks. Reversibility of this posttranslational modification after inhibitor removal indicates that *Giardia* possesses DNA damage reparatory mechanisms. Aphidicolin treatment causes dissociation of the nuclear and cytoplasmic cycles. While DNA synthesis and entry to mitosis are stopped, the cytoplasmic cycle and its processes continue. We also focused on characterization of nuclear division during *Giardia* encystation with respect to cyst wall formation and flagellar apparatus arrangement. Nuclei are divided by semi-open mitosis in early phase of encystation in a precyst before cyst wall formation. After the karyokinesis, nuclei stayed in pairs and were interconnected with several inter-nuclear bridges formed by fusion of nuclear envelopes. Each interconnected nuclear pair is associated with one basal body tetrad of the undivided diplomonad mastigont.

Keywords: *Giardia intestinalis*, cell cycle, encystation, flow cytometry, mitosis

ABSTRAKT

Giardia je jednobuněčný parazitický organismus, který je zdrojem průjmových onemocnění po celém světě. Má minimální genomovou výbavu a zjednodušené molekulární a metabolické dráhy. V tomto ohledu je to vhodný modelový organismus pro studium regulace buněčného cyklu a pro definici minimální genetické a proteinové výbavy nutné pro reprodukci eukaryotické buňky. V životním cyklu giardie se vyskytují dvě stádia: patogenní trofozoit a infekční cysta, která dokáže přežít ve vnějších podmínkách. Nové znalosti o encystaci mohou být významné z terapeutického hlediska, protože na tento proces je zacílen vývoj vakcíny a léků. Protože studium buněčného cyklu vyžaduje synchronizovanou populaci, studovali jsme vliv synchronizační látky aphidicolinu na jednotlivé buněčné děje během buněčného cyklu trofozoitů giardie. Naše výsledky ukázaly, že aphidicolin zastavil syntézu DNA a trofozoiti byli zablokováni podle obsahu DNA na hranici G1/S fáze. Následná inhibice vstupu do mitózy a cytokineze naznačuje, že *Giardia* má funkční kontrolní bod při poškozené DNA. Aphidicolin působí při dlouhodobé inkubaci a vyšších koncentracích vedlejší efekty; detekovali jsme pozitivní signál pro fosforylovaný histon H2A, který je u savčích buněk součástí signalizační dráhy spuštěné jako reakce na dvouřetězcové zlomy v DNA. Reverzibilita této posttranslační modifikace po odstranění inhibitoru ukazuje, že *Giardia* má reparační mechanismy poškození DNA. Inkubace s aphidicolinem působí disociaci jaderného a cytoplazmatického cyklu. Zatímco syntéza DNA a vstup do mitózy jsou zastaveny, cytoplazmatický cyklus pokračuje. Zaměřili jsme se také na popis jaderného dělení během encystace ve vztahu k tvorbě cystové stěny a přestavbě bičíkového aparátu. Jaderné dělení proběhlo semi-open mitózou za účasti dvou mitotických vřetének v rané fázi encystace před vznikem cystové stěny. Jádra zůstala po rozdělení v párech a byla propojená několika můstky, které vznikly fúzí jaderných membrán. Každý propojený pár jader je spojený s jednou tetrádou bazálních tělísek nerozděleného mastigontu diplomonády.

Klíčová slova: *Giardia intestinalis*, buněčný cyklus, encystace, průtoková cytometrie, mitóza

ACKNOWLEDGEMENT

CONTENT:

1. AIMS OF THE THESIS

Giardia intestinalis was considered one of the earliest branching eukaryotic organisms. Though the discovery of mitochondrial genes in its genome and description of mitosomes showed it is not as primitive as originally believed, it still possesses some primitive characteristics. It has an unusual cell structure with two nearly identical nuclei and complex cytoskeleton, a small genome and minimalistic genome equipment, and simplified molecular and metabolic pathways. In this respect, it is a promising model organism for studying cell cycle regulation and to define the minimal genetic and protein equipment required for the functional reproduction of the eukaryotic cell. Studying cell cycle regulatory molecules requires a synchronized population, which was not available in *Giardia*. We studied more thoroughly the influence of one DNA replication inhibitor, mycotoxin aphidicolin, recently used as a tool for *Giardia* synchronization. *Giardia* also represents a health risk, being a worldwide cause of diarrhea in humans, and it is important to understand the mechanisms of encystation as the prerequisite for transition into a new host. Despite of great expansion in biochemical and molecular methods, which enabled the characterization of single molecules during differentiation and has provided great insight about cyst wall formation, the basic description of nuclei behavior and the flagellar apparatus reorganization during encystation and excystation is still unknown. Possible exchange of genetic material in cyst and the presence of meiotic genes in *Giardia* genome along with prediction of sexual process in *Giardia* focus even more the attention on the enigmatic nuclei division during encystation.

OBJECTIVES:

- To study the effect and reversibility of the synchronization drug aphidicolin on individual cell characteristics during the cell cycle of trophozoites. The purpose of this study was to determine the extent and for which parameters the population can be regarded as synchronized.

- To characterize individual phases of encystation in respect to cyst wall formation in *Giardia*, to identify the stage of encystation when the nuclei divides and determine how these two processes are interconnected.

- To find out which type of mitosis occurs in encystation, how the mitotic spindle is nucleated. And to further follow the behavior of flagellar apparatus, which is tightly coordinated with karyokinesis in *Giardia*.

2. INTRODUCTION

2.1. Introduction to *Giardia intestinalis*

Giardia intestinalis (Lambl, 1859) Alexeieff, 1914 (syn. *Giardia lamblia*, *Giardia duodenalis*) was first observed by van Leeuwenhoek in 1681. It was described in detail by Lambl in 1859, who placed it into the genus *Cercomonas* and named it *Cercomonas intestinalis*. In 1882, Künstler was the first to use the generic name *Giardia* for *Giardia agilis*, a species from tadpoles. Alexeieff (1914) then found that the human species is congeneric with that from amphibians (Kulda and Nohýnková 1995).

Further studies were possible thanks to the cultivation and completion of life cycle (encystation and excystation) *in vitro*. Karapetyan (1962) initiated cultivation *in vitro* of *Giardia* trophozoites in xenic cultures. Trophozoites, washed from duodenal content of infected people, were inoculated to complex medium together with *Candida guiliermondi* and chick fibroblasts (Karapetyan 1962). Meyer (1970) was the first to cultivate *G. intestinalis* axenically using yeast extract to substitute for living yeast (Clark and Diamond 2002). Bingham and Meyer (1979) introduced excystation *in vitro* using cysts purified from stool as a natural source of trophozoites for inoculum of axenic cultures. Excystation was induced by mimicking environmental conditions in the stomach and upper small intestine. This was achieved by exposing the cysts to acidic pH, followed by neutralization with bicarbonate, and then the cysts were transferred to growth medium with neutral pH (Bingham and Meyer 1979). Gillin et al. (1987, 1988) and Schupp et al. (1988) introduced differentiation of cultured trophozoites into cysts (encystation *in vitro*). The protocol mimics the conditions in lower jejunum and ileum, where encystation takes place as found using animal models. The encystation medium enriched in bile has slightly alkaline pH of 7.8. Studies of *Giardia* differentiation are important because of its significant impact on human health. *Giardia* is a widespread cause of diarrhea and it was included in the "Neglected Disease Initiative" of the WHO (Savioli et al. 2006).

In the last 20 years *Giardia* is also attractive from the evolutionary point of view, as it was considered to be among one of the earliest branching eukaryotes. Together with other Metamonada and putatively amitochondriate groups like Parabasala, Microsporidia and Archamoeba, it was placed to Archezoa (Cavalier-Smith 1989). Archezoa were believed to diverge from eukaryotes before mitochondria acquisition

and therefore they were considered ancient and primitive (Keeling 1998). However, due to the ongoing genome project, putative mitochondria proteins were found in the *Giardia* genome. The first evidence was the discovery of a gene for chaperonin cpn60. Chaperonin cpn60 is strongly similar to gene from α-proteobacteria, which is thought to be the closest living relative of the prokaryotes that gave rise to mitochondria (Roger et al. 1998). A few years later came the direct evidence that *Giardia* possess double membrane bound organelle without genome, which was named mitosome. Proteins related to those associated with mitochondria localize to mitosome. This was solid evidence that *Giardia* once had mitochondria (Tovar et al. 2003; Knight 2004). Nucleoli, which were previously thought to be missing, were discovered recently at the anterior part of each nucleus (Jiménez-García et al. 2008). *Giardia* however retains some primitive characteristics: absence of peroxisomes, typical Golgi apparatus and myosin, it encodes for the bacterial arginine pathway and contains only few introns in its compact genome (Morrison et al. 2007).

Organisms morphologically identical to human parasites affect many mammalian hosts, besides humans and other primates, they are found in carnivores, rodents, lagomorphs, ruminants, non-ruminants and edentates; they also infect reptiles (Kulda and Nohýnková 1995). Using allozyme electrophoresis, restriction fragment length polymorphism, molecular karyotyping and other DNA- based techniques; a high degree of genetic variation was found among isolates of *G. intestinalis* of human and animal origin (Bertram et al. 1983; Nash et al. 1985). It is now evident that the morphologically indistinguishable parasites belong to several *G. intestinalis* genotypes known as assemblages. Currently, eight assemblages have been determined. All human isolates belong to assemblages A or B; these are also the assemblages with the low degree of host specificity, infecting dogs, cats, livestock, rodents and some species of wild animals (Mayrhofer et al. 1995). Other assemblages (C-G) are more host specific in comparison with assemblages A and B. These infect dogs (assemblage C-D), hoofed livestock, particularly cattle (E), cats (F) and rats (G). Recently, assemblage H has been described in seal and gull, and dedicated to marine vertebrates (Lasek-Nesselquist et al 2010). It seems that genotypes can correlate with infectivity and clinical outcome of disease, and with rate of proliferation *in vitro*. Recent studies showed that assemblages represent distinct evolutionary lineages (Thompson 2004) and there is an ongoing debate

whether *G. intestinalis* assemblages should be reclassified to separate species (Caccio and Ryan 2008; Monis et al. 2009).

2.2. *Giardia* trophozoite

The trophozoite is a pear-shaped, octo-flagellated cell approximately 12-15 μm long and 5-9 μm wide. It is flattened ventrally and rounded dorsally. A major part of ventral surface is modified into an adhesive disc. The trophozoite possesses two morphologically indistinguishable nuclei situated with mirror symmetry along longitudinal axis in the anterior part of the cell. A rod-shaped median body is situated posterior to the nuclei and disc (Kulda and Nohýnková 1995).

2.2.1. Plasma membrane and endomembrane system

The plasma membrane of *Giardia* trophozoite is covered with a coat from variable surface proteins (VSP). The coat covers the whole surface of the cell and it is constantly changing so the trophozoite can avoid the host immune response (Nash 2002). There are around 235-275 genes encoding for VSP in *Giardia* genome, but only one VSP protein is found on the surface of the trophozoite at the time (Morrison et al. 2007). Antigenic variation is probably regulated at the posttranscriptional level by a mechanism similar to RNA interference (RNAi) (Prucca et al. 2008). Expression of the VSPs is downregulated during encystation, the coat is lost, and the proteins occur within peripheral vesicles that underlie plasma membrane of the trophozoite (McCaffery et al. 1994a). The major membrane associated proteins are cysteine-rich proteins ranging in size from 20 to 200 kDa with highly variable N-terminal domain and frequent CXXC motifs (C-cysteine, X-any amino acid). The C terminus is conserved; it contains hydrophobic membrane spanning region and cytoplasmic tail CRGKA, which is important for targeting protein into the plasma membrane (Marti et al. 2003a; Prucca and Luján 2009).

Giardia was thought to lack many components of the endomembrane system - apparent endoplasmic reticulum (ER), Golgi complex, mitochondria, peroxisomes or lysosomes. *Giardia* however has a type of distinct membranous organelles underlying the dorsal plasma membrane of the trophozoite, known as the peripheral vesicles (PV). They show characteristics of both endosomes and lysosomes: acidic environment and the presence of hydrolytic enzymes, acid phosphatases, proteinases

and RNases. These vesicles may be associated with ER (Lanfredi-Rangel et al. 1998). Endoplasmic reticulum is a membranous organelle continuous with nuclear membrane and its sacs extend throughout the cytosol. Its main role is protein and lipid biosynthesis, and storage for intracellular Ca^{2+} (Koch 1990). Tubulo-vesicular system corresponding to ER in *Giardia* has been detected by transmission electron microscopy (McCaffery et al. 1994a). A *Giardia* homolog of molecular chaperonin Bip was localized in immunoelectron microscopy using antibodies (Gupta et al. 1994) in membrane sacks on cryosections, thus the presence of ER in *Giardia* was confirmed (Soltys et al. 1996). Further genes coding for ER specific proteins, a protein disulfide isomerase (PDI-3), which is ER resident protein involved in disulphide bond formation in newly synthesized proteins, and an α subunit of the signal recognition particle (SRα), which targets signal peptide-containing proteins into ER have been identified in *Giardia* genome (Knodler et al. 1999; Svärd et al. 1999).

2.2.2. Cytoskeleton

The complex, mostly microtubular *Giardia* cytoskeleton plays important role in the cell attachment, motility, cell division and encystation/excystation processes (Elmendorf et al. 2003). The microfilamentous cytoskeleton of *Giardia* is poorly understood. Recently, it was shown that actin localizes to the cell cortex, the two nuclei and all flagellar axonemes and it was suggested that it could play a role in the cell shape, membrane trafficking and cytokinesis (Paredez et al. 2011).

Microtubular cytoskeleton in *Giarida* consists of four pairs of flagella, adhesive disc, median body and funis (Kulda and Nohýnková 1995). As in typical eukaryote, *Giardia* microtubules comprise of α; β tubulins. The *Giardia* genome possesses two copies of α tubulin and three copies of β tubulin (Morrison et al. 2007). Tubulins in eukaryotes are subjected to several posttranslational modifications, acetylation, and tyrosination/detyrosination, polyglycylation and polyglutamylation, which correlates to microtubule stability (MacRae 1997). Modifications are also present in *Giardia* tubulins. Acetylated α tubulin is present in all microtubular structures of interphase trophozoite (Soltys and Gupta 1994). Several putative tubulin tyrosine ligases found in the *Giardia* genome indicate the existence of the tyrosination/detyrosination cycle at C terminus of α tubulin (Elmendorf et al. 2003). High performance liquid chromatography (HPLC) and mass spectroscopy provided evidence for both

polyglycylation and polyglutamylation of *Giardia* tubulins (Weber et al. 1996). Immunofluorescence staining revealed polyglycylated tubulin in the flagellar axonemes, with lower levels in the median body and was found weakly on adhesive disc (Campanati et al. 1999). Polyglutamylation of tubulin was detected only on proximal halves of flagella (Boggild et al. 2002). *Giardia* possesses typical microtubule organizing center proteins: γ tubulin and centrin (Belhadri et al. 1995; Morrison et al. 2007). Gamma tubulin, which is essential for microtubule nucleation and formation of mitotic spindles in protist, fungi and animal cells, localizes in the basal body region in interphase and late mitotic *Giardia* cells (Nohýnková et al. 2000). Centrin, which is associated with basal bodies/centrioles and functions in the duplication and segregation of centrosomes (Salisbury 1995), was found in the basal bodies region throughout the whole *Giardia* cell cycle (Belhadri et al. 1995). *Giardia* single copy actin gene has a very low homology with actins from other species (58%). It lacks the core set of actin- binding proteins (ABPs), including ARP2/3 complex and formins, though it is able to form filaments *in vitro* (Drouin et al. 1995; Elmendorf et al. 2003; Paredez et al. 2011).

All eight flagella originate from basal bodies. Basal bodies are arranged in two groups (tetrads) and are positioned symmetrically close to each other in the midline between the nuclei. Basal bodies form pairs in each tetrad. Flagella with canonical eukaryotic microtubular structure 9+2 form bilaterally symmetrical pairs of four flagellar types: anteriolateral, posteriolateral, caudal and ventral. Pairs of flagella do not correspond to the basal body pairs. Each basal body pair is formed by basal bodies of different flagellar types (Nohýnková et al. 2006). The left lateral basal body pair bears left anteriolateral and ventral axoneme; the left middle basal body pair bears left caudal and posteriolateral axonemes; the right middle basal body pair bears right caudal and ventral axonemes; the right lateral basal body pair bears right anteriolateral and posteriolateral axonemes (Nohýnková et al. 2006).

Each flagellar type has different cellular localization and associated structures of yet unknown composition and functions. Flagella have long intracytoplasmic portions of axonemes not bounded by membranes. Intracytoplasmic axonemes of anteriolateral flagella accompany striated lamellae called marginal plates and fibrous structure - dense rods. Intracytoplasmic axonemes of posteriolateral flagella are associated with dense rods as well. Intracytoplasmic axonemes of the caudal flagella are associated with sheets of microtubules called funis. The ventral flagella are

equipped with a finlike extension containing a paraflagellar rod (Kulda and Nohýnková 1995).

In diplomonads, supranuclear microtubules nucleated from banded collars - microtubular organizing centers - situated close to the proximal base of basal bodies of the caudal flagella forming two symmetrical bands. In *Giardia*, these bands are asymmetrically developed. The band originating from the right tetrad, viewed from the dorsal cell side, is rudimentary. From the left tetrad originate a single layer of approximately 40 parallel supranuclear microtubules that runs clockwise and forms the skeleton basis of the adhesive disc, a unique structure in *Giardia*, which serves as an attachment organelle to intestine as well as to artificial surface. Each microtubule of the disc runs along its whole length accompanied by a microribbon composed mainly of giardins. Microribbons are heavily inter-linked with cross-bridges (Holberton 1981).

Another unique microtubular enigmatic structure present in *Giardia* is a median body. It is a membrane-unbound bundle of microtubules situated dorsally to caudal axonemes (Kulda and Nohýnková 1995). A specific marker of a median body is a filamentous protein named the median body protein (Marshall and Holberton 1993). The question about nucleation center of median body microtubules led to suggestion that median body can serve as a microtubular organizing centre itself (Marshall and Holberton 1993; Meng et al. 1996). Median body is a cell cycle dependent structure. It gradually disappears during mitosis, it is absent in progeny and in young trophozoites and reaches its maximum size in G2 phase, before the onset of mitosis (Sagolla et al. 2006). The disappearing and reappearing of the median body during cell division supports the proposed function of median body as storage of prepolymerized microtubules for fast daughter adhesive disc assembly during cytokinesis (Soloviev 1963).

2.2.3. Two nuclei and karyotype

Two nuclei in *Giardia* were originally considered identical because of morphology and other characteristics namely equal size (1.2 x 1.5 μm), and shape, equivalent DNA content, and the same transcriptional activity (Kabnick and Peattie 1990; Erlandsen and Rasch 1994). Binding of probes for each of the five chromosomes to both nuclei, further indicated that each nucleus has at least one complete copy of the genome (Yu et al. 2002). Recently, nucleolus has been detected

at the anterior part of each nucleus (Jiménez-García et al. 2008). Gradually differences between the nuclei were observed. Benchimol (2004d) found different number of nuclear pores between the nuclei, which generally correlates with nuclear transcriptional activity. Autoradiography analysis with [H^3] thymidine showed that nuclear replication in both nuclei occurs simultaneously at least 70% of the time, revealing some degree of asynchronicity in DNA synthesis (Wiesehahn et al. 1984). Our cytogenetic analysis revealed differences in chromosome numbers and DNA content between the nuclei (Tůmová et al. 2007a). Expression of the small nucleolar RNA (snoRNA) *GlsR17* occurs primarily in nucleolus of only one nucleus (Saraiya and Wang 2008), and stably transfected episomal plasmids enter and are maintained only in one nucleus through many subsequent cell divisions (Yu et al. 2002).

Though chromosomes in *Giardia* condense during mitosis, the cytological studies of karyotypes were complicated because of incomprehensiveness of condensed chromosomes due to the small size of the nuclei and a low number of mitotic cells in an asynchronous population. Light microscopic studies showed different results: four chromosomal bodies were presented by Kabnick and Peattie (1990), Erlandsen and Rasch (1994) found five chromosomal bodies with Feulgen staining, and Červa and Nohýnková (1992) found nine granules representing chromosomes. Therefore, in *Giardia*, molecular karyotyping with pulsed field gel electrophoresis (PFGE) preceded karyotyping, employing techniques of classical cytogenetics. Adam et al. (1988) showed with specific chromosome probes, the presence of five distinct chromosomal linkage groups. Higher number of bands presented in other studies (Korman et al. 1992), might represent size variants of chromosomes in major groups (Adam et al. 2000). Chromosome number seems to vary between isolates (Upcroft and Upcroft 1999). The heterogeneity might be a result of changes in hypervariable subtelomeric region (LeBlancq and Adam 1998).

2.2.4. Genome ploidy and meiosis

Ploidy of nuclei in *Giardia* was a matter of debate. Kabnick and Peattie (1990) regarded each nucleus as haploid. Erlandsen and Rasch (1994) measured the genomic DNA content of Feulgen stained nuclei by laser scanning confocal microscopy. Based on DNA content per nucleus (chromosome number and size), they concluded that each of the chromosomes in each nucleus would consist of 10-12 copies. Adam (2001) suggested that *Giardia* is tetraploid, based on four size variants

of chromosome 1 and a number of alleles of *vsp*A6 and *vsp*C5 located on different chromosomes (Yang and Adam 1994). In model proposed by Bernarder et al. (2001), based on trophozoite DNA content measured with flow cytometry in different cell and life cycle stages, *Giardia* trophozoites in G1 phase are tetraploid (4N), therefore each nucleus in G1 is diploid (2N) and the cell cycles between genomic ploidy (4N and 8N). During encystation occurs another round of nuclei division and DNA replication, giving rise to the cyst with four tetraploid nuclei - together 16N (4x4N). Excyzoite, as well as cyst, also has 16N (4x4N) and undergoes two rounds of cell division without DNA replication, resulting in four trophozoites, each 4N (2x2N). Variability in genomic ploidy is common also in life cycle of other eukaryotic lineages. The polyploidization can be either terminal or cyclic. Terminal polyploidization is connected with terminal cell differentiation e.g. in somatic nuclei of ciliates. When increase in ploidy is cyclic, it is later reduced by either asexual reproduction like in *Giardia* and *Entamoeba* or by sexual reproduction e.g., in plants (Parfrey et al. 2008).

The question of the sexual recombination in *Giardia* has been raised and discussed thoroughly. Partly because of a low level of allelic sequence heterozygosity (ASH) <0.02% in genotype A in *Giardia* WB isolate. Such a low level of ASH is unusual for an asexual organism with higher ploidy, because the individual nuclei are expected to accumulate different mutations (Adam 2001). However, there is a significant difference in allelic heterozygosity between genotypes, while the genome draft of *G. intestinalis* GS (genotype B) revealed the allelic sequence divergence of 0.5% (Franzén et al. 2009). Still, the low level of ASH suggests that some genetic exchange takes place, though it was never observed in *Giardia*.

A search for meiotic genes in *Giardia* genome revealed 17 homologues coding the "core meiotic recombination machinery" that function in meiosis in higher eukaryotes (Ramesh et al. 2005). Though some of these proteins function also in other processes, at least five are exclusively meiotic: Dmc1, Spo11, Mnd1, Hop1 and Hop2. Therefore, there is a suggestion that meiosis may still be operating in *Giardia*, because these proteins would not be retained in genome (Ramesh et al. 2005). Although it is possible these genes might have taken over different functions after loss of meiosis in *Giardia*, like in DNA damage repair, from which the meiosis might have originally evolved (Villeneuve and Hillers 2001). Some of these genes

were found also in other protists that were originally considered asexual like *Entamoeba*, *Encephalitozoon*, *Leishmania* and *Trypanosoma*. In *Trypanosoma brucei*, there has been proven genetic exchange between clones transfected with green fluorescent protein (GFP) and red fluorescent protein (RFP), resulting in yellow hybrids in vector tse-tse fly salivary glands (Gibson et al. 2008). These results show that meiosis arose in a common ancestor of all eukaryotes. With growing evidence that meiosis or some kind of genetic recombination occurs in *Giardia*, there was great effort to find a proof for it. There might be several reasons why the direct evidence was missing: 1) the recombination might occur infrequently and was not yet observe, 2) it might be furtive and escape attention e.g. during encystation or 3) it was already observed but not recognized (Birky 2005). Recently, Poxleitner et al. (2008b) showed signs of genetic recombination between two non-daughter nuclei in cyst. Episome transfected to only one of the two nuclei of trophozoites was detected by fluorescent in situ hybridization, in less than a third of cysts, in three of four nuclei. This might be a consequence of nuclear envelope fusion, documented on TEM (transmission electron microscope) and genetic transfer between non-daughter nuclei (Poxleitner et al. 2008b). While the plasmid was never observed in all four nuclei, it seems that the nuclear fusion would be restricted only to two nuclei. As follow-up study, the expression of three meiotic specific genes (Spo11, Hop1 and Dmc1) was measured during *Giardia* encystation. However, it did not show any unambiguous results, as these genes are expressed either in trophozoites (Melo et al. 2008).

2.3. Cell cycle

2.3.1. Cell cycle in model eukaryotic cell

Cell cycle is a sequence of events that lead to reproduction of cell. Cell cycle regulation is highly conserved among eukaryotes. The basic principles of cell cycle regulation were discovered and described mainly on two model organisms: fission yeast (*Schizosaccharomyces pombe*) (Mitchison 1971) and budding yeast (*Saccharomyces cerevisiae*) (Hartwell 1974) by isolating and studying haploid temperature sensitive cell division cycle (cdc) mutants. Many studies are also carried on animal models like *Xenopus laevis* early embryo or on *in vitro* cultured mammalian cell lines (Morgan 2007).

Cell cycle comprises four phases: G1, S, G2 and M phase. From G1 (the first gap phase) cell enters the cell cycle. In unfavorable conditions or as a response to inhibitory signals, cell can exit the cell cycle from G1 to dormant phase G0 and wait until the conditions are favorable and return to the cell cycle. In case of multicellular organism, cells in some tissues stay in G0 for a lifetime of organism. About one third of the cycle occupies S phase, during which DNA is replicated. In G2 (the second gap phase) the cell grows and prepares for division. The M phase, which takes a much shorter time in comparison with other cell cycles phases, comprises of mitosis, nuclear division, and cytokinesis, the cell division (Hartwell et al. 1974).

Cell cycle control mechanisms control order and timing of cell-cycle events. Later events of cell cycle are dependent on completion of earlier events. Three major regulatory checkpoints guide: 1) progression through Start in late G1, the G1/S checkpoint; 2) the entry into mitosis, the G2/M checkpoint; and 3) chromosome segregation at the metaphase-anaphase transition, the spindle assembly checkpoint (SAC) (Hartwell and Weinert 1989). Because it is crucial that the genome integrity is preserved in an undisturbed form the main control mechanisms, present in entry and during S phase and M phase, ensure that each newly formed daughter cell receives a complete genome without any mutations or deletions (Nurse 2002). These checkpoints prevent replication of damaged DNA or segregation of damaged chromosomes in mitosis by triggering DNA damage response, which blocks the cell cycle progression to give the cell time to repair DNA damage. Proliferation of the cell with damaged DNA can otherwise lead to genomic instability, which can lead to cell death or in multicellular organisms to tumorigenesis. In mitosis, SAC monitors the attachment of all chromosomal kintechores of sister chromatids to microtubule in the mitotic spindle, the bi-orientation of sister chromatids to both poles of mitotic spindle, and guides the chromosome segregation during metaphase-anaphase transition into two daughter cells. In case of even a single unattached kinetochore, the anaphase is blocked by inhibition APC^{Cdc20} and securin destruction sister chromatid separation is therefore prevented (Hartwell and Weinert 1989; Morgan 2007). Exit from mitosis controls mitotic exit network (Bettignies and Johnston 2003).

Regulation of all processes during cell cycle is guided by a complex of serine/threonine protein kinases, called cyclin-dependent kinases (Cdks). Cdks are activated by the binding of a regulatory cyclin subunit. While Cdks levels are stable

throughout the cell cycle, cyclin levels change. This is due to changes in cyclin gene expression and the protein degradation by their ubiquitination and consequent destruction in protease complex – the proteasome. Two main ubiquitin-protein ligases in cell cycle are SCF (Skp, Cullin, F-box containing complex), which are crucial for G1/S transition and production of the anaphase promoting complex (APC), which promotes metaphase-to-anaphase transition. For Cdks activation is besides of cyclin binding, crucial also phosphorylation of the conserved Thr 160 residue, near the kinase active site by Cdk-activating kinase (CAK) and dephosphorylation of two inhibitory phosphorylations on the conserved Thr 14 and Tyr 15 residues (which are phosphorylated by Wee1 kinase) by Cdc25 phosphatase (Nurse 2002). The activation of Cdk complex further results in phosphorylation of Ser and Thr residues downstream in the cell cycle machinery substrates. Different Cdk complexes operate in different cell cycle phases and each cyclin-Cdk complex promotes activation of the next complex in sequence. In animal cells, G1 is under control of G1 complex - cyclin D/Cdk6, Cdk4. G1/S transition controls G1/S-Cdk complex - cyclin E/Cdk2 and its role is to trigger transition through Start, launch DNA replication and centrosome duplication and activate S-Cdks. S-Cdk complexes - cyclin E; A/Cdk2, Cdk1 control S phase, mainly the DNA replication and activation of M-Cdks. G2/M transition and M-phase is controlled by M-Cdk - cyclin B/Cdk1. Main role of this complex is to control mitotic spindle assembly and chromosome alignment at the spindle midzone. M-Cdks eventually activate APC, which triggers sister chromatid separation and inactivation of cyclin-Cdk complexes (Sánchez and Dynlacht 2005; Morgan 2007). Unidirectional transition from one cell cycle stage to the next is directed not only by activation of the next cyclin-Cdk complex in sequence but also by inactivation and inhibition of Cdk complexes, which can be regulated in many ways. Cdk inhibitor proteins (CKIs) play an important negative regulatory role in the cell cycle; they bind to complex cyclin-Cdk and inactivate it. These proteins operate mainly in G1 and prevent cell to enter the cell cycle prematurely. For example, they are activated in response to DNA damage or unfavorable environmental conditions. Their defects or loss of function can cause deregulation of the cell cycle and can possibly lead to cancer in multicellular organisms (Peter and Herskowitz 1994; Foster 2008).

2.3.2. Cell cycle in *Giardia* and other parasitic protists

Up to recently, cell cycle regulation in parasitic protists was not well understood. More thorough studies of the cell cycle, aimed mainly at finding new antiparasitic drugs, enabled genome projects in *Entamoeba, Plasmodium, Trypanosoma, Cryptosporidium* and other protists (http://eupathdb.org/eupathdb) some of which are already completed. These projects supported the search for cell cycle regulatory molecules. Cell cycle regulation in parasitic protists has many different features from canonical regulation in eukaryotic cells, because of their complex life cycles and ability to live in changing environmental conditions (Hammarton et al. 2003).

The completed *Giardia* genome project of assemblage A (isolate WB) http://giardiadb.org/giardiadb/, to which assemblages B (isolate GS) and assemblage E (isolate P15) were recently added, provides information about cell cycle regulatory gene equipment in *Giardia*. *Giardia* has one of the smallest genomes in eukaryotes - 12 Mb for haploid genome. Though many regulatory pathways are simplified in this minimalistic genome, the cell cycle in *Giardia* is regulated with the conserved regulatory mechanisms in typical eukaryotic cell (Morrison et al. 2007). *Giardia* proceeds through all four typical eukaryotic cell cycle phases. The first studies about *Giardia* cell cycle by flow cytometry based on DNA content showed that G1 is the dominant phase in an unsynchronized population (Hoyne et al. 1989; Sandhu et al. 2004). Bernarder et al. (2001) on the other hand presented in his on flow cytometry based study a different model, that dominant and the longest phase in *Giardia* cell cycle is G2. This result was further confirmed by Reiner et al. (2008) and Poxleitner et al. (2008a). G2+M phase takes up to 66% of the cell cycle duration and G1 takes only about 12% of the cell cycle duration in *Giardia*.

Various inhibitors are employed for cell cycle analysis. Aphidicolin (APH), a DNA synthesis inhibitor, was used to synchronize *Giardia* trophozoites via disrupting S phase (Reiner et al. 2008). Aphidicolin is a mycotoxin from a group of tetracyclic diterpenoids produced by fungi *Cephalospora aphidicola* or *Nigrospora oryzae* (Spadari et al. 1982). When applied to most eukaryotic organisms, it induces replication fork that stalls and inhibits DNA replication due to its competitive binding with dNTP to eukaryotic DNA α polymerase, (Huberman 1981; Spadari et al. 1982). Aphidicolin has been used relatively successfully as a tool for cell cycle synchronization in various cell lines, including plant and vertebrate cells (Samuels et al. 1998; Uzbekov et al. 1998; Kues et al. 2000). After aphidicolin treatment cells are

arrested in the G1/S phase border and after release from this block, they are supposed to move to S phase and G2 as a synchronized population. However, the level of synchronization is often reduced after one cell cycle (O´Connor and Jackman 1996).

Aphidicolin induced inhibition of DNA synthesis and consequent mitosis in nuclei in the *Trypanosoma brucei* bloodstream did not inhibit DNA synthesis in kinetoplast and cytokinesis, which led to dissociation of nuclear and kinetoplast cycles (Ploubidou et al. 1999).

In various kinds of mammalian cells, G1 is uniformly the dominant and the longest phase of the cycle. The duration and prevalence of different cell cycle phases have not been studied thoroughly in many species of parasitic protist, but the known scarce results suggest that arrangement of cell cycle phases differs among different species. In free-living diplomonads *Spironucleus barkhanus* and *S. salmonicida,* flow cytometry cell cycle analysis reveal that population is evenly distributed between peaks corresponding to G1 and G2 (Roxström-Lindquist et al. 2010). In *Trichomonas vaginalis,* different groups found different dominant phases in flow cytometry analysis of an unsynchronized population; Riley et al. (1994) show that G2 phase is dominant, on the other hand Zubáčová et al. (2008) indicate the G1 phase as dominant. In bloodstream and procyclic forms of *Trypanosoma brucei*, the dominant phase is G1 (Siegel et al. 2008; Forsythe et al. 2009). In *Entamoeba histolytica,* it is difficult to assess distinct cell cycle phases, as there are no discernible peaks corresponding to individual cell cycle phases. The population comprises of cells with different number of nuclei and even nuclei within one cell differ in their ploidy (Lohia et al. 2007). Axenic populations are more variable in the number of nuclei and their ploidy than xenic populations grown with bacterial flora. Polyploidy is also more frequent in older populations than in freshly subcultured isolates (Mukherjee et al. 2008).

2.3.2.1. G1 and S phase

G1 phase in *Giardia* is short; it occupies only 12% of the cell cycle duration. Freshly divided G1 trophozoites are small and lack median bodies, which appear again during G1. DNA replication takes about 22% of the cell cycle duration in *Giardia* (Reiner et al. 2008), which corresponds to the duration of S phase in mammalian cells. The simplified DNA synthesis machinery in *Giardia* has origins of replication out of the original hexameric origin recognition complex (ORC) present

in mammalian cells, which comprises Orc1-6, only two proteins (Orc4, Orc1) (Morrison et al. 2007). Similarly only one protein Orc1 out of ORC is present in *Trypanosoma brucei* or *Entamoeba histolytica* (Hammarton 2007; Lohia et al. 2007). Simplified pre-replicative complex (pre-RC) in *Giardia* consists only of Cdc6 and Mcm 2-7, with the helicase activity to promote unwinding of DNA at the origin of replication. In additional to these two complexes, *Entamoeba* or *Trypanosoma* also have the Mcm 9-10 complex (Liu et al. 2009). *Giardia* further lacks several regulatory initiator proteins involved in replication e.g. Cdt1, Dpb11, Cdc45, Dbf4, Mcm10 and geminin. It has three replicative B-type DNA polymerases (Polα, Polδ, Polε), like *Trichomonas vaginalis* or *Saccharomyces cerevisiae* (Morrison et al. 2007). Four orthologues of human Cdks: Cdc2/Cdk1-like 1-4 and one ortholog of cyclin activating kinase (CAK) were found in *Giardia* genome (Guo and Stiller 2004). In *Entamoeba histolytica,* trophozoites undergo endoreplication cycles, resulting in cells that contain different number of nuclei with different amount of DNA content (Banerjee et al. 2002). *Entamoeba* genome encodes a large number of proteins required for DNA replication licensing, although with different function. It further lacks some crucial regulators like Cdt1, geminin and others, which may lead to loss of replication licensing to once per cell cycle (Lohia et al. 2007).

2.3.2.2. G2 and M phase

Transition from G2 to M phase requires activation of cyclin B/Cdk1complex. In its genome *Giardia* possesses homologues of both, cyclin B and Cdk1 (Smith et al. 1998). Homolog of Cdc25 phosphatase, which dephosphorylates the inhibitory phosphorylation sites on Cdks and help activate cyclin/Cdk complexes, was not found (Morrison et al. 2007). The homolog of Wee 1 kinase, which is responsible for the inhibitory phosphorylations on Cdks is present (Manning et al. 2011). The expression of cyclin B measured at the mRNA level increases in G2 phase *Giardia* trophozoites, which corresponds with increasing level of cyclin B in G2 phase in the typical eukaryotic cell cycle (Reiner et al. 2008). *Giardia* possesses important key mitotic regulator – the aurora kinase. Aurora kinases are activated in mitosis and regulate centrosome duplication, spindle assembly, sister chromatid segregation and cleavage furrow formation in eukaryotes. In metazoans aurora kinases (AK) family comprises two members: AK A, AK B, mammalian germ cells also contain AK C, whose function is not well understood (Andrews et al. 2003). The single aurora gene

in *Giardia* has a 61% amino acid sequence homology to human aurora kinase A (Davids et al. 2008). Yeast cells possess also only a single member of aurora kinase family (Ipl1), which functions closely resemble metazoans aurora B (Shirk et al. 2011). Phosphorylated active form of aurora kinase localizes in *Giardia* to the basal body region, adhesive disc, mitotic spindle and anterior paraflagellar rods. Activated form of aurora kinase is only present in *Giardia* in mitosis. Specific inhibitors of aurora kinase prevent mitosis and block cytokinesis. *Giardia* trophozoites blocked in mitosis, are still able to replicate DNA and give rise to polyploid cells (Davids et al. 2008). Another important mitotic kinase, polo-like kinase (Plk) was also found in *Giardia* genome but currently there is no data about the localization or activity (Morrison et al. 2007; Manning et al. 2011). Other important mitotic regulatory complexes such as the spindle assembly checkpoint machinery, APC, and the mitotic exit network are almost unexplored in *Giardia*. These complexes play an important role in the cell cycle regulation particularly in mitosis in the destruction of regulatory proteins by their ubiquitination and consequent degradation in protease complexes – the proteasomes. *Giardia* genome codes for a single gene for ubiquitin, ubiquitin ribosomal fusion gene, E1 and E2 enzymes, multiple protein ubiquitin ligase systems and for proteasome 20S typical eukaryotic complex (Gallego et al. 2007).

There has been quite a lot of controversy about modes of mitosis and cell division in *Giardia* in initial studies.

For a long time, the process of mitosis itself was not described in detail. Although there has been a study showing the mitotic spindles in karyokinesis of *Giardia* trophozoites on fluorescence microscopy (Nohýnková et al. 2000), there were still doubts whether *Giardia* possesses mitotic spindles. Solari et al. (2003) and Benchimol (2004b) suggested that nuclei in *Giardia* might be divided in a unique way by adhesive disc intervention, as shown on electron micrographs. However, a few years later, came the detailed documentation and description of mitosis course in *Giardia*, based on fluorescence and electron microscopy, from two different laboratories. Chromosomes condense in early prophase, while the nuclei are still in an interphase position. In the late prophase, the nuclei migrate in the midline of the cell, one above the other. Viewed from dorsal side, the left nucleus migrates anteriorly and the right nucleus posteriorly.

A mitotic bipolar spindle starts to nucleate in the prophase as well. Around each nucleus assembles one mitotic spindle. It is composed of extranuclear and

intranuclear microtubules, with two spindle poles. At each spindle pole region, there are two basal bodies and probably only one of them is nucleating the relevant half of the spindle (Sagolla et al. 2006; Tůmová et al. 2007a). Assembly of kinetochores on the centromeric chromatin and the attachment of mitotic spindle microtubules to them are essential for correct chromosome segregation. The centromere contains cenH3, a centromeric variant of H3 histone, which recruits kinetochore proteins, motors and other structural and regulatory proteins to centromere (Van Hooser et al. 2001). *Giardia* possesses homologues of all core histones, two copies of histone H2a, H2b, H3 and three copies of H4. Linker H1 histone is missing in the *Giardia* genome (Wu et al. 2000). *Giardia* has two variants of H3: H3b and cenH3. CenH3 localizes to discrete foci in both the interphase nuclei and to the mitotic spindle poles in anaphase and seems to be associated with the centromere (Dawson et al. 2007). The nuclear envelope does not break apart during mitosis in *Giardia* and only some of the microtubules of extranuclear mitotic spindle enter the nuclear envelope. The type of *Giardia* mitosis has been described as semi-open orthomitosis according to Raikov (1994); (Sagolla et al. 2006; Tůmová et al. 2007b).

The chromosomes are then segregated in anaphase to opposite sides of dividing cell according to left-right symmetry of the cell. There has been a debate about distribution of the two nuclei into daughter cells due to the lack of a detailed description of mitosis,. Suggested models proposed either 1) equational distribution, according which each daughter cell receives one copy of each mother nucleus or 2) reductional distribution when both nuclei from one mother nucleus are segregated to the same daughter cell (Yu et al. 2002). Results from fluorescent in situ hybridization (FISH) analysis of dividing cells revealed that nuclei are distributed to daughter cells equally (Ghosh et al. 2001; Sagolla et al. 2006). The equational distribution of nuclei into daughter trophozoites was also confirmed by Tůmová et al. (2007a).

The modes of mitosis are variable among protists. A type of closed mitosis (pleuromitosis) with extranuclear spindle microtubules that do not penetrate nuclear membrane but are connected to the kinetochores on the nuclear membrane, was described in parabasalids like *Trichomonas vaginalis* (Gómez-Conde et al. 2000) and *Tritrichomonas foetus* (Ribeiro et al. 2002). The nuclear envelope does not break either in kinetoplastids like *Trypanosoma brucei* or in schizont of *Plasmodium falciparum*, where the karyokinesis is not accompanied by chromosome

condensation (Raikov 1994). Closed pleuromitosis occurrs in *Entamoeba histolytica*; the chromosomes do not condensate during mitosis (Chávez-Munguía et al. 2006).

2.3.2.3. Division of flagellar apparatus and adhesive disc

During the flagellar apparatus reorganization in *Giardia* mitosis and cell division, the flagella are distributed into daughter cells in a semi-conservative manner. All four pairs of flagella are maintained and distributed to daughter cells and eight new flagella are formed *de novo*. However each daughter cell receives different half set of mother flagella (Nohýnková et al. 2006).

Parent anteriolateral and caudal flagella are segregated equally between daughter cells. The flagella of the mother ventral and posteriolateral pairs are segregated unequally; one daughter cell receives both ventral and the other both posteriolateral flagella. All mother flagella are transformed during the migration, with the exception of the caudal flagella. Interphase pairs of basal bodies stay together during migration, but the pairs of flagella are separated from each other, which enables the transformation of parent posteriolateral and ventral flagella into daughter anteriolateral flagellar pairs. Each parent anteriolateral flagellum moves to the opposite side of the cell with respect to its interphase position and form the right caudal flagellum in each daughter cell. Caudal flagella that do not undergo transformation during cell division form the left caudal flagellum in each daughter cell. During the reorientation, the basal body also starts to duplicate and the newly assembling daughter flagella will emerge. The pairs of ventral and posteriolateral flagella are assembled *de novo* in daughter cells (Nohýnková et al. 2006). Gamma tubulin might play a role in its assembly, which is a universal component of microtubular organizing center (MTOC) in eukaryotes. It has been detected by immunofluorescence at the basis of four out of eight basal bodies in *Giardia* during interphase; however it disappears at early mitosis and appears again at late mitosis concurrently with *de novo* assembly with flagella in daughter cells (Nohýnková et al. 2000).

Individual basal bodies in *Giardia*, within the basal body pairs described earlier, are of different age and relates to the basal body/flagella reorientation and transformation. This is also known from other flagellated organisms; it is well described in unicellular algae that bear flagella that are different in size and function. Moreover, during cell division when each daughter cell only receives one half of

parental apparatus, it has to produce the other half *de novo* and also comprises the flagella transformation (Beech et al. 1991).

As mentioned earlier, there was a difference of opinions, due to experimental discrepancies, on plane of the cell division. More specifically, whether *Giardia* divides while attached or swimming (Kabnick and Peattie 1990; Ghosh et al. 2001; Yu et al. 2002; Benchimol 2004a, b). In these studies, three modes of cytokinesis that could occur during cell division were suggested: 1) ventral-ventral; 2) dorsal-dorsal and 3) ventral-dorsal. Benchimol (2004a) suggested that all three modes of cytokinesis occur in *Giardia*. Tůmová et al. (2007b) described in detail the mode of the cell division, in which an important role in *Giardia* cytokinesis plays its unique attachment organelle, the adhesive disc. The trophozoite stays attached during the whole course of mitosis. The disassembly of parental disc starts concurrently with formation of two daughter adhesive discs on dorsal side of mother cell, which determines the ventral side of daughter trophozoites. On electron micrographs, the disc disintegration accompanies shortening of giardin ribbons on the disc microtubules leading to their eventual loss. New daughter adhesive discs nucleate in counter clockwise direction from the left caudal flagellum, which is the mature and the oldest flagellum. With the parental disc disintegration, the daughter trophozoites proceed to swimming phase and continue in the process of cell division. The whole process is finished when daughter trophozoites attach, with their newly assembled adhesive discs and they still stay connected with tail cytoplasmic bridge which, as the trophozoites move apart, is getting thinner and finally it is cleaved and retracted. However, the mode of contraction and the proteins that might play role are unknown. Typical contractile ring composed of actin and myosin that works at the final stage of cytokinesis in animal cells must be modified in *Giardia*, because no myosin was found in its genome (Morrison et al. 2007).

2.4. Differentiation

2.4.1. Differentiation and cell cycle interconnection

Cell differentiation is a key process in development of a multicellular organism or in various processes in multicellular organisms e. g. in the hematopoiesis. Differentiation encompasses many levels; it involves changes in gene expression, genome ploidy, signaling pathways, metabolism or cell morphology. The differentiation and cell cycle progression are believed to be two mutually exclusive

processes in terminally differentiating cells. A differentiated cell signals a stop to proliferation and to exit the cell cycle (Myster and Duronio 2000). It was shown that in mammalian cells the exit point is in G1 phase (the dominant phase of the cell cycle) (Huleman and Boonstra 2001). In unicellular organisms, differentiation is a periodical adaptation to changing environmental conditions (different hosts) during life cycle. For example, *Trypanosoma brucei* transforms from a slender to stumpy form in bloodstream of the mammalian host and then to procyclic form in a tse tse fly midgut (Matthews 1999). *Naegleria gruberi* differentiates from an amoebic form into a flagellate or the cyst stage (Lee 2010); *Acanthamoeba* or *Entamoeba* form a protective coat and transform into the cyst (Chávez-Munguia et al. 2005; Chatterjee et al. 2009). Protists as well as cells in multicellular organism stop the proliferation before onset of differentiation. However, in many species some events of cell cycle like DNA synthesis or mitosis also proceed during differentiation. Though this question is almost unexplored, it seems that unicellular organisms have a specific exit point in the cell cycle from which they can enter differentiation process. In *Trypanosoma brucei*, transformation from slender to stumpy form occurs in dominant cell cycle phase G0/G1 (Fenn and Matthews 2007). As stated previously, the dominant cell cycle phase in *Giardia* is G2 phase, which occupies most of the cell cycle. Results from a synchronized culture showed, that cells in early G2 are most prone to enter the encystation process (Reiner et al. 2008).

2.4.2. Encystation in *Giardia*
2.4.2.1. The cyst wall assembly and secretory pathway

The cyst wall in *Giardia* is formed from outer filamentous layer, which is 0.3 - 0.5 μm thick, and inner membranous layer consisting of two membranes, which border the peritrophic space (Lujan et al 1997). Filamentous layer is composed of carbohydrates (63%) and four proteins (37%). The dominant carbohydrate is β-(1-3) linked N-acetyl galactosamine (GalNAc). GalNAc is synthesized from glucose in a pathway activated during encystation (Karr and Jarroll 2004). Three small cyst wall proteins (CWP1-3) are highly homologous. They contain leucine rich repeats (LRRs) cysteine rich domain and amino-terminal signal peptides. The CWP2 has a 121 - residue carboxy-terminal tail, which is not present in the other two proteins. All three proteins are co-expressed during encystation and transported to nascent cyst wall in encystation specific vesicles (ESVs) (Lujan et al. 1995; Mowatt et al. 1995; Sun et al.

2003). Recently, the fourth cyst wall protein was discovered. It is a 170 kDa high cysteine non-variant cyst protein (HCNCp). This protein is, more than to other CWPs, similar to VSP. It is rich in cysteine (13.9%) but is only upregulated in the later stages of encystation and it is transported in ESVs as other CWPs (Davids et al. 2006).

In *Giardia*, there were described two excretory secretory pathways. They divide after export of the material from ER: a constitutive pathway for VSP transport on plasma membrane in trophozoite and an inducible pathway, which transports cyst wall material (CWM) during encystation. Both pathways work simultaneously in the early phases of encystation (Marti et al. 2003a). However, VSP was never found in ESVs (McCaffery et al. 1994b). These two pathways have different kinetics, while CWPs are stored in ESVs for hours and undergo posttranslational processing; VSP goes directly to the plasma membrane within minutes.

The ESV compartments that transport CWM were visualized for the first time in encysting cells by Gillin et al. (1987). Marti et al. (2003a) suggested that newly synthesized cyst wall material is sorted away from constitutively secreted cargo exported from ER. The targeting of CWP from ER into ESVs is signal dependent. The amino-terminal signal peptide and LRR likely target them to the secretory pathway (Hehl et al. 2000; Marti et al. 2003a; Sun et al. 2003). Stefanic et al. (2009) brought the evidence about the roles of COPII and Rab1 GTPase in the transport of CWM to ESV. As ESVs share some Golgi characteristics, they are reminiscent of cis Golgi compartment neogenesis. They mature on their way to plasma membrane, progressing from cis to trans stage (Stefanic et al. 2009) and they are associated with Golgi markers like β´COPI; GiYip1, clathrin and dynamin (Marti et al. 2003a, b). The maturation process of vesicles includes retrograde transport to ER. Stefanic et al. (2006) showed that Hsp70-Bip is exported to ESV and then actively retrieved to ER, as it does not colocalize with ESVs during later stages of encystation. During the maturation of ESVs, the CWPs are posttranslationally modified. Cargo is delayed in ESVs and subjected to post-processing. There was described the proteolytic cleavage of CWP2 C-terminus by lysosomal cysteine proteinase (Gottig et al. 2006; Konrad et al. 2010); phosphorylation of CWPs (Slavin et al. 2002); or formation of disulphide bonds within CWP1 and 2 (Hehl et al. 2000). The disulphide-bonded heterodimers in ESVs can be unfolded by treatment of dithiotreitol (DTT) and consequently lead to reversible disappearance of ESV (Reiner et al. 2001).

Despite growing knowledge about ESV formation, its maturation, and transport of CWM to the cell surface, there is still limited information about the final step of cyst wall formation - the ESVs fusion with the cell membrane and cargo release. The transmembrane SNARE proteins (soluble-N-ethylmaleimide-sensitive factor attachment protein receptors) play a crucial role in membrane fusion in eukaryotic cells (Harbury 1998). In thorough genomic search, 17 putative SNARE proteins were found in the *Giardia* genome. Distinct SNARE proteins localize to different subcellular compartments in *Giardia* and knockdown experiments showed that only some of the proteins are essential, while others are dispensable for the cell. In non-encysting trophozoites, they colocalize mainly with PV and ER and weakly with ESVs in encysting cells. (Elias et al. 2008). Reiner et al. (1990) suggested ESVs content is released by exocytosis. Benchimol (2004c) claimed that ESVs release via exocytosis with incomplete membrane fusion. Empty membranous fragments, observed around nascent cyst wall, support this hypothesis. Membranous fragments can then be resealed into empty vesicles and then endocytosed. Recent data show that the CWM in ESVs is partitioned into two fractions during the pathway in the later stage of encystation. These fractions are further sequentially sorted and secreted on the cell surface. The presorted material is then secreted at different rates. CWP1 and processed CWP2 are excreted quickly within a few minutes and polymerize to form the first layer of cyst wall and the rest of the condensed CWM is secreted slowly within hours to form the second layer. Cysts with normal appearance are formed when the processing of CWP2 within ESVs is abolished with protease inhibitor. However these cysts are not water resistant (Konrad et al. 2010).

2.4.2.2. Gene regulation and signal transduction in encystation

Once it possible to trigger encystation process, the regulation of expression of encystation specific genes was further studied. One of the regulating molecules might be cholesterol. Cholesterol deprivation alters membrane fluidity. This results in changing the activity of membrane bound enzymes and signal transport, consequently affecting the regulation of transcription of encystation specific genes (Luján et al. 1996). Several transcription factors were shown to be involved in encystation, the first was Myb2. The Myb transcription factors regulate developmental processes and cell cycle in fungi, plant and mammals (Sun et al. 2002). Homologues of few other transcription factors or DNA-binding proteins

affecting regulation of transcription in cell proliferation, development and differentiation in various eukaryotes were found in *Giardia* and bind to promoters of encystation specific genes. Examples of these include a member of the ARID family of transcription factors (AT-rich interaction domain), GARP or WRKY proteins. However, none of these proteins seem to function exclusively in encystation (Sun et al. 2006; Wang et al. 2007; Pan et al. 2009). Carranza and Luján (2009) favored the explanation that encystation specific genes are in trophozoites blocked by transcription repressors, which is released from DNA during differentiation. Sonda et al. (2010) showed that gene expression in encystation is also regulated by histone acetylation. Microarray analysis revealed that inhibition of histone deacetylase (HDAC) down-regulates transcription factors Myb2, CWP 2-3, and glucosamine-6-phosphate deaminase (Sonda et al. 2010).

Homologues of various proteins involved in signal transduction pathways in cell proliferation and differentitation were found in *Giardia*; however their function in encystation is not well understood. Most of these proteins change their localization and activity during encystation. *Giardia* possesses two homologs of extracellular signal regulated kinases (ERK1, 2) from the mitogen activated protein kinase (MAPK) family. Both are expressed in trophozoites and encysting cells, however during encystation their activity decreases (Ellis et al. 2003). Several signaling proteins are upregulated during encystation: protein phosphatase 2A (PP2A); its knock-down results in decreased number of ESVs and cyst (Lauwaet et al. 2007); protein kinase B and C (PKB, PKC) (Kim et al. 2005; Bazan-Tejeda et al. 2007). Arginine deiminase (ADI), an energy metabolism enzyme in *Giardia*, catalyzes arginine to citrulline and results in energy production under anaerobic conditions. It has been suggested that ADI is involved in transduction pathways controlling encystation (Touz et al. 2008).

2.4.3. Excystation in *Giardia*

Excystation is a process of leaving the protective coat, which undergo cyst (oocyst)-forming pathogenic protozoans, for example *Entamoeba histolytica*, *Balantidium coli*, *Cryptosporidium sp*. or *Toxoplasma gondii*, to initiate the infection in a new host. *Giardia* cysts ingested by a mammalian host excyst shortly after entering the small intestine. Scanning electron microscopy of *Giardia muris* and *Giardia intestinalis* by Coggins and Schaefer (1984) and Buchel et al. (1987),

revealed more detailed pictures of excysting cells. In cyst, the peritrophic space separates the plasmalemma and cyst wall (Erlandsen et al. 1990). In the beginning of excystation, the peritrophic space starts to enlarge (Hetsko et al. 1998); the lacunal space at the cyst periphery fuse and enclosed protozoan is released from the cyst wall. These pictures were the first evidence of *Giardia muris* excysting trophozoite was the emergence of flagella from a small opening at one cyst pole. Flagellar motion enlarges the opening, from which emerges a whole trophozoite, leaving the empty cyst wall case. Emerging trophozoites, with irregular cell shape and no apparent adhesive disc, almost immediately initiate cell division and daughter adhesive discs together with daughter flagella start to appear (Coggins and Schaefer 1984). Freshly excysted trophozoite possesses preventral flange, which according to Hetsko et al. (1998), might enable the attachment while the adhesive disc has not yet been formed.

It is crucial that cyst wall, which on one side protects organism against unfavorable conditions in outer environment, would be also permeable and sensitive to external stimuli in intestinal milieu. Cytoplasmic pH 6.9 in cyst changes relevantly to changes in external pH (Hetsko et al. 1998).

Peripheral vacuoles contain cysteine proteases. These enzymes are released to peritrophic space and degradate the cyst wall proteins. Inhibition of these proteases by various inhibitors blocks the excystation (Feely et al. 1991; Ward et al. 1997). Exposure of cyst to polyclonal serum against purified cyst wall or to wheat germ agglutinin, specific to N-acetyl glucosamine (GlcNAc) which is present in cyst wall, prevents excystation, probably by interfering with the proteolysis of cyst wall glycoproteins (Meng et al. 1996). The protein kinase A (PKA), PP2A and conserved calcium binding regulatory protein calmodulin mediated pathways are crucial for excystation. PKA dependent pathway plays critical role in metabolism, cell growth and differentiation in eukaryotic cells and has the same affect in other parasitic protists like *Leishmania* and *Trypanosoma*. Inhibition of PKA, PP2A and calmodulin block the excystation (Bernal et al. 1998; Abel et al. 2001; Reiner et al. 2003; Lauwaet et al. 2007).

Excystation is very complex and quick process. It is not well understood whether the cyst contains preformed mRNA for the proteins involved in excystation or if the involved genes are transcribed *de novo*. Differential mRNA display analysis showed that specific transcripts appear, disappear or change their abundance during different

excystation stages. Genes that change their expression are involved in regulation of protein degradation (e.g. proteasome subunits), cytoskeleton assembly/disassembly (α; β tubulin) and mitosis (e.g. kinesin 5, Mad2) (Birkeland et al. 2010).

3. LIST OF ORIGINAL PAPERS

- **Cytogenetic evidence for diversity of two nuclei within a single diplomonad cell of *Giardia*.**
  Pavla Tůmová, <u>Klára Hofštetrová</u>, Eva Nohýnková, Ondřej Hovorka and Jiří Král
  Chromosoma (2007), 116 (1): 65-78 (IF=4.065)

- ***Giardia intestinalis*: Aphidicolin influence on the trophozoite cell cycle.**
  <u>Klára Hofštetrová</u>, Magdalena Uzlíková, Pavla Tůmová, Karin Troell, Staffan G. Svärd and Eva Nohýnková
  Experimental Parasitology (2010), 124: 159-166 (IF=1.751).

- **How nuclei of *Giardia* pass through cell differentiation: semi-open mitosis followed by nuclear interconnection.**
  <u>Klára Jiráková</u>, Jaroslav Kulda, and Eva Nohýnková
  Protist (2011), Epub ahead of print (IF=3.329).

- **Mitotic checkpoints in a binucleated protozoan parasite *Giardia intestinalis***
  Kristýna Marková, <u>Klára Jiráková</u>, Magdalena Uzlíková, Pavla Tůmová, Jaroslav Kulda, and Eva Nohýnková
  Eukaryotic Cell, in review

4. RESULTS

4.1. Aphidicolin influence on cell cycle

Studying the cell cycle, especially cell cycle regulatory molecules which oscillate during various cell cycle phases, requires a synchronized population. Synchronization of cell population may be achieved by different approaches. It is likely that this is most often achived by inhibiting either DNA replication or nuclei division using specific inhibitors. We studied the influence of reversible and irreversible aphidicolin concentrations on *Giardia* trophozoites, namely DNA synthesis, DNA damage and characteristics of cell cycle progression, i.e. cell population growth, mitotic index, cell size and presence of median bodies.

The influence of aphidicolin on the *Giardia* cell cycle is both dose and time dependent. The working concentration of 5 μg/ml was adjusted, based on the initial experiments. DNA content of propidium iodide (PI) stained trophozoites in logarithmic phase of growth was measured by flow cytometry. We found that approximately 70% of untreated cells resided in G2/M corresponding to DNA content 8N and the rest of population was in G1/S phase (corresponding to 4N). This population distribution in cell cycle phases was supported by multiparameter flow cytometry analysis of the population stained with PI and antibody against cyclin B, a G2 marker. The positive signal for cyclin B was present mainly in cells corresponding to G2/M, in comparison with the low level of positivity for cyclin B in cells corresponding to G1/S.

Aphidicolin treatment inhibited the DNA synthesis. Flow cytometry histograms of DNA content showed that even after short incubation period (that did not cover the whole length of the cell cycle), almost 80% of trophozoites shifted to and were blocked in G1/S phase, which led to dramatic decrease in the number of cells in G2/M. Incorporation of 5–bromo-2´-deoxy-uridine (BrdU), which is a synthetic nucleotide – an analog to thymidine - and it is used as a marker for DNA synthesis in many cell types (Hasbold and Hodgkin 2000), provided direct proof that DNA synthesis was disrupted by aphidicolin treatment. Our results from immunofluorescence showed, that BrdU was incorporated into the DNA of ~33% of untreated *Giardia* cells. The DNA was replicated asynchronously as demonstrated by asymmetry in fluorescence signal between the two nuclei. In 10% of the cells, only one of the two nuclei showed a positive signal for BrdU incorporation. This observation corresponded to nuclear asynchronous behavior at the onset of prophase

and anaphase during mitosis (Tůmová et al. 2007a). After a short period of incubation with aphidicolin, the incorporation of BrdU had almost ceased though in some nuclei it was present as a weak signal represented as single dots. However, it differed significantly from a homogenous signal in the whole nucleus of untreated cells.

The aphidicolin, as well as treatment with other DNA synthesis inhibitory drugs, had negative side effects. Aphidicolin induces chromosomal gaps and DNA double strand breaks (DSB), especially at common fragile sites, probably due to stalling the replication forks (Glover 2006). Guarding mechanisms have evolved to detect the damaged DNA and prevent its propagation to progeny. In DSBs recognition and their repair, the phosphorylated form of histone H2A plays an essential role (Zhou and Elledge 2000). *Giardia* possesses two copies of this core histone, which in its sequence contain the well conserved phosphorylation site on C terminus. We found that this posttranslational modification was present in aphidicolin treated *Giardia* trophozoites and could be detected with the antibody against phosphorylated H2A on immunofluorescence. Phosphorylated H2A was already present either in one or both nuclei of the 55% of cells after 6 hours of incubation with aphidicolin. The presence of signal in only one nucleus likely corresponded to the asynchronicity in the DNA synthesis between the nuclei. The percentage of cells containing phosphorylated H2A and the presence of signal in both nuclei increased with prolonged incubation with aphidicolin and reached 99% after 48 hours. The fluorescence signal for phosphorylated H2A was detected not only as a consequence of aphidicolin treatment, but it also occurrs naturally in untreated trophozoites (cca in 17% of cells). This signal appears only as single dots and usually in only one of the two nuclei in comparison with full signal in aphidicolin treated cells.

Another side effect of aphidicolin treatment was the causative dissociation of nuclear and cytoplasmic cycles. While the nuclear cycle was stopped at the G1/S border, the cytoplasmic cycle and its processes (protein synthesis, increase in cell size) continued. *Giardia* trophozoites grew significantly in cell size with prolonged aphidicolin treatment. The aphidicolin treated trophozoites were longer by 34% and wider by 44% in comparison with untreated cells after 48 hours of incubation with drug. The protein synthesis was unperturbed and continued; the amount of proteins was significantly higher in aphidicolin treated cells, which was monitored by measuring the protein concentration. Correspondingly, these trophozoites contained

almost in 100% median bodies and these were bigger than what was measured in untreated cells. This microtubular organelle undergoes assembly and disassembly during cell cycle. Therefore it can be regarded as a cell cycle marker since it is missing after cytokinesis in G1 cells and it is highly manifested in G2 cells. As mentioned earlier, based on flow cytometry analysis, mitotic cyclin B was present mainly in G2 trophozoites. We also found higher levels of this cyclin on western blots in aphidicolin treated cells in comparison with untreated cells.

Consequently, the blocking of DNA synthesis induced by aphidicolin also inhibited the nuclei division and cytokinesis. The DNA damage checkpoint, monitoring the unfinished S phase, is therefore active in *Giardia*. Decrease in the presence of phosphorylated H2A after release from aphidicolin, further suggests the reparation of DSB through DNA repair mechanism. However, further studies are needed to demonstrate whether components of DNA damage checkpoint and the signaling cascade are present and activated in *Giardia*. Our results showed that in lower concentration and shorter incubation period, the effect of aphidicolin was reversible. The cells started to divide quickly after the release from the block, as the mitotic index of these trophozoites increased.

4.2. Albendazole influence on cell cycle

A microtubular polymerization inhibitor albendazole prevented nuclei division in *Giardia* by blocking the mitotic spindle assembly. However, the cytokinesis continued in most cells resulting in aberrant trophozoites containing either none, one or two nuclei. We measured DNA content in albendazole treated trophozoites by flow cytometry. In shorter incubation intervals (3 hours), the distribution of a treated population on a DNA histogram resembled control cells without drug treatment. After 7 hours of incubation with the drug, an increased peak corresponding to G1/S phase and a new peak with DNA content higher than 8N started to appear. After 24 hours of incubation with albendazole three distinctive peaks were formed, one corresponded to G1/S, one approximately to G2 and one was between 8N and 16N DNA content. When comparing flow cytometry results with morphological profiles of albendazole treated population, three cell sub-populations could be defined: 1) cells with one G2 nucleus corresponding to G1 peak; 2) cells with either two G2 nuclei or with one G2 nucleus with re-replicated DNA, both corresponding to G2 peak and 3) cells with two nuclei that have proceeded another round of replication,

corresponding to peak between 8N and 16N. The second round of DNA replication in nuclei that did not undergo karyokinesis was further documented with BrdU incorporation and chromosomal spreads. After 12 hours of incubation with albendazole, BrdU was detected in nuclei of aberrant cells. Chromosomal spreads in a significant portion of cells after 24 hours albendazole treatment showed up to twenty condensed chromosomes per nucleus (average number per nucleus in typical mitotic *Giardia* cell is ten (Tůmová et al. 2007a). *Giardia* must override or lack some of the control mechanisms, because replication in eukaryotic cells is licensed to occur only once per cell cycle.

4.3. Nuclear division and DNA replication during encystation

The completion of *Giardia* life cycle is crucial for its successful transmission to a new host. The whole life cycle of *Giardia* can be performed *in vitro* and therefore, processes occurring during encystation and excystation can be studied. Our studies of encystation and excystation were focused on nuclei division, DNA replication and flagellar apparatus reorganization in both processes. To follow DNA replication during differentiation, we performed flow cytometry analysis of DNA content on PI stained cells, BrdU incorporation and the inhibitory effects of albendazole.

DNA content of *in vitro* gained cysts, measured by flow cytometry, confirmed that cysts had double the amount of DNA than trophozoites in G2 phase, corresponding to 16N as stated previously by Bernarder et al. (2001). To determine the timing of DNA replication during encystation, we performed BrdU incorporation in encysting cells. Positive staining for BrdU was occurred in 36% of cysts. In all BrdU positive cysts, all four nuclei showed BrdU signal. DNA replication therefore occurred in each nucleus and followed the nuclear division.

To check whether karyokinesis in encystation proceeds with the aid of the mitotic spindle, we used albendazole which is known to block mitotic spindle assembly in *Giardia* trophozoites (Nohýnková et al. 2000). Albendazole treatment prevented nuclei division, which indicated the presence of an undescribed mitotic spindle in nuclear division during encystation. Albendazole however did not inhibit the cyst wall formation. The produced cysts with two nuclei possessed a mature cyst wall that was resistant to water treatment. Interestingly in non-divided nuclei another round of DNA replication occurred. DNA content of cysts formed in the presence of

albendazole, measured by flow cytometry, was equal to untreated cysts (16N). These cysts were viable according to trypan blue dye exclusion.

4.4. Nuclear division and cell organization during differentiation

Two nucleated *Giardia* trophozoites differentiation into four nucleated cysts has been well known fact for many decades. However, so far nobody has elucidated and described in detail nuclei division during the encystation or in the cyst, partially because the encystation process is unsynchronized and the cells cannot be as easily oriented as the trophozoites. Albendazole induced inhibition of nuclear division in encysting cells indicated the presence of microtubular mitotic spindle; we therefore focused on visualizing the nuclei division.

The studies of ultrastructure in encysting cells on electron microscope revealed that division of both nuclei occurred in the early phase of encystation in a precyst. Precyst was a rounded non adherent stage. It contained abundant glycogen granules and enlarged endoplasmic reticulum corresponding to nascent ESVs transporting CWP to cyst wall, which was not yet formed; the precyst was still covered by plasmatic membrane. The nuclei divided by semi-open mitosis corresponding to nuclei division in *Giardia* trophozoites (Sagolla et al. 2006; Tůmová et al. 2007a). Two microtubular mitotic spindles were formed; each composed of extranuclear and intranuclear microtubules. The nuclear membrane did not break apart during mitosis and was perforated only for the single microtubules to enter the nucleus at the poles. A basal body was situated at the proximity to the pole, where the microtubules concentrated. But though we were not able to accurately determine the positioning of two mitotic spindles due to the rounded cell, it seems that contrary to the trophozoites the two mitotic spindles were not parallel to each other.

Nuclei after mitosis stayed in pairs with part of plasmatic membranes lying close together - resembling diplokaryons. The ventral disc was fragmented into several pieces composed of microtubules with adjacent microribbons. As revealed with immunofluorescence imaging, phosphorylation including that of aurora kinase, did not accompany the adhesive disc fragmentation during encystation in contrast to disassembly of the disc in trophozoite division. Nuclei during division had a characteristic irregular shape, from the nuclear envelope projected ER. This lobular shape also maintained nuclei in early cysts, but in mature cysts with assembled cyst wall, the nuclei were mostly rounded due to decrease of ER expansion as ESV

production was ceased in cysts. The nuclei within the pair were interconnected with cytoplasmic bridges. Each nuclear pair was interconnected with up to three small bridges that can vary in size. As only few precysts contained nuclear pairs without the interconnection, we propose that nuclei interconnected shortly after karyokinesis by a two-step fusion, with the outer nuclear envelopes fusing first as we documented. This was followed by fusion of inner nuclear membranes, linking the content of both nuclei. These inter-nuclear bridges were present either in precysts, or in cysts of any origin: in *in vitro* formed mature cysts that are resistant to water treatment or even in wild-type cysts gained from animals or human patients.

During the whole encystation process from trophozoite into mature cyst only one single flagellar apparatus comprising four pairs of flagella and eight adjacent basal bodies remained preserved. The karyokinesis in encystation occurred without duplication of flagellar axonemes and basal bodies, which is in contrast to karyokinesis in trophozoites, where these two processes are interconnected (Nohýnková et al. 2006). Confocal microscopy using an antibody against acetylated tubulin showed that the arrangement of axonemes in cyst was preserved as that in interphase trophozoite. The nuclear pairs were situated adjacent to the basal bodies tetrads at one cyst pole. This characteristic distribution of nuclear pairs was confirmed by counting the nuclear position in wild-type cysts stained with Gömöri trichrome, where 99% of the cysts had this nuclear arrangement. Ultrastructural analysis confirmed these observations, and further revealed that in each nuclear pair just one nucleus was positioned in close proximity of the basal bodies mediating the nuclear pair association to basal bodies.

4.5. Excystation

The excystation of *Giardia* was described in 1980s´ using scanning electron microscopy. However, up to date basic structural description of freshly excysted trophozoite was missing. Moreover it is not understood how the nuclear pairs and single flagellar apparatus are distributed in two subsequent cell divisions that follow the excystation. During the excystation the first six backward directed flagella, namely caudal, posteriolateral and ventral emerged from a single opening. The anteriolateral flagella together with nuclei were the last to emerge from the cyst. The freshly excysted trophozoite did not have typical shape of interphase trophozoite. Its cytoskeleton comprised the single flagellar apparatus and two duplicated

microtubular structures as shown with immunostaining. The single flagellar apparatus remained in the same position as in the interphase trophozoite or the cyst. Microtubular arcs corresponding to defragmented adhesive disc were positioned left or right next to backward directed flagella. Trophozoite had one more, so far undescribed, cytoskeletal microtubular structure stained with anti-acetylated tubulin; these were two microtubular bundles lying symmetrically along the caudal flagella. These likely corresponded to median bodies. Both of these microtubular structures (defragmented disc and microtubular bundles) disappeared during cell division. Two nuclear pairs lay on sides adjacent to two tetrads of basal bodies. We did not manage to follow in detail nuclei distribution and flagellar apparatus reorganization in cell division. However, we found that during cytokinesis the new adhesive discs in the forming daughter trophozoites were oriented with ventral/ventral axial symmetry. They were developing in the opposite directions to each other, winding counter clockwise corresponding to typical cytokinesis of trophozoite (Tůmová et al. 2007b). Distribution of parental flagella between daughter trophozoites in the cell division after excystation was similar to that of mitotic trophozoites (Nohýnková et al. 2006). The anteriolateral and posteriolateral flagellar pairs received progeny from the mother trophozoite, while ventral and posteriolateral pairs were assembled *de novo* and were observed as short axonemes on fluorescence microscopy or Giemsa staining in freshly divided cells.

4.6. Summary of results

Aphidicolin influence on cell cycle

- DNA replication inhibitor aphidicolin causes inhibition of DNA synthesis in *Giardia*: trophozoites are arrested at the G1/S border according to their DNA content. Consequent inhibition of entry into mitosis and cytokinesis indicates that *Giardia* has functioning DNA damage checkpoint.

- Presence of phosphorylated histone H2A, a marker of double strand breaks, suggests that aphidicolin may cause DNA damage in *Giardia*. Reversibility of this posttranslational modification after inhibitor removal indicates that *Giardia* possesses DNA damage reparatory mechanisms.

- Aphidicolin treatment causes dissociation of nuclear and cytoplasmic cycles. While DNA synthesis and entry to mitosis are stopped, the cytoplasmic cycle and its processes continue: increasing cell size, corresponding to higher protein content and higher percentage of cells containing median bodies.

Albendazole influence on cell cycle

- Albendazole inhibits nuclei division in *Giardia* trophozoites by blocking mitotic spindle assembly. Nuclei that did not undergo karyokinesis proceed to the second round of DNA replication. The control mechanism of allowing DNA synthesis only once per cell cycle seems to be missing or circumvented in *Giardia*.

Nuclear division and DNA replication during encystation

- Replication of DNA during *Giardia* encystation occurs after nuclei division. BrdU incorporation revealed that DNA replication occurred in all four nuclei within the cyst.

- Albendazole blocks nuclei division during *Giardia* encystation. However, it does not prevent cyst wall formation – these two processes are not interconnected. The nuclei within cysts formed in the presence of albendazole undergo another round of DNA replication without previous karyokinesis.

Nuclear division and cell organization during differentiation

- Nuclei division occurs in early phase of encystation before cyst wall formation in a precyst. Each nucleus is divided by its own mitotic spindle composed of extranuclear and intranuclear microtubules. Nuclei are divided by semi-open mitosis as in trophozoites.

- Nuclei after the karyokinesis stay in pairs on one cyst pole. Nuclei in pairs are interconnected with several inter-nuclear bridges, formed by fusion of both nuclear membranes. This nuclear organization in cyst persists in mature wild-type, as well in *in vitro*, formed cysts.

- Flagellar apparatus does not replicate during karyokinesis in encystation, which is in contrast to karyokinesis in trophozoites. The arrangement of flagellar apparatus remains same as in interphase trophozoite. In each nuclear pair only one nucleus is associated with one tetrad of basal bodies.

Excystation

- Excyzoite is rounded; four nuclei are still organized in two pairs. The cytoskeleton comprises a single flagellar apparatus, which remains in the same arrangement as in the trophozoite and the cyst. Next to backward directed axonemes are fragments of adhesive disc. Along caudal flagella lie two microtubular bundles which likely correspond to median bodies.

5. REFERENCES

Abel ES, Davids BJ, Robles LD, Loflin CE, Gillin FD, Chakrabarti R (2001). Possible roles of protein kinase A in cell motility and excystation of the early diverging eukaryote Giardia lamblia. J Biol Chem 276: 10320-10329

Adam RD, Nash TE, and Wellems TE (1988). The *Giardia lamblia* trophozoite contains sets of closely related chromosomes. Nucleic Acids Res 16: 4555-4567

Adam RD (2000). The Giardia lamblia genome. Int J Parasitol 30: 475-484

Adam RD (2001). Biology of Giardia lamblia. Clin Microbiol Rev 14: 447-475

Andrews PD, Knatko E, Moore WJ, Swedlow JR (2003). Mitotic mechanics: the auroras come into view. Curr Opin Cell Biol 15: 672–683

Banerjee S, Das S, Lohia A (2002). Eukaryotic chekcpointss are absent in the cell division cycle of Entamoeba histolytica. J Biosc 27: 567-572

Bazán-Tejeda ML, Argüello-García R, Bermúdez-Cruz RM, Robles-Flores M, Ortega-Pierres G (2007). Protein kinase C isoforms from Giardia duodenalis: identification and functional characterization of a beta-like molecule during encystment. Arch Microbiol 187: 55-66

Beech PL, Heimann K, and Melkonian M (1991). Development of the flagellar apparatus during the cell cycle in unicellular algae. Protoplasma 164: 23-37

Belhadri A (1995). Presence of centrin in the human parasite Giardia: a further indication of its ubiquity in eukaryotes Biochem Biophys Res Commun 214: 597-601

Benchimol M (2004a). Mitosis in *Giardia lamblia*: multiple modes of cytokinesis. Protist 155: 33-44

Benchimol M (2004b). Participation of the adhesive disc during karyokinesis in *Giardia lamblia*. Biol Cell 96: 291-301

Benchimol M (2004c). The release of secretory vesicle in encysting Giardia lamblia. FEMS Microbiol Lett 235: 81-87

Benchimol M (2004d). Giardia lamblia: behavior of the nuclear envelope. Parasitol Res 94: 254-264

Bernal RM, Tovar R, Santos JI, Muñoz ML (1998). Possible role of calmodulin in excystation of Giardia lamblia. Parasitol Res84: 687-693

Bernander R, Palm JE, Svard SG (2001). Genome ploidy in different stages of the Giardia lamblia life cycle. Cell Microbiology 3: 55-62

Bertram MA, Meyer EA, Lile JD, Morse SA (1983). A comparison of isozymes of five axenic Giardia isolates. J Parasitol 69: 793-801

de Bettignies G, Johnston LH (2003). The mitotic exit network. Curr Biol 13: R301

Bingham AK, Meyer EA (1979). Giardia excystation can be induced in vitro in acidic solutions. Nature 277: 301-302

Birkeland SR, Preheim SP, Davids BJ, Cipriano MJ, Palm D, Reiner DS, Svärd SG, Gillin FD, McArthur AG (2010). Transcriptome analyses of the Giardia lamblia life cycle. Mol Biochem Parasitol 174: 62-65

Birky CW Jr (2005). Sex: is giardia doing it in the dark? Curr Biol 15: R56-58

Boggild AK, Sundermann CA, Estridge BH (2002). Post-translational glutamylation and tyrosination in tubulin of tritrichomonads and the diplomonad Giardia intestinalis Parasitol Res 88: 58-62

Buchel LA, Gorenflot A, Chochillon C, Savel J, Gobert JG (1987). In vitro excystation of Giardia from humans: a scanning electron microscopy study J Parasitol 73: 487-493

Cacciò SM, Ryan U (2008). Molecular epidemiology of giardiasis. Mol Biochem Parasitol 160: 75-80

Campanati L, Bré MH, Levilliers N, de Souza W (1999). Expression of tubulin polyglycylation in Giardia lamblia. Biol Cell 91: 499-506

Carranza PG, Lujan HD (2009). New insights regarding the biology of Giardia lamblia. Microbes Infect 12: 71-80

Cavalier-Smith T (1989) Molecular phylogeny. Archaebacteria and Archezoa. Nature 339: l00-101

Clark CG, Diamond LS (2002). Methods for cultivation of luminal parasitic protists of clinical importance. Clin Microbiol Rev 15: 329-341

Coggins JR, Schaefer FW 3rd (1984). Giardia muris: scanning electron microscopy of in vitro excystation. Exp Parasitol 57: 62-67

Craig EA, Gambill BD, Nelson RJ (1993) Heat shock proteins: molecular chaperones of protein biogenesis. Microbiol Rev 57: 402-414

Červa L, and Nohýnková E (1992). A light microscopic study of the course of cellular division of *Giardia intestinalis* trophozoites grown *in vitro*. Folia Parasitol 39: 97-104

Davids BJ, Reiner DS, Birkeland SR, Preheim SP, Cipriano MJ, McArthur AG, Gillin FD (2006). A new family of giardial cysteine-rich non-VSP protein genes and a novel cyst protein. Mol Biochem Parasitol 152: 80-89

Davids BJ, Williams S, Lauwaet T, Palanca T, Gillin FD (2008). Giardia lamblia aurora kinase: a regulator of mitosis in a binucleate parasite Curr Opin Microbiol 10: 554-559

Dawson SC, Sagolla MS, Cande WZ (2007). The cenH3 histone variant defines centromeres in Giardia intestinalis. Chromosoma 116: 175-184

Drouin G, Moniz de Sá M, Zuker M (1995). The Giardia lamblia actin gene and the phylogeny of eukaryotes. J Mol Evol 41: 841-849

Elias EV, Quiroga R, Gottig N, Nakanishi H, Nash TE, Neiman A, Lujan HD (2008). Characterization of SNAREs determines the absence of a typical Golgi apparatus in the ancient eukaryote Giardia lamblia. J Biol Chem 283: 35996-36010

Ellis JG 4th, Davila M, Chakrabarti R (2003). Potential involvement of extracellular signal-regulated kinase 1 and 2 in encystation of a primitive eukaryote, Giardia lamblia. Stage-specific activation and intracellular localization. J Biol Chem 278: 1936-1945

Elmendorf HG, Dawson SC, McCaffery JM (2003). The cytoskeleton of Giardia lamblia. Int J Parasitol 33: 3-28

Erlandsen SL, and Rasch EM (1994). The DNA content of trophozoites and cysts of *Giardia lamblia* by microdensitometric quantitation of Feulgen staining and examination by laser scanning confocal microscopy. J Histochem Cytochem 42: 1413-1416

Erlandsen SL, Bemrick WJ, Schupp DE, Shields JM, Jarroll EL, Sauch JF, Pawley JB (1990). High-resolution immunogold localization of Giardia cyst wall antigens using field emission SEM with secondary and backscatter electron imaging. J Histochem Cytochem 38: 625-632

Fan JB, Korman SH, Cantor CR, and Smith CL (1991). *Giardia lamblia*: haploid genome size determined by pulse field gel electrophoresis is less than 12 Mb. Nucleic Acids Res 19: 1905-1908

Feely DE, Gardner MD, Hardin EL (1991). Excystation of Giardia muris induced by a phosphate-bicarbonate medium: localization of acid phosphatase. J Parasitol 77: 441-448

Fenn K, Matthews KR (2007). The cell biology of Trypanosoma brucei differentiation. Curr Opin Microbiol 10: 539-546

Forsythe GR, McCulloch R, Hammarton TC (2009). Hydroxyurea-induced synchronisation of bloodstream stage Trypanosoma brucei. Mol Biochem Parasitol 164: 131-136

Foster I (2008). Cancer: A cell cycle defect. Radiography 14: 144-149

Franzén O, Jerlström-Hultqvist J, Castro E, Sherwood E, Ankarklev J, Reiner DS, Palm D, Andersson JO, Andersson B, Svärd SG (2009). Draft genome sequencing of giardia intestinalis assemblage B isolate GS: is human giardiasis caused by two different species? PLoS Pathog 5: e1000560

Gaechter V, Schraner E, Wild P, Hehl AB (2008). The single dynamin family protein in the primitive protozoan Giardia lamblia is essential for stage conversion and endocytic transport. Traffic 9: 57-71

Gallego E, Alvarado M, Wasserman M (2007). Identification and expression of the protein ubiquitination system in Giardia intestinalis. Parasitol Res 101: 1-7

Ghosh S, Frisardi M, Rogers R, and Samuelson J (2001). How *Giardia* swim and divide. Infect Immun 69: 7866-7872

Gibson W, Peacock L, Ferris V, Williams K, Bailey M (2008). The use of yellow fluorescent hybrids to indicate mating in Trypanosoma brucei. Parasit Vectors 1: 4

Gillin FD, Boucher SE, Rossi SS, Reiner DS (1989). Giardia lamblia: the roles of bile, lactic acid, and pH in the completion of the life cycle in vitro. Exp Parasitol 69: 164-174

Gillin FD, Reiner DS, Boucher SE (1988). Small-intestinal factors promote encystation of Giardia lamblia in vitro. Infect Immun 56: 705-707

Gillin FD, Reiner DS, Gault MJ, Douglas H, Das S, Wunderlich A, Sauch JF (1987). Encystation and expression of cyst antigens by Giardia lamblia in vitro. Science 235: 1040-1043

Glover, TW (2006). Common fragile sites. Cancer Lett 232: 4-12

Gómez-Conde E, Mena-López R, Hernández-Jaúregui P, González-Camacho M, Arroyo R (2000). Trichomonas vaginalis: chromatin and mitotic spindle during mitosis. Exp Parasitol 96: 130-138

González J, Cornejo A, Santos MR, Cordero EM, Gutiérrez B, Porcile P, Mortara RA, Sagua H, Da Silveira JF, Araya JE (2003). A novel protein

phosphatase 2A (PP2A) is involved in the transformation of human protozoan parasite Trypanosoma cruzi. Biochem J 374: 647-656

Gottig N, Elías EV, Quiroga R, Nores MJ, Solari AJ, Touz MC, Luján HD (2006). Active and passive mechanisms drive secretory granule biogenesis during differentiation of the intestinal parasite Giardia lamblia. J Biol Chem 281: 18156-18166

Guo ZH, and Stiller JW (2004). Comparative genomics of cyclin-dependent kinases suggest co-evolution of the RNAP IIC-terminal domain and CTD-directed CDKs. BMC Genomics 5: 69

Gupta RS, Aitken K, Falah M, Singh B (1994) Cloning of Giardia lamblia heat shock protein HSP70 homologs: implications regarding origin of eukaryotic cells and of endoplasmic reticulum. Proc Natl Acad Sci U S A 91: 2895-2899

Hammarton TC, Mottram JC, and Doerig CD (2003). The cell cycle of parasitic protozoa: potential for chemotherapeutic exploitation. Prog Cell Cycle Res 5: 91-101

Hammarton TC (2007). Cell cycle regulation in Trypanosoma brucei. Mol Biochem Parasitol 153: 1-8

Harbury PA (1998). Springs and zippers: coiled coils in SNARE-mediated membrane fusion. Structure 6: 1487-1491

Hartwell L, and Weinert T (1989). Checkpoints: controls that ensure the order of cell cycle events. Science 246: 629–634

Hartwell LH, Culotti J, Pringle JR, Reid BJ (1974). Genetic control of the cell division cycle in yeast. Science183: 46-51

Hartwell LH (1974). Saccharomyces cerevisiae cell cycle. Bacteriol Rev 38: 164-198
Hasbold J, Hodgkin PD (2000). Flow cytometric cell division tracking using nuclei. Cytometry 40: 230-237

Hehl AB, Marti M, Köhler P (2000). Stage-specific expression and targeting of cyst wall protein-green fluorescent protein chimeras in Giardia. Mol Biol Cell 11: 1789-1800

Hetsko ML, McCaffery JM, Svärd SG, Meng TC, Que X, Gillin FD (1998). Cellular and transcriptional changes during excystation of Giardia lamblia in vitro. Exp Parasitol 88:172-183

Holberton DV (1981). Arrangement of subunits in microribbons from Giardia. J Cell Sci 47: 167-185

Hoyne GF, Boreham PF, Parsons PG, Ward C, Biggs B (1989). The effect of drugs on the cell cycle of Giardia intestinalis. Parasitology 3: 333-339

Huberman JA (1981). New views of the biochemistry of eucaryotic DNA replication revealed by aphidicolin, an unusual inhibitor of DNA polymerase alpha. Cell 23: 647-648

Hulleman E, Boonstra J (2001). Regulation of G1 phase progression by growth factors and the extracellular matrix. Cell Mol Life Sci 58: 80-93

Chatterjee A, Ghosh SK, Jang K, Bullitt E, Moore L, Robbins PW, Samuelson J (2009). Evidence for a "wattle and daub" model of the cyst wall of entamoeba. PLoS Pathog 5: e1000498

Chávez-Munguía B, Cedillo-Rivera R, Martínez-Palomo A (2004). The ultrastructure of the cyst wall of Giardia lamblia. J Eukaryot Microbiol 51: 220-226

Chávez-Munguía B, Omaña-Molina M, González-Lázaro M, González-Robles A, Bonilla P, Martínez-Palomo A (2005) Ultrastructural study of encystation and excystation in Acanthamoeba castellanii. J Eukaryot Microbiol 52: 153-158

Chávez-Munguía B, Tsutsumi V, Martínez-Palomo A (2006). Entamoeba histolytica: ultrastructure of the chromosomes and the mitotic spindle. Exp Parasitol 114: 235-239

Jiménez-García LF, Zavala G, Chávez-Munguía B, Ramos-Godínez Mdel P, López-Velázquez G, Segura-Valdez Mde L, Montañez C, Hehl AB, Argüello-García R, Ortega-Pierres G (2008). Identification of nucleoli in the early branching protist Giardia duodenalis. Int J Parasitol 38: 1297-1304

Kabnick KS, Peattie DA (1990). In situ analyses reveal that the two nuclei of Giardia lamblia are equivalent. J Cell Sci 95: 353-360

Karapetyan A (1962). In vitro cultivation of Giardia duodenalis. J Parasitol 48: 337-340

Karr CD, Jarroll EL (2004). Cyst wall synthese: N-acetygalactosaminyltransferase activity is induced to form the novel N-acetylgalactosamine polysacharide in the *Giardia* cyst wall. Microbiology 150: 1237-1243

Keeling PJ (1998). A kingdom´s progress: Archezoa and the origin of eukaryotes. BioEssays 20: 87-95

Kim KT, Mok MT, Edwards MR (2005). Protein kinase B from Giardia intestinalis. Biochem Biophys Res Commun 334: 333-341

Knight J (2004). *Giardia*: Not so special, after all? Nature 429: 236-237

Knodler LA, Noiva R, Mehta K, McCaffery JM, Aley SB, Svärd SG, Nystul TG, Reiner DS, Silberman JD, Gillin FD (1999). Novel protein-disulfide isomerases from the early-diverging protist Giardia lamblia. J Biol Chem 274: 29805-29811

Koch GL (1990). The endoplasmic reticulum and calcium storage. Bioessays 12: 527-531

Konrad C, Spycher C, Hehl AB (2010). Selective condensation drives partitioning and sequential secretion of cyst wall proteins in differentiating Giardia lamblia. PLoS Pathog 6(4): e1000835

Korman SH, Le Blancq SM, Deckelbaum RJ, Van der Ploeg LH (1992). Investigation of human giardiasis by, karyotype analysis. J Clin Invest 89: 1725-1733

Kues WA, Anger M, Carnwath JW, Paul D, Motlik J, Niemann H (2000). Cell cycle synchronization of porcine fetal fibroblasts: effects of serum deprivation and reversible cell cycle inhibitors. Biol Reprod 62: 412-419

Kulda J, and Nohýnková E (1995). Flagellates of the human intestine and of intestines of other species. In: Kreier JP (Ed.), Parasitic Protozoa, vol. II. Academic Press, New York, pp: 225–422

Kumar P, and Wang CC (2006). Dissociation of cytokinesis initiation from mitotic control in an eukaryote. Eukaryot Cell 5: 92-102

Lanfredi-Rangel A, Attias M, de Carvalho TM, Kattenbach WM, De Souza W (1998). The peripheral vesicles of trophozoites of the primitive protozoan Giardia lamblia may correspond to early and late endosomes and to lysosomes. J Struct Biol 123: 225-235

Lanfredi-Rangel A, Attias M, Reiner DS, Gillin FD, De Souza W (2003). Fine structure of the biogenesis of Giardia lamblia encystation secretory vesicles. J Struct Biol 143: 153-163

Lasek-Nesselquist E, Welch DM, Sogin ML (2010). The identification of a new Giardia duodenalis assemblage in marine vertebrates and a preliminary analysis of G. duodenalis population biology in marine systems. Int J Parasitol 40: 1063-1074

Lauwaet T, Davids BJ, Torres-Escobar A, Birkeland SR, Cipriano MJ, Preheim SP, Palm D, Svärd SG, McArthur AG, Gillin FD (2007). Protein phosphatase 2A plays a crucial role in Giardia lamblia differentiation. Mol Biochem Parasitol 152: 80-89

LeBlancq SM, and Adam RD (1998). Structural basis for karyotype heterogeneity in *Giardia lamblia*. Mol Biochem Parasitol 97: 199-208

Lee J (2010). De novo formation of basal bodies during cellular differentiation of Naegleria gruberi: progress and hypotheses. Semin Cell Dev Biol 21: 156-162

Liu Y, Richards TA, Aves SJ (2009). Ancient diversification of eukaryotic MCM DNA replication proteins. BMC Evol Biol 17: 9-60

Lohia A, Mukherjee C, Majumder S, Dastidar PG (2007) Genome re-duplication and irregular segregation occur during the cell cycle of Entamoeba histolytica. Biosci Rep 27: 373-384

Luján HD, Marotta A, Mowatt MR, Sciaky N, Lippincott-Schwartz J, Nash TE (1995). Developmental induction of Golgi structure and function in the primitive eukaryote Giardia lamblia. J Biol Chem 270: 612-618

Luján HD, Mowatt MR, Byrd LG, Nash TE (1996). Cholesterol starvation induces differentiation of the intestinal parasite Giardia lamblia. Proc Natl Acad Sci U-S-A 93: 7628-7633

Luján HD, Mowatt MR, Conrad JT, Bowers B, Nash TE (1995). Identification of a novel Giardia lamblia cyst wall protein with leucine-rich repeats. Implications for secretory granule formation and protein assembly into the cyst wall. J Biol Chem 270: 29307-29313

Luján HD, Mowatt MR, Nash TE (1997). Mechanisms of Giardia lamblia differentiation into cysts. Microbiol Mol Biol Rev 61: 294-304

Manning G, Reiner DS, Lauwaet T, Dacre M, Smith A, Zhai Y, Svard S, Gillin FD (2011). The minimal kinome of Giardia lamblia illuminates early kinase evolution and unique parasite biology. Genome Biol 12: R66

Marshall J, Holberton DV (1993). Sequence and structure of a new coiled coil protein from a microtubule bundle in Giardia. J Mol Biol 231: 521-530

Marti M, Li Y, Schraner EM, Wild P, Köhler P, Hehl AB (2003a). The secretory apparatus of an ancient eukaryote: protein sorting to separate export pathways occurs before formation of transient Golgi-like compartments. Mol Biol Cell 14: 1433-1447

Marti M, Regös A, Li Y, Schraner EM, Wild P, Müller N, Knopf LG, Hehl AB (2003b) An ancestral secretory apparatus in the protozoan parasite Giardia intestinalis. J Biol Chem 278: 24837-24848

Matthews KR (1999). Developments in the differentiation of Trypanosoma brucei. Parasitol Today15: 76-80

Mayrhofer G, Andrews RH, Ey PL, Chilton NB (1995). Division of Giardia isolates from humans into two genetically distinct assemblages by electrophoretic analysis of enzymes encoded at 27 loci and comparison with Giardia muris. Parasitology 111: 11-17

McArthur AG, Morrison HG, Nixon JEJ, Passamaneck NQE, Kim U, Hinkle G, Crocker MK, Holder ME, Farr R, and Reich CI, et al. (2000). The *Giardia* genome project database. FEMS Microbiol Lett 189: 271-273

McCaffery JM, Faubert GM, Gillin FD (1994a). Giardia lamblia: traffic of a trophozoite variant surface protein and a major cyst wall epitope during growth, encystation, and antigenic switching. Exp Parasitol 79: 236-249

McCaffery JM, Gillin FD (1994b). Giardia lamblia: ultrastructural basis of protein transport during growth and encystation. Exp Parasitol 79: 220-235

MacRae TH (1997). Tubulin post-translational modifications-enzymes and their mechanisms of action. Eur J Biochem 244: 265-278

Melo SP, Gómez V, Castellanos IC, Alvarado ME, Hernández PC, Gallego A, Wasserman M (2008). Transcription of meiotic-like-pathway genes in Giardia intestinalis. Mem Inst Oswaldo Cruz 103: 347-350

Meng TC, Aley SB, Svard SG, Smith MW, Huang B, Kim J, Gillin FD (1996). Immunolocalization and sequence of caltractin/centrin from the early branching eukaryote Giardia lamblia. Mol Biochem Parasitol 81: 101-110

Mitchison JM (1971). The Biology of The Cell Cycle (Cambridge: Cambridge University Press)

Monis PT, Caccio SM, Thompson RC (2009). Variation in Giardia: towards a taxonomic revision of the genus. Trends Parasitol 25: 93-100

Morgan DO (2007). The Cell Cycle. Principles of control (New Science Press Ltd)

Morrison HG, McArthur AG, Gillin FD, Aley SB, Adam RD, Olsen GJ, Best AA, Cande WZ, Chen F, Cipriano MJ, Davids BJ, Dawson SC, Elmendorf HG, Hehl AB, Holder ME, Huse SM, Kim UU, Lasek-Nesselquist E, Manning G, Nigam A, Nixon JE, Palm D, Passamaneck NE, Prabhu A, Reich CI, Reiner DS, Samuelson J, Svard SG, Sogin ML (2007). Genomic minimalism in the early diverging intestinal parasite Giardia lamblia. Science 317: 1921-1926

Mowatt MR, Luján HD, Cotten DB, Bowers B, Yee J, Nash TE, Stibbs HH (1995). Developmentally regulated expression of a Giardia lamblia cyst wall protein gene. Mol Microbiol 15: 955-963

Mukherjee C, Clark CG, Lohia A (2008). Entamoeba shows reversible variation in ploidy under different growth conditions and between life cycle phases. PLoS Negl Trop Dis 2: e281

Myster DL, Duronio RJ (2000). To differentiate or not to differentiate? Curr Biol 10: R302-304

Nash TE, McCutchan T, Keister D, Dame JB, Conrad JD, Gillin FD (1985). Restriction-endonuclease analysis of DNA from 15 Giardia isolates obtained from humans and animals. J Infect Dis 152: 64-73

Nash TE (2002). Surface antigenic variation in Giardia lamblia. Mol Microbiol 45: 585-590

Nohýnková E, Dráber P, Reischig J, Kulda J (2000). Localization of gamma-tubulin in interphase and mitotic cells of a unicellular eukaryote, *Giardia intestinalis*. Europ J Cell Biol 79: 438-445

Nohýnková E, Tumová P, Kulda J (2006). Cell division of Giardia intestinalis: flagellar developmental cycle involves transformation and exchange of flagella between mastigonts of a diplomonad cell. Eukaryot Cell 5: 753-761

Nurse P (2002). Cyclin dependent kinases and cell cycle control (Nobel lecture). Chem Biolchem 3: 596-603

O´Connor PM and Jacman J (1996). Cell cycle-materials and methods (ed. M., Pagano). Springer-Verlag Berlin Heidelberg.

Pan YJ, Cho CC, Kao YY, Sun CH (2009). A novel WRKY-like protein involved in transcriptional activation of cyst wall protein genes in Giardia lamblia. J Biol Chem 284: 17975-17988

Paredez AR, Assaf ZJ, Sept D, Timofejeva L, Dawson SC, Wang CJ, Cande WZ (2011). An actin cytoskeleton with evolutionarily conserved functions in the absence of canonical actin-binding proteins. Proc Natl Acad Sci U S A 108: 6151-6156

Parfrey LW, Lahr DJ, Katz LA (2008). The dynamic nature of eukaryotic genomes. Mol Biol Evol 25: 787-794

Peter M, Herskowitz I (1994). Joining the complex: cyclin-dependent kinase inhibitory proteins and the cell cycle. Cell 79: 181-184

Ploubidou A, Robinson DR, Docherty RC, Ogbadoyi EO, and Gull K (1999). Evidence for novel cell cycle checkpoints in trypanosomes: kinetoplast segregation and cytokinesis in the absence of mitosis. J Cell Sci 112: 4641-4650

Poxleitner MK, Carpenter ML, Mancuso JJ, Wang CJ, Dawson SC, Cande WZ (2008b). Evidence for karyogamy and exchange of genetic material in the binucleate intestinal parasite *Giardia intestinalis*. Science 319:1530-1533

Poxleitner MK, Dawson SC, Cande WZ (2008a). Cell cycle synchrony in Giardia intestinalis cultures achieved by using nocodazole and aphidicolin. Eukaryot Cell 7: 569-574

Praefcke GJ, McMahon HT (2004) The dynamin superfamily: universal membrane tubulation and fission molecules? Nat Rev Mol Cell Biol 5: 133-147

Prucca CG, Lujan HD (2009). Antigenic variation in Giardia lamblia. Cell Microbiol 11: 1706-1715

Prucca CG, Slavin I, Quiroga R, Elías EV, Rivero FD, Saura A, Carranza PG, Luján HD (2008). Antigenic variation in Giardia lamblia is regulated by RNA interference. Nature 456: 750-754

Raikov IB (1994). The diversity of forms of mitosis in Protozoa: a comparative review. Eur J Protistol 30: 253-269

Ramesh MA, Malik SB, and Logsdon JM (2005). A phylogenetic inventory of meiotic genes: evidence for sex in *Giardia* and an early eukaryotic origin of meiosis. Curr Biol 15: 185-191

Reiner DS, McCaffery M, Gillin FD (1990). Sorting of cyst wall proteins to a regulated secretory pathway during differentiation of the primitive eukaryote, Giardia lamblia. Eur J Cell Biol 53: 142-153

Reiner DS, Hetsko ML, Meszaros JG, Sun CH, Morrison HG, Brunton LL, Gillin FD (2003). Calcium signaling in excystation of the early diverging eukaryote, Giardia lamblia. J Biol Chem 278: 2533-2540

Reiner DS, McCaffery JM, Gillin FD (2001). Reversible interruption of Giardia lamblia cyst wall protein transport in a novel regulated secretory pathway. Cell Microbiol 3: 459-472

Reiner DS, Ankarklev J, Troell K, Palm D, Bernander R, Gillin FD, Andersson JO, Svärd SG (2008). Synchronisation of Giardia lamblia: identification of cell cycle stage-specific genes and a differentiation restriction point. Int J Parasitol 38: 935-944

Ribeiro KC, Mariante RM, Coutinho LL, Benchimol M (2002). Nucleus behavior during the closed mitosis of Tritrichomonas foetus. Biol Cell 94: 289-301

Riley DE, Krieger JN, Miner D, Rabinovitch PS (1994). Trichomonas vaginalis: dominant G2 period and G2 phase arrest in a representative of an early branching eukaryotic lineage. J Eukaryot Microbiol 41: 408-414

Roger AJ, Svärd SG, Tovar J, Clark CG, Smith MW, Gillin FD, Sogin ML (1998). A mitochondrial-like chaperonin 60 gene in Giardia lamblia: evidence that diplomonads once harbored an endosymbiont related to the progenitor of mitochondria. Proc Natl Acad Sci U S A 95: 229-234

Roxström-Lindquist K, Jerlström-Hultqvist J, Jørgensen A, Troell K, Svärd SG, Andersson JO (2010). Large genomic differences between the

morphologically indistinguishable diplomonads Spironucleus barkhanus and Spironucleus salmonicida. BMC Genomics 21: 11:258

Sagolla MS, Dawson SC, Mancuso JJ, Cande WZ (2006). Three-dimensional analysis of mitosis and cytokinesis in the binucleate parasite Giardia intestinalis. J Cell Sci 19: 4889-4900

Salisbury JL (1995). Centrin, centrosomes, and mitotic spindle poles. Curr Opin Cell Biol 7: 39-45

Samuels AL, Meehl J, Lipe M, and Staehelin LA (1998). Optimizing conditions for tobacco BY-2 cell cycle synchronization Protoplasma 202: 232-236

Sandhu H, Mahajan RC, Ganguly NK (2004). Flowcytometric assessment of the effect of drugs on Giardia lamblia trophozoites in vitro. Mol Cell Biochem 265: 151-160

Sánchez I, Dynlacht BD (2005). New insights into cyclins, CDKs, and cell cycle control. Semin Cell Dev Biol 16: 311-321

Saraiya AA, Wang CC (2008). SnoRNA, a novel precursor of microRNA in Giardia lamblia. PLoS Pathog 4: e1000224

Savioli L, Smith H, Thompson A (2006). Giardia and Cryptosporidium join the 'Neglected Diseases Initiative'. Trends Parasitol 22: 203-208

Schupp DG, Januschka MM, Sherlock LA, Stibbs HH, Meyer EA, Bemrick WJ, Erlandsen SL (1988). Production of viable Giardia cysts in vitro: determination by fluorogenic dye staining, excystation, and animal infectivity in the mouse and Mongolian gerbil. Gastroenterology 95: 1-10

Shirk K, Jin H, Giddings TH Jr, Winey M, Yu HG (2011). The Aurora kinase Ipl1 is necessary for spindle pole body cohesion during budding yeast meiosis. J Cell Sci 124: 2891-2896

Siegel TN, Hekstra DR, Cross GA (2008). Analysis of the Trypanosoma brucei cell cycle by quantitative DAPI imaging. Mol Biochem Parasitol 160: 171-174

Singh N, Bhattacharya S, Paul J (2011). Entamoeba invadens: dynamics of DNA synthesis during differentiation from trophozoite to cyst. Exp Parasitol 127: 329-333

Slavin I, Saura A, Carranza PG (2002). Dephosphorylation of cyst wall proteins by a secreted lysosomal acid phosphatase is essential forexcystation of *Giardia lamblia*. Mol Biochem Parasitol 122: 95–98

Smith MW, Aley SB, Sogin M, Gillin FD, and Evans GA (1998). Sequence survey of the *Giardia lamblia* genome. Mol Biochem Parasitol 15: 267-280

Solari AJ, Rahn M, Saura A, and Lujan HD (2003). A unique mechanism of nuclear division in *Giardia lamblia* involves components of the ventral disc and the nuclear envelope. Biocell 27: 329-346

Soloviev MM (1963). Studies on division of *Lamblia duodenalis* in cultures. Med Parazitol Parazit Bolezni 32: 96-101

Soltys BJ, Falah M, Gupta RS (1996). Identification of endoplasmic reticulum in the primitive eukaryote Giardia lamblia using cryoelectron microscopy and antibody to Bip. J Cell Sci 109: 1909-1917

Sonda S, Morf L, Bottova I, Baetschmann H, Rehrauer H, Caflisch A, Hakimi MA, Hehl AB (2010). Epigenetic mechanisms regulate stage differentiation in the minimized protozoan Giardia lamblia. Mol Microbiol 76: 48-67

Spadari S, Sala F, and Pedrali-Noy G (1982). Aphidicolin: a specific inhibitor of nuclear DNA replication in eukaryotes. Trends Biochem Sci 7: 29-30

Stefanic S, Palm D, Svärd SG, Hehl AB (2006). Organelle proteomics reveals cargo maturation mechanisms associated with Golgi-like encystation vesicles in the early-diverged protozoan Giardia lamblia. J Biol Chem 281: 7595-7604

Stefanic S, Morf L, Kulangara C, Regös A, Sonda S, Schraner E, Spycher C, Wild P, Hehl AB (2009). Neogenesis and maturation of transient Golgi-like cisternae in a simple eukaryote. J Cell Sci 122: 2846-2856

Svärd SG, Rafferty C, McCaffery JM, Smith MW, Reiner DS, Gillin FD (1999). A signal recognition particle receptor gene from the early-diverging eukaryote, Giardia lamblia. Mol Biochem Parasitol 98: 253-264

Sun CH, Palm D, McArthur AG, Svärd SG, Gillin FD (2002). A novel Myb-related protein involved in transcriptional activation of encystation genes in Giardia lamblia. Mol Microbiol 46: 971-984

Sun CH, McCaffery JM, Reiner DS, Gillin FD (2003). Mining the Giardia lamblia genome for new cyst wall proteins. J Biol Chem 24: 21701-21708

Sun CH, Su LH, Gillin FD (2006). Novel plant-GARP-like transcription factors in Giardia lamblia. Mol Biochem Parasitol 146: 45-57

Tachezy J. Dolezal P. in Origin of Mitochondria and Hydrogenosomes, eds Martin W, Muller M (Springer Berlin/Heidelberg), pp 105-133

Thompson RCA (2004). The zoonotic significance and molecular epidemiology of *Giardia* and giardiasis. Vet Parasitol 126: 15-35

Touz MC, Rópolo AS, Rivero MR, Vranych CV, Conrad JT, Svard SG, Nash TE (2008). Arginine deiminase has multiple regulatory roles in the biology of Giardia lamblia. J Cell Sci 121: 2930-2938

Tovar J, Leon-Avila G, Sanchez LB, Šuťák R, Tachezy J, Giezen N, Hernandez M, Müller M, and Lucocq JM (2003). Mitochondrial remnant organelles of *Giardia intestinalis* function in iron sulphur protein maturation. Nature 426: 172-174

Tůmová P, Hofštetrová K, Nohýnková E, Hovorka O, Král J (2007a). Cytogenetic evidence for heterogeneity of two *Giardia* nuclei. Chromosoma 116: 65-78

Tůmová P, Kulda J, Nohýnková E (2007b). Cell division of *Giardia intestinalis*: assembly and disassembly of the adhesive disc, and the cytokinesis. Cell Motility Cytoskelet 64: 288-298

Upcroft JA, Abedinia M, Upcroft P (2003). Rearranged subtelomeric rRNA genes in Giardia duodenalis. Eukaryot Cell 4: 484-486

Upcroft P, and Upcroft JA (1999). Organization and structure of the *Giardia* genome. Protist 150: 17-23

Uzbekov R, Chartrain I, Philippe M and Arlot-Bonnemains Y (1998). Cell Cycle Analysis and Synchronization of the *Xenopus* Cell Line XL2. Exp Cell Res 242: 60-68

Van Hooser AA, Ouspenski II, Gregson HC, Starr DA, Yen TJ, Goldberg ML, Yokomori K, Earnshaw WC, Sullivan KF, Brinkley BR (2001). Specification of kinetochore-forming chromatin by the histone H3 variant CENP-A. Chromosome Res 10: 267-277

Villeneuve AM, Hillers KJ (2001). Whence meiosis? Cell 106: 647-650

Wang CH, Su LH, Sun CH (2007). A novel ARID/Bright-like protein involved in transcriptional activation of cyst wall protein 1 gene in Giardia lamblia. J Biol Chem 282: 8905-8914

Ward W, Alvarado L, Rawlings ND, Engel JC, Franklin C, McKerrow JH (1997). A primitive enzyme for a primitive cell: the protease required for excystation of Giardia. Cell 89: 437-444

Weber K, Schneider A, Müller N, Plessmann U (1996). Polyglycylation of tubulin in the diplomonad Giardia lamblia, one of the oldest eukaryotes. FEBS Lett 393: 27-30

Weber K, Schneider A, Westermann S, Müller N, Plessmann U (1997). Posttranslational modifications of alpha- and beta-tubulin in Giardia lamblia, an ancient eukaryote. FEBS Lett 419: 87-91

Wiesehahn GP, Jarroll EL, Lindmark DG, Meyer EA, Hallick LM (1984). Giardia lamblia: autoradiographic analysis of nuclear replication. Exp Parasitol 58: 94-100

Wu G, McArthur AG, Fiser A, Šali A, Sogin ML, and Müller M (2000). Core Histones of the Amitochondriate Protist, Giardia lamblia. Mol Biol Evol 17: 1156-1163

Yang YM, and Adam RD (1994). Allele-specific expression of a variant-specific surface protein (VSP) of *Giardia lamblia*. Nucleic Acids Res 22: 2102-2108

Yu LZ, Birky CW, and Adam RD (2002). The two nuclei of *Giardia* each have complete copies of the genome and are partitioned equationally at cytokinesis. Eukaryot Cell 1: 191-199

Zhou BB, Elledge SJ (2000). The DNA damage response: putting checkpoints in perspective. Nature 408: 433–439

Zubáčová Z, Cimbůrek Z, Tachezy J (2008). Comparative analysis of trichomonad genome sizes and karyotypes. Mol Biochem Parasitol 161: 49-54

6. APPENDIX: ORIGINAL PAPERS

RESEARCH ARTICLE

Cytogenetic evidence for diversity of two nuclei within a single diplomonad cell of *Giardia*

Pavla Tůmová · Klára Hofštetrová · Eva Nohýnková ·
Ondřej Hovorka · Jiří Král

Abstract *Giardia intestinalis* is an ancient protist that causes the most commonly reported human diarrheal disease of parasitic origin worldwide. An intriguing feature of the *Giardia* cell is the presence of two morphologically similar nuclei, generally considered equivalent, in spite of the fact that their karyotypes are unknown. We found that within a single cell, the two nuclei differ both in the number and the size of chromosomes and that representatives of two major genetic groups of *G. intestinalis* possess different karyotypes. Odd chromosome numbers indicate aneuploidy of *Giardia* nuclei, and their stable occurrence is suggestive of a long-term asexuality. A semi-open type of *Giardia* mitosis excludes a chromosome interfusion between the nuclei. Differences in karyotype and DNA content, and cell cycle-dependent asynchrony are indicative of diversity of the two *Giardia* nuclei.

Communicated by E.A. Nigg

P. Tůmová (✉) · K. Hofštetrová · E. Nohýnková
Department of Tropical Medicine,
First Faculty of Medicine,
Charles University in Prague,
Studničkova 7,
Prague 2 12800, Czech Republic
e-mail: ptumo@lf1.cuni.cz

O. Hovorka
Institute of Microbiology,
Academy of Sciences,
Prague, Czech Republic

J. Král
Department of Genetics and Microbiology,
Charles University in Prague,
Prague, Czech Republic

Introduction

Giardia intestinalis is a unicellular parasitic eukaryote that causes giardiasis—the most commonly reported human intestinal infection of protozoan origin. *Giardia* is considered to be asexual (Adam 2001). It has two life cycle stages: a flagellated trophozoite that inhabits the small intestine and causes the disease, and a resistant cyst that is discharged with feces and serves to transmit infection. Besides its medical importance, *Giardia* is an organism of exciting evolutionary significance. It has been generally assumed to represent an ancient eukaryote based on sequencing data (e.g., 16S rRNA, elongation factor E1α, HSP70, and cathepsin B), ultrastructure (the lack of mitochondria, microbodies, and an absence of discernible nucleolus), and prokaryote-like features found in *Giardia*-metabolism (Gillin et al. 1996; Lloyd and Harris 2002). However, mitochondrion-derived genes are present in the nuclear genome of *Giardia*, suggesting its evolution from a mitochondria-bearing ancestor (Roger et al. 1998), and subcellular compartments that might be a remnant of mitochondria have been reported recently (Tovar et al. 2003). Nevertheless, *Giardia* is still currently placed among the most basal eukaryotes (Adam 2001; Ali and Hill 2003).

Giardia belongs to diplomonads, a group of protists both parasitic and free-living, with axial cell symmetry (Brugerolle 1991). A peculiar feature of a diplomonad trophozoite is the presence of two symmetrically arranged nuclei of equal size and appearance, each being associated with four flagella and microtubular fibers (i.e., karyomastigont). In a *Giardia* trophozoite, each of the two nuclei has at least one complete copy of the genome (Yu et al. 2002), similar quantities of DNA (Kabnick and Peattie 1990; Bernander et al. 2001)—which replicate simultaneously at least 70% of the time (Wiesehahn et al. 1984), and approxi-

mately equal numbers of rDNA genes (Kabnick and Peattie 1990). The nuclei are transcriptionally active (Kabnick and Peattie 1990), and proteins appear to be targeted equally into both of them (Elmendorf et al. 2000). However, questions concerning the homology of the two nuclei, their origin, the evolutionary significance, and the function of this diplokaryosity are still far from being understood. The simplest hypothesis, based on cladistic analysis of morphological characteristics, proposes that diplokaryotic diplomonads arose by a duplication of karyomastigont of monokaryotic enteromonads (Siddall et al. 1992). Molecular phylogenetics supports also an opposite scenario: that a common ancestor of diplomonads and enteromonads had a double karyomastigont (Kolisko et al. 2005). Cavalier-Smith (1995) proposed that the diplokaryotic stage might have played a key role in the evolution of meiosis.

G. intestinalis possesses a small genome. The generally accepted size of the haploid genome is about 12 Mb, estimated from sum of sizes of chromosomes separated by pulsed field gel electrophoresis (PFGE) (Fan et al. 1991) and supported from data obtained by genome sequencing (www.mbl.edu/Giardia; Adam 2000). Knowledge on *Giardia* karyotype comes almost exclusively from electrophoretic karyotyping using PFGE. The results of PFGE and sequence analysis indicate that chromosomes of *Giardia* are dynamic; frequent rearrangements and recombinations have been reported from telomeric arrays of rDNA genes and from subtelomeric repeats. Inner parts of chromosomes seem to be more stable (Adam 1992; Upcroft and Upcroft 1999; Upcroft et al. 2005). A common consensus is that there are five chromosome linkage groups defined by using chromosome-specific probes (Adam et al. 1988; Le Blancq and Adam 1998), that homologous chromosomes are present in several copies, and that their size variability is a hallmark of heterogeneity of molecular karyotypes of *Giardia* isolates (Le Blancq and Adam 1998). The presence of up to four size variants of chromosome 1 (Adam 1992; Adam et al. 1988; Le Blancq and Adam 1998) led to the suggestion that *Giardia* trophozoite can be tetraploid (Hou et al. 1995). A similar conclusion was made based on flow cytometry measurement of DNA content of nonsynchronized *Giardia* cells (Bernander et al. 2001). By using fluorescence in situ hybridization with low copy number gene probes, the presence of at least one chromosome from each of the five linkage groups has been demonstrated per interphase nucleus (Yu et al. 2002). However, the actual distribution of chromosomes between the nuclei (i.e., the karyotype and ploidy of each nucleus within a single cell) is virtually unknown, although *Giardia* chromosomes do condense. Earlier microscopists mentioned eight chromatin granules in each nucleus (Rodenwaldt 1912; Prowazek and Werner 1914) fusing into four prophase chromosomes (Kofoid and Christiansen 1915; Filice 1952). More recent

observations describe four to nine chromosome-like bodies per dividing nucleus (Kabnick and Peattie 1990; Erlandsen and Rasch 1994; Červa and Nohýnková 1992). The scatter in the results has been probably caused by resolution limits of light microscopy to distinguish small-sized chromosomes packed within dividing nuclei of fixed and stained trophozoites. Moreover, due to the complexity of the *Giardia* cytoskeleton (Brugerolle 1975), its rearrangement during division (Nohýnková et al. 2006), the small size of the two parallel-dividing nuclei, and the poor recognition of *Giardia* cell symmetry, even the process of cell division, is still not fully understood (Adam 2001; Elmendorf et al. 2003).

In this paper, we analyze karyotypes of *Giardia* nuclei and chromosome behavior during cell division by using conventional cytogenetic techniques, which have never been employed to study *Giardia*. For this purpose, we adapted a spreading technique, which includes hypotonic treatment, and employed a technique of enrichment of cultured *Giardia* populations with mitotic cells developed in our laboratory. The results presented in this study show that the two *Giardia* nuclei are not equivalent because they do not possess the same chromosome number and, consequently, the same karyotype.

Materials and methods

Cell cultures and their enrichment with mitotic cells

Four isolates of *G. intestinalis* belonging to two different genetic groups (assemblages; for a review see Thompson and Monis 2004) were examined: two human isolates (HP-1 and WB-1B) of the assemblage A, and one human (HH) and one chinchilla isolate (CH-105) of the assemblage B (Šedinová et al. 2003; Monis et al. 2003). The HP-1 is a Prague line of Portland-1 (ATCC 30888) provided by E.A. Meyer (Oregon Health Sciences University, Portland, USA), the cloned line WB-1B [derived from the original isolate WB (ATCC 30957) from a patient with a chronic symptomatic giardiasis] was provided by J.A. Upcroft (QIMR, Brisbane, Australia), and the isolates HH (from an acute case of human giardiasis after visiting India) and CH-105 (from a chinchilla with acute diarrhea) were isolated in Prague in 1999 and 1990, respectively.

Trophozoites were grown axenically in a modified TYI-S-33 medium supplemented with bovine bile (Keister 1983). To enrich the cultured population with mitotic cells, a method based on albendazole treatment was used (Nohýnková et al. 2006). Briefly, trophozoites from a late log-phase of growth (nearly a confluent monolayer) were exposed to 100 ng/ml albendazole (Sigma) in fresh TYI-S-33 medium at 37°C for 7 h. After exposure, the medium, together with albendazole-affected free-swimming cells, was

quickly discarded, and the attached nonaffected trophozoites were briefly washed with a freshly prepared albendazole-free medium and immediately incubated in a medium without the drug for the next 15 to 30 min at 37°C to initiate mitosis. Slides for Giemsa- and immunostaining, and for laser scanning cytometry (LSC), were prepared in a 3-mm-deep anaerobic perfusion chamber (Sigma) to allow cells to attach on either the slide or coverslip at the bottom of the chamber. For chromosome preparations, drug-free medium was discarded after incubation, and adherent trophozoites were detached by cold phosphate-buffered saline (PBS; pH 7.2), resuspended, harvested by centrifugation ($1{,}600{\times}g$, 10 min, 4°C), and immediately used. No differences in the karyotype pattern and the course of mitosis have been observed between cells from the enriched and the wild-type populations, respectively.

In vitro encystation, harvesting cysts, and excystation

The isolate HP-1 was used to complete the life cycle of *Giardia* in vitro. To encyst, trophozoites were incubated in preencystation medium TYI-S-33 without bile (pH 6.8) for 72 h. The spent medium with swimming trophozoites was discarded, and the attached cells were overlaid with encystation TYI-S-33 medium supplemented with 250 µg/ml of porcine bile and 5 mM lactic acid (pH 7.8) (Gillin et al. 1989). After 20 h of incubation, cysts were harvested by centrifugation ($800{\times}g$; 10 min; 4°C), resuspended in cold distilled water to lyse the trophozoites, and maintained at 4°C for at least 5 days. To excyst, the in vitro prepared cysts in cold distilled water were mixed with 0.0075 N HCl/ 10 mM L-cysteine hydrochloride/10 mM ascorbic acid in Hank's buffer (pH 7). After 37 min of incubation at 37°C, the same volume of 1 M NaHCO$_3$ was added, and the tube was spun at $800{\times}g$/10 min. The supernatant was carefully removed, and fresh TYI-S-33 with ferricyanide ammonium citrate (22.8 µg/ml *w/v*) and arginine (2 µg/ml *w/v*) was poured on the pellet. The tube was incubated at 37°C. A confluent monolayer of trophozoites was formed within 5 days. For chromosome preparations, the first subpassage was used.

Cell preparations and immunofluorescence labeling

For Giemsa staining, the slides were quickly air-dried, fixed with methanol for 5 min, and stained with Giemsa solution (8% in neutral-buffered distilled water) for 30 min.

Immunofluorescence staining was carried out according to (Nohýnková et al. 2000). Cells attached to coverslips were fixed in ice-cold methanol (−20°C, 5 min), permeabilized with acetone (−20°C, 5 min), and air-dried. After rehydration and quenching, the cells were exposed to a primary antibody followed by fluorescein isothiocyanate

(FITC)-conjugated secondary antibody. Monoclonal antibody 6-11B-1 against the acetylated N-terminal domain of alpha-tubulin was used as a marker of the mitotic spindle (Nohýnková et al. 2000). The slides were mounted in Vectashield with propidium iodide (PI) to stain DNA and examined with a laser scanning confocal microscope (FluoView 1000; Olympus).

Transmission electron microscopy

Cells were fixed with 2.5% glutaraldehyde in 0.1 M cacodylate buffer/5 mM CaCl$_2$, postfixed with 1% OsO$_4$/ 0.8% potassium ferricyanide/5 mM CaCl$_2$ in the same buffer, dehydrated in acetone, and embedded in Epon. Ultrathin sections were examined after staining with uranyl acetate/lead citrate with a JEOL 1010 electron microscope.

Chromosome preparations and evaluation of karyotype

Washed trophozoites were hypotonized in 75 mM KCl (15 min) and centrifuged ($870{\times}g$, 6 min), and the pellet was fixed with three changes of freshly prepared methanol: acetic acid (3:1) (10, 20, and 30 min). The fixative solution was mixed immediately before use. Between each step, cells were centrifuged at $3{,}500{\times}g$ for 5 min. A final suspension of fixed cells was dropped on the slides and air-dried overnight at room temperature. For chromosome visualization, the slides were stained (1 min) with PI (50 µg/ml in a solution containing 0.1 mg/ml RNase A, 0.1% Nonidet-P-40, and 0.1% trisodium citrate). Preparations were observed using an Olympus BX40 fluorescence microscope, and figures were photographed on Ilford PAN 100 black-and-white film. Image processing occurred through high-resolution scanning and magnification on a computer.

For evaluation of karyotypes, only figures with fully confined chromosomes in both nuclei were used. For the number of chromosomes, over 200 late-prophase figures per isolate were evaluated in at least three independent experiments. The minimum period between two experiments was 1 month. The correlation between the frequency of a minor karyotype pattern and its deviation from the prevailing one (difference in numbers of chromosomes) was tested by Kendall test. For chromosome size, 10 to 20 figures were measured on printed images. Relative chromosome length was calculated as a percentage of total chromosome length of the set of a given nucleus (Passarge 1974). Distribution of relative chromosome lengths in isolates HP-1 and WB-1B was compared by a standard homogeneity test.

Chromosome banding techniques

C-banding was carried out according to Sumner (1972), with some modifications. Briefly, preparations were incubated in

0.2 N HCl for 45 min, rinsed with distilled water, then immersed into saturated Ba(OH)$_2$ at 50°C for 3–5 min, rinsed with distilled water, and renatured in 2xSSC (pH 7) at 60°C for 75 min. Air-dried preparations were stained with 20% Giemsa in Sörensen phosphate buffer (pH 6.8) for 5 h.

For fluorescence banding, the slides were preincubated in McIlvaine buffer/10 mM MgCl$_2$ (pH 7) for 10 min and stained. Staining procedures were modified according to Sola et al. (1992); the same buffer was used in staining experiments unless otherwise specified. For chromomycin staining, a slide was overlaid with 150 µl of fluorochrome solution (0.5 mg/ml chromomycin in the buffer) under a coverslip (24×60 mm) and incubated for 15 min, then rinsed with the same buffer, dipped into HEPES/NaCl buffer (pH 7) containing methyl green (0.12 mg/ml) for 15 min, briefly rinsed with HEPES/NaCl buffer, and mounted in glycerol/propyl gallate. Before DAPI treatment, the slides were placed in a solution of 0.35 mg/ml methyl green in the McIlvaine buffer for 15 min, then stained for 15 min in DAPI solution (0.5 mg/ml DAPI in the buffer), rinsed in the same buffer, and mounted in glycerol/propyl gallate. Staining steps were performed in the dark. The preparations were inspected using an Olympus AX 70 Provis microscope.

DNA replication

To detect DNA replication, an immunofluorescence assay using the BrdU Labeling and Detection Kit I (Roche) was carried out following the instructions by the manufacturer. Briefly, trophozoites from a log-phase of growth were exposed to BrdU labeling reagent (50 min, 37°C), washed, fixed in 70% ethanol/50 mM glycine HCl (pH 2; 30 min, −20°C), then incubated with anti-BrdU antibody (diluted 1:10 with 66 mM Tris/0.66 mM MgCl$_2$/1 mM 2-mercaptoethanol, 30 min, 37°C) followed by an FITC-conjugated secondary antibody (diluted 1:10 with PBS; 30 min, 37°C) and mounted in Vectashield. The slides were examined with an Olympus BX 40 fluorescence microscope. Over 300 cells with detected DNA replication were evaluated for comparison of the level of BrdU incorporation. Three categories were introduced for the evaluation of BrdU incorporation between both nuclei: the same signal intensity, different signal intensity, and a signal present only in one nucleus.

Laser scanning cytometry

For comparison of DNA content based on emitted fluorescence intensity of both nuclei, the isolate HP-1 was used. DNA of methanol-fixed cells was stained with DAPI (1 µg/ml in bidistilled water) for 5 min at room temperature. Analysis was performed on a laser scanning computer iCys attached to an Olympus IX71 microscope. For excitation diode, 405-nm violet laser was used; emission was detected on 463/39-nm filter set. Two parameters had been evaluated for the DNA content comparison of both trophozoite nuclei: the integral of fluorescence and the

Fig. 1 Karyotype of *Giardia intestinalis*. **a** A late prophase plate of clone WB-1B showing the 9+11 karyotype pattern: one nucleus (*located left on the plate*) contains nine chromosomes, and the other one contains 11 chromosomes. **b** A late prophase plate of isolate HH to demonstrate the 10+11 karyotype pattern: one nucleus (*located left*) contains 10 chromosomes, and the other nucleus contains 11 chromosomes. **c**–**f** Karyograms of four isolates of *Giardia intestinalis*. **c** WB-1B. **d** HP-1. **e** HH. **f** CH-105. *Each row* corresponds to a single trophozoite nucleus. Chromosomes are rowed up according to their length. The plates in (**a**) and (**b**) were used for karyogram construction in (**c**) and (**e**), respectively. *Bar* 3 µm
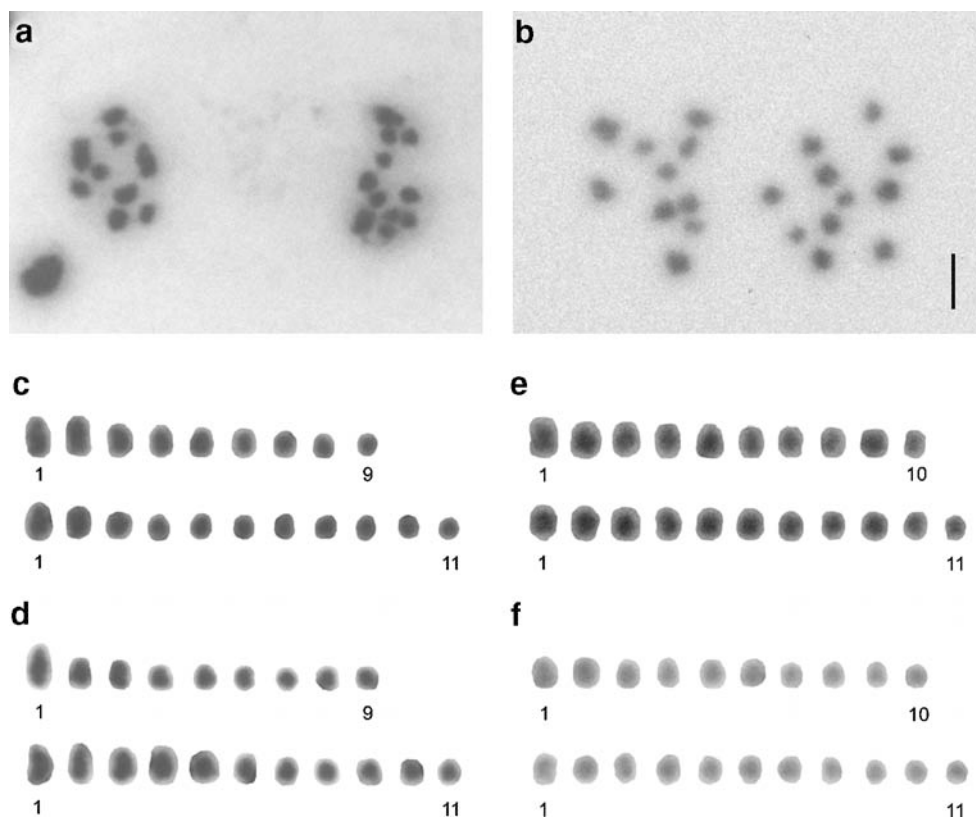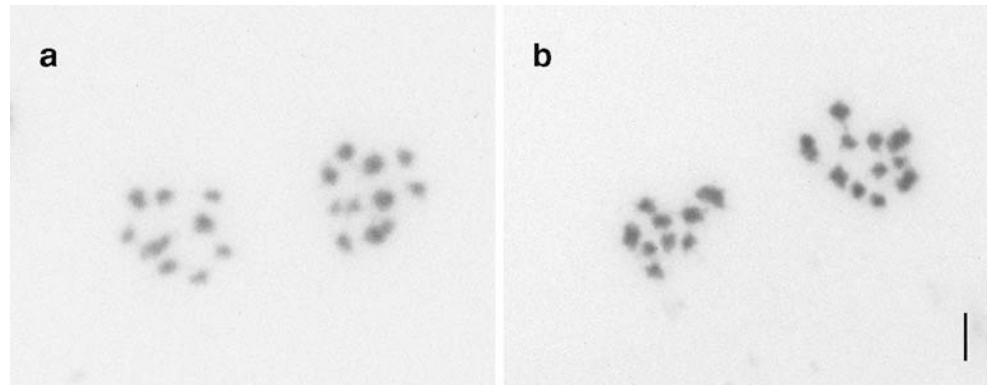
Fig. 2 Late prophase plates of isolate HP-1 demonstrating karyotype of a cell from **a** a wild-type culture, **b** an enriched culture by means of albenda-zole. *Bar* 3 μm

maximum pixel value. Nuclei that fell outside the scatter-gram dynamic range were excluded from further analysis. To categorize nuclei, we used only events from the R1 region (Fig. 7a). The ratio of the integral of fluorescence to the average pixel value (ratio of integral of fluorescence/area) allowed us to distinguish six subpopulations of nuclei, which were marked with different colors (Fig. 7b). The color gating of 1,000 nuclei was transferred back into the image to analyze the presence of the nuclear subpopulations within each cell (Fig. 7c). To compare the values of the emitted fluorescence from both nuclei, 270 cells were measured, and the values were analyzed by a Student *t* test.

Results

Karyotype analysis

Chromosomes of *Giardia* were minute (0.8 to 2.4 μm in length), ovoid to rod-like, without any apparent primary and secondary constrictions. They consisted of two tiny chromatids, which separated in metaphase (see below). C-banding did not reveal blocks of constitutive heterochro-matin in any of the chromosomes. Also, application of fluorochromes that specifically stain chromosome areas of AT- or GC-rich DNA (DAPI and chromomycin A_3,

Table 1 Distribution of chromosome numbers in the studied isolates

Isolate	Prevailing karyotype	Other variants					
	Percentage	Percentage					
	(Actual ratio)	(Actual ratio)					
HP-1[a]	9+11	9+10	10+11	9+12	10+10	11+11	
	93.5	3.3	1.4	0.9	0.5	0.5	
	(200/214)	(7/214)	(3/214)	(2/214)	(1/214)	(1/214)	
HP-1[b]	9+11	9+10	9+12	8+11	8+10	10+11	11+11
	90.5	4.9	1.4	1.4	0.9	0.5	0.5
	(200/221)	(11/221)	(3/221)	(3/221)	(2/221)	(1/221)	(1/221)
HP-1[c]	9+11	9+10	10+11	8+11	8+10	9+12	
	88.5	6.2	2.2	1.3	1.3	0.4	
	(200/226)	(14/226)	(5/226)	(3/226)	(3/226)	(1/226)	
WB-1B[a]	9+11	9+10	9+12	8+12	10+11		
	87.3	5.7	4.4	1.3	1.3		
	(200/229)	(13/229)	(10/226)	(3/229)	(3/229)		
HH[a]	10+11	9+11	10+10	10+12	9+10	11+11	
	87.7	5.3	2.2	2.2	1.8	0.9	
	(200/228)	(12/228)	(5/228)	(5/228)	(4/228)	(2/228)	
CH-105[a]	10+11	10+10	9+11	11+11	9+10	10+12	9+12
	84.4	5.5	4.6	2.1	1.7	1.3	0.4
	(200/237)	(13/237)	(11/237)	(5/237)	(4/237)	(3/237)	(1/237)

The correlation between frequency of a minor karyotype and its deviation from prevailing karyotype (difference of numbers of chromosomes) tested by Kendall test is highly significant (Kendall $\tau=-0.407$, $p=0.0013$, $N=31$)
[a] Population enriched with mitotic cells
[b] Wild-type population
[c] First passage after excystation

respectively) did not differentiate bands, except for a tiny signal at the end of one or two chromosomes after chromomycin staining (data not shown).

In a single cell, the two nuclei exhibited different chromosome numbers and differed also in chromosome sizes (Fig. 1a,b). The same differences were found in mitotic cells from wild-type populations and from those enriched with mitotic cells by using albendazole (Fig. 2). Regarding the distribution of numbers of chromosomes between the two nuclei, a comparative analysis of four *Giardia* isolates revealed two dominant karyotype patterns:

9+11 (isolates WB-1B and HP-1) and 10+11 (isolates HH and CH-105) with odd chromosome numbers in one or both nuclei (Fig. 1c–f) (Table 1). The isolates WB-1B plus HP-1 and HH plus CH-105, representing two major genetic groups of *G. intestinalis* (assemblages A and B, respectively), thus differed as to the total chromosome number per cell, possessing 20 and 21 chromosomes, respectively. Besides the dominant pattern, minor variants were detected in each isolate (Table 1). To explore stability of the asymmetry of *Giardia* karyotypes, the isolate HP-1 was followed up during a period of 4 years (approximately

Fig. 3 Comparative analysis of DNA content of the two *Giardia* nuclei by laser scanning cytometry. **a** To categorize nuclei, only events from R1 region are used. Nuclei that fall outside the scattergram dynamic range are excluded from further analysis. **b** Nuclei of R1 region are separated into six subpopulations (*marked by different colors*) according to Ratio of Integral of Fluorescence to Average Pixel value. **c** Trophozoites with color-gated nuclei featuring a different DNA content of each nucleus. To orient *Giardia* trophozoites, cells are stained with anti-acetylated tubulin antibody (6-11B-1)
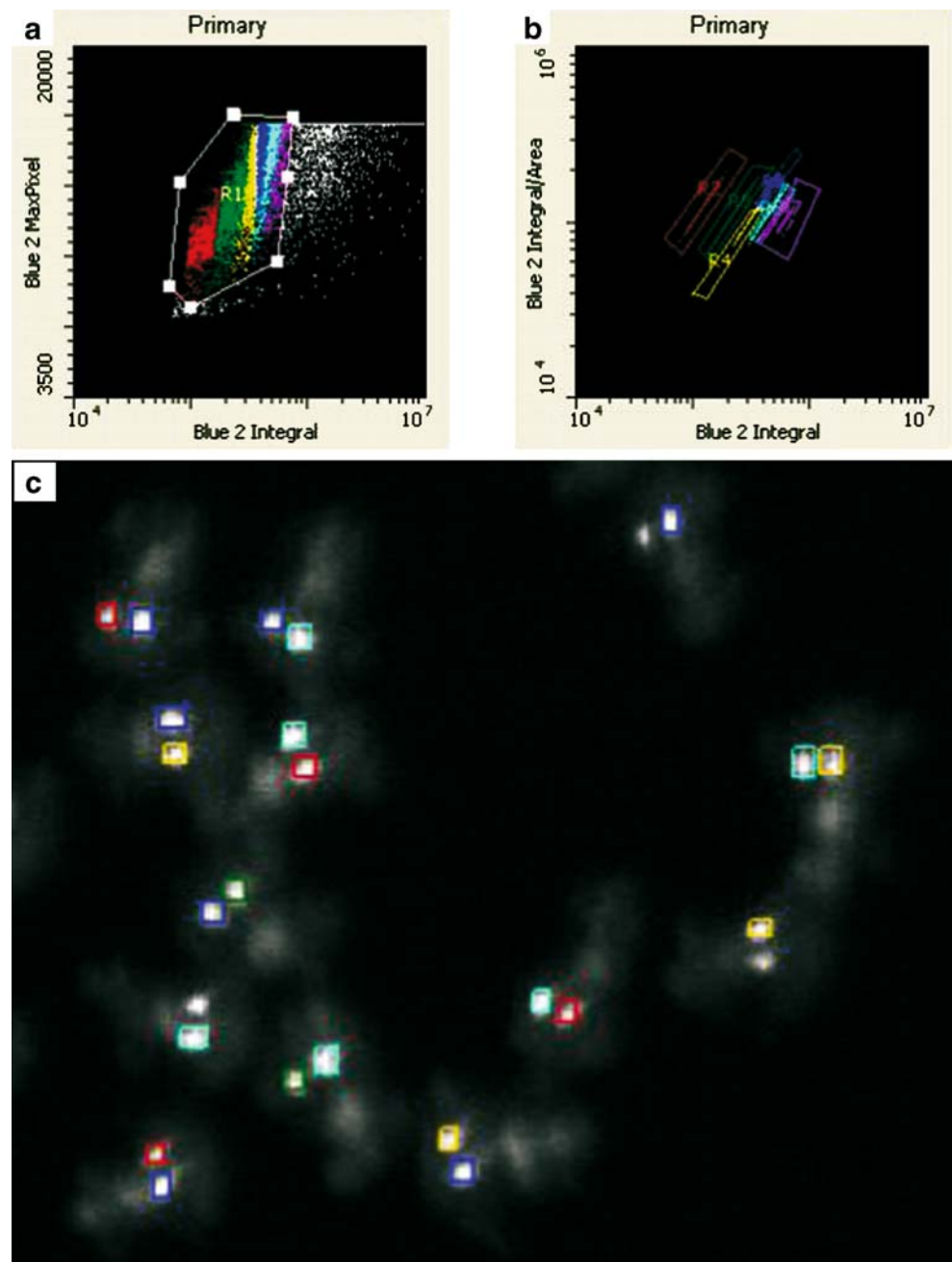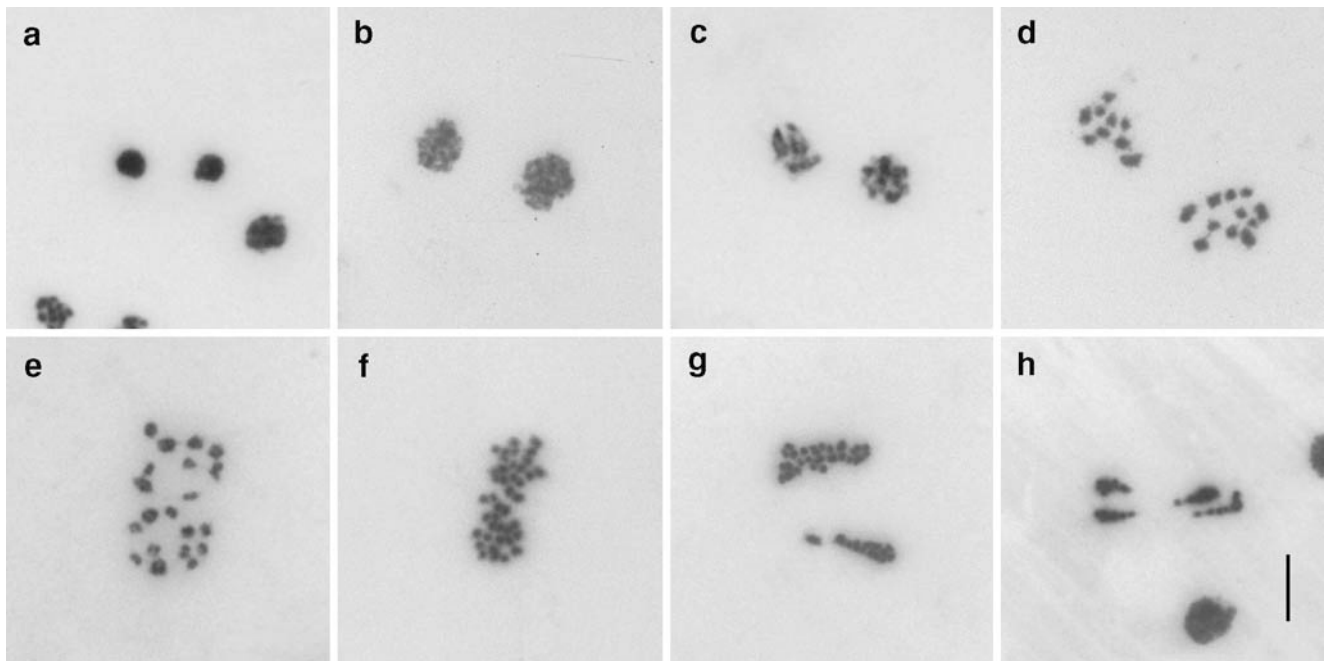
Fig. 4 The course of *Giardia* mitosis on hypotonized preparations stained with propidium iodide to show chromosome behavior during sequential events. **a** *Interphase* Small compact nuclei. **b** *Early prophase* Loosened nuclei with fibrogranular appearance. **c** *Prophase* Gradual condensation of chromosomes. **d** *Late prophase* Fully condensed chromosomes in two clusters (one per nucleus), in which each chromosome separates into two small chromatids (**e**). **f** *Metaphase* Two irregular clusters of chromatids. **g** *Anaphase* Alignments of chromatids which segregate laterally to form daughter nuclei in telophase (**h**). *Bar* 6 μm

3,800 generations in vitro) and during an entire life cycle completed in vitro. In both cases, the distribution of the dominant karyotype pattern did not change (Table 1).

Corresponding nuclei (i.e., nuclei with the same number of chromosomes) of isolates WB-1B and HP-1 belonging to the same genetic group differed significantly in the distribution of relative chromosome lengths (Fig. 1c,d). One or several chromosomes of unique length were observed in one or both nuclei of these *Giardia* isolates (Figs. 1 and 2).

Differences in DNA content between the two nuclei of interphase trophozoite

LSC showed differences ($p<0.0001$) in the DNA content between two interphase nuclei. By a quantitative analysis of the DNA content, six subpopulations of nuclei were detected (Fig. 3a,b). Median fluorescence intensity, which is in proportion to DNA content, for these subpopulations was as follows: R2 (red) 130834, R3 (green) 236836, R4
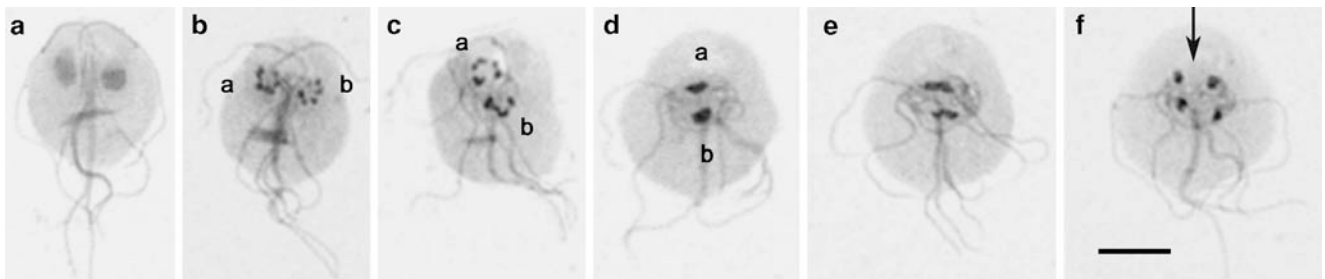

Fig. 5 The course of *Giardia* mitosis in relationship to cell morphology. Dorsal view. Giemsa staining. **a** *Interphase cell* The two nuclei are located side by side along the longitudinal cell axis. **b** *Early prophase* In each nucleus, chromatin forms several irregular "bodies". The two nuclei start to migrate from interphase, left/right position to mitotic anterior/posterior position. **c** *Late prophase* The nuclei reach the tandem mitotic position. **d** *Metaphase* Chromatin forms a compact body in the center of each nucleus. **e** *Anaphase* A left–right stretching of the chromatin material in each of the simultaneously dividing nuclei. **f** *Telophase* Two small daughter nuclei are formed from each mother nucleus so that after cytokinesis, each daughter cell receives one copy of each mother nucleus. *Arrow* indicates cytokinesis direction. Left nucleus (**a**), right nucleus (**b**). *Bar* 5 μm

(yellow) 319857, R5 (blue) 417580, R6 (cyan) 497743, R7 (magenta) 608123 (Fig. 3b). In a logarithmically growing nonsynchronous population, up to 82% of cells harbored nuclei from different subpopulations (Fig. 3c).

The course of mitosis: the behavior of chromosomes, nuclei, and mitotic spindle assembly

In spread chromosome preparations, nuclei of hypotonized interphase and mitotic cells stained with propidium iodide or DAPI were followed to demonstrate the chromosome behavior during the *Giardia* cell cycle. This was enabled by finding that the method of preparation did not affect bilateral topology of the two nuclei. Ventral or dorsal positions of the hypotonized cells were not possible to differentiate on the slides. Compact interphase nuclei (Fig. 4a) enlarged, became fibrous, and loosened in early prophase (Fig. 4b). Within the fibrous matrix, chromosome condensation took place gradually. Hence, the early-prophase chromosomes shared an indefinite profile (Fig. 4c), becoming clearly discernible in late prophase (Fig. 4d). In some late prophase cells, differentiation of chromosomes to chromatids was observed (Fig. 4e). During metaphase, in each nucleus the minute chromatids formed a large cluster (Fig. 4f). In anaphase, the cluster stretched laterally with discrete chromatids being lined up next to each other. Frequently, the chromatids coming from a single

nucleus were aligned in two parallel rows (Fig. 4g). Subsequently, the chromatids clustered on either pole to give the origin of small compact daughter nuclei (Fig. 4h).

Giemsa staining was used to show how the chromosome behavior observed in hypotonized preparations corresponds to mitotic behavior of nuclei in intact trophozoites (viewed from dorsal side). Interphase trophozoites possessed two oval nuclei located in the anterior cell half; left and right to the longitudinal cell axis (Fig. 5a). At the onset of prophase, chromatin in each nucleus condensed into irregular "chromatin bodies" not countable due to their overlapping (Fig. 5b). Following this, the dividing nuclei gradually moved to the midline, the left one anteriorly and the right one posteriorly, so that they were arranged in tandem in metaphase. The chromatin bodies persisted during nuclear migration (Fig. 5c) up to metaphase when they concentrated to a single compact, centrally located chromatin cluster in each nucleus (Fig. 5d), similarly to the bulk of chromatids demonstrated above. Anaphase started as a poleward left–right stretching of chromatin material along the longitudinal axis of the dividing nuclei (Fig. 5e) and terminated when four daughter nuclei (two from each parent nucleus) were formed (Fig. 5f). Cytokinesis proceeded between the separated nuclei in anterior–posterior direction in accord with the longitudinal body axis of the mother cell, so that each progeny received one copy of each mother nucleus (Fig. 5f).

Fig. 6 The two mitotic spindles in a single *Giardia* cell visualized by immunofluorescence staining. Spindle microtubules are labeled with anti-acetylated tubulin antibody (6-11B-1); DNA is stained with propidium iodide. **a** *Metaphase/anaphase* Two spindles (*arrowheads*)—one per a nucleus—are located parallel to each other. **b** *Telophase* Lateral (*left/right*) elongation of the spindles. **c** Chromatin (*red*) behavior during metaphase to telophase. **d** Double labeling of the same nuclei to show that the spindles (*green*) prevent mixing of chromatin (*red*). *Bar* 2 μm
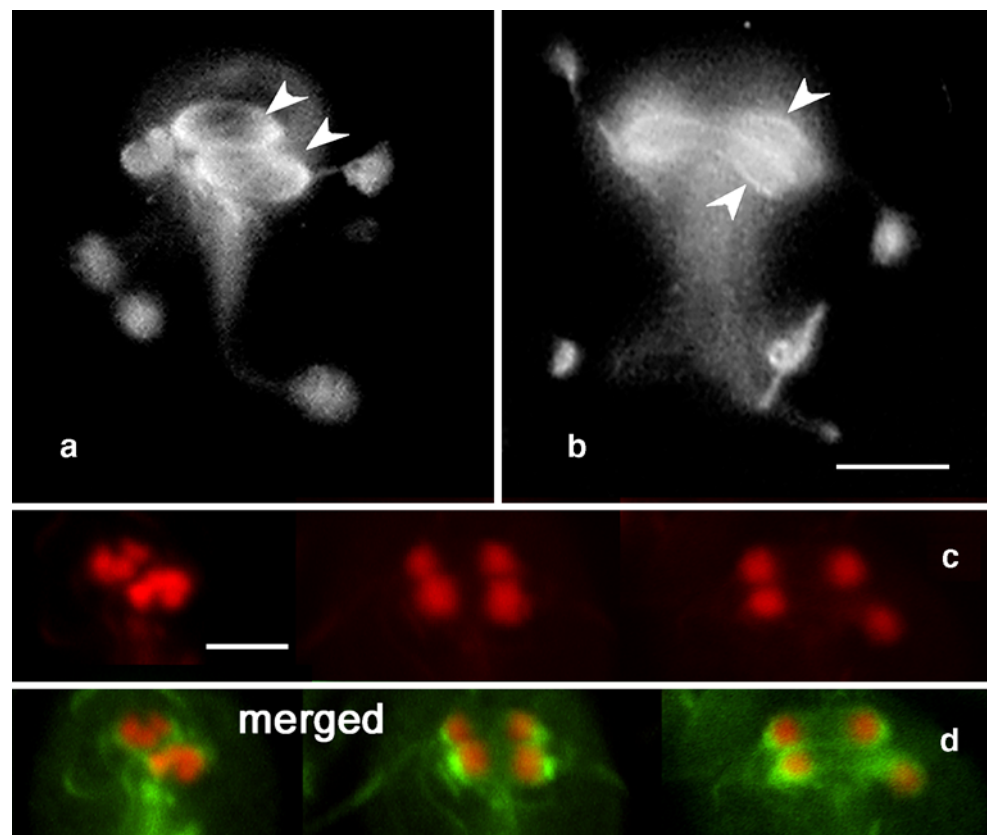
In immunofluorescence experiments, labeling of mitotic *Giardia* cells with anti-α-tubulin antibody demonstrated assembly of two mitotic spindles per cell (Fig. 6). In metaphase and anaphase, the two spindles were located parallel to each other, oriented perpendicularly to longitudinal body axis of the dividing cell. Each spindle was limited by the thin microtubule envelope (Fig. 6).

Transmission electron microscopy revealed an intact nuclear membrane of each of the dividing nuclei, which persisted throughout the whole course of mitosis, and two mitotic spindles (one per nucleus) composed of intranuclear and extranuclear microtubules (Fig. 7). At each nuclear pole, close to the respective spindle pole, the nuclear membrane formed a small cup-like impression. Only this region of the membrane was perforated to form narrow pores through which several spindle microtubules individually entered the nucleoplasm (Fig. 7c). On longitudinal sections through the dividing nuclei, a few microtubules lying parallel to the axis of the division were occasionally visible (Fig. 7b,c). On cross sections, three to four small bundles of five to seven

microtubules each were usually irregularly distributed within the nucleoplasm (Fig. 7d). Neither kinetochore-like structures nor condensed chromosomes were observed. In addition to intranuclear microtubules, some 50 extranuclear spindle microtubules formed an external corset tethering the nuclear envelope (Fig. 7d). Both intranuclear and extranuclear spindle microtubules emerged from a spindle pole neighboring the basal body pair in the cytoplasm (not shown). The arrangement of *Giardia* mitosis conformed semi-open orthomitosis according to Raikov's (1994) classification.

Cell-cycle-dependent asynchrony of the two nuclei

Within a dividing cell, the two nuclei did not undergo the entire course of mitosis synchronously. In all isolates, two short phases of asynchrony were observed in approximately 30–70% of the mitotic cells. (1) In early prophase (50–70% of cells), condensation of the interphase chromatin into mitotic chromosomes went on faster in the nucleus that
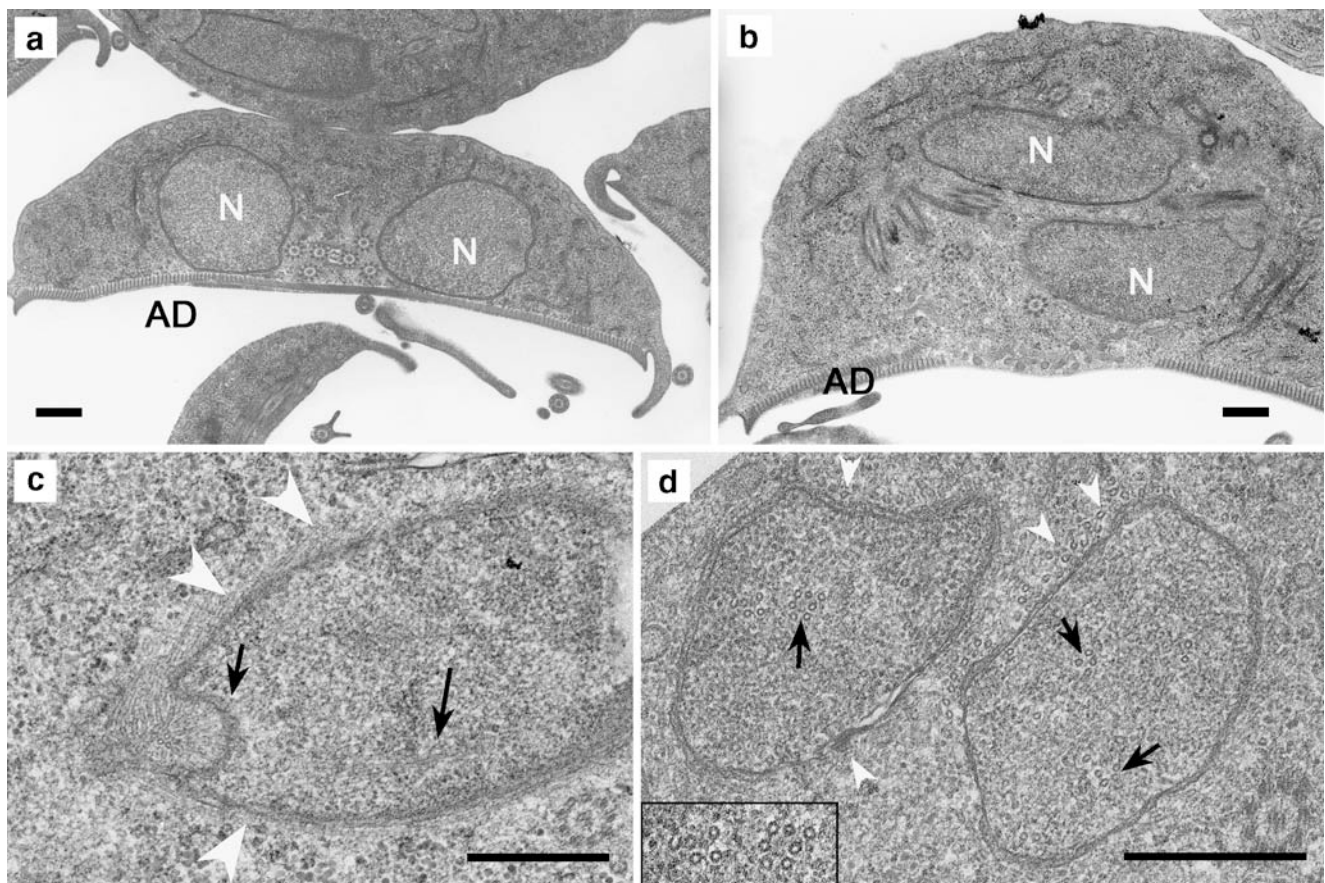

Fig. 7 Ultrastructure of the mitotic spindles. **a** A cross section of a trophozoite in interphase. The two nuclei are situated near the adhesive disk with flagellar axonemes in-between. **b** A cross section of a trophozoite in metaphase. The dividing nuclei at the superimposed position are located between the reorganized flagella axonemes. **c** A longitudinal section of a metaphase nucleus. The extranuclear microtubules (*arrowheads*) run along the intact nuclear envelope. The intranuclear microtubules (*arrow*) enter the nucleoplasm through the perforated area at the pole. **d** A cross section of metaphase nuclei. In each, extranuclear microtubules (*arrowheads*) parallel externally the nuclear envelope. Within the nuclei, the intranuclear microtubules (*arrows*) form small clusters of up to seven microtubules (*inset*). Nucleus (*N*), adhesive disk (*AD*). *Bar* 500 nm
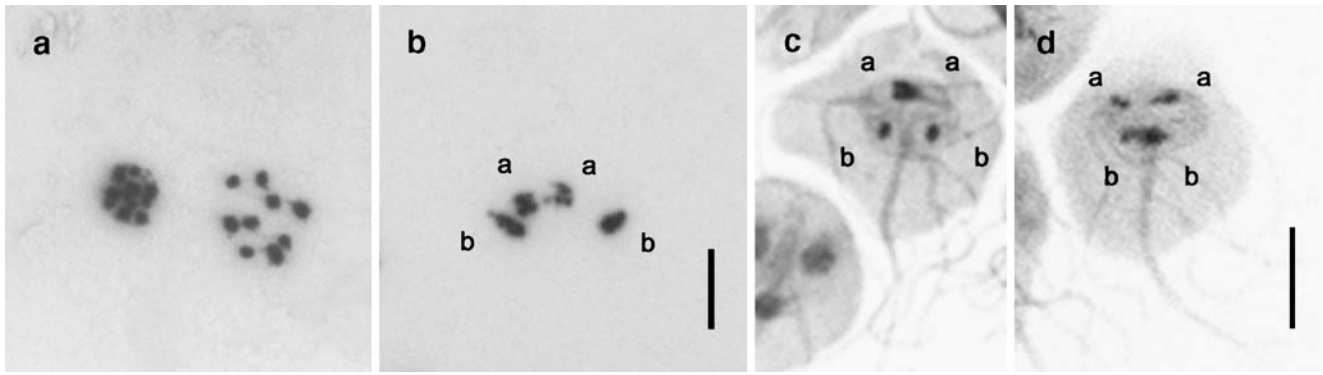
Fig. 8 The asynchronous nuclear division on hypotonized (**a**, **b**) and nonhypotonized (**c**, **d**) preparations. **a** *Prophase* Faster chromosome condensation is evident in the nucleus with nine chromosomes.

b, **d** *Anaphase* Lateral segregation of chromatids and formation of daughter nuclei proceed slower in nucleus (*a*) (**b**, **c**) or in nucleus (*b*) (**d**). **a**, **b** *Bar* 6 μm. **c**, **d** *Bar* 5 μm

contained the smaller number of chromosomes (Fig. 8a). (2) In anaphase (30% of cells), the lateral stretching of chromatids went on faster in one of the two dividing nuclei (Fig. 8b–d). Meanwhile, the slower progressing nucleus caught up with the faster one so that in both nuclei, the same level of chromosome condensation was achieved in late prophase and four daughter nuclei (two from each of the parent nucleus) were synchronously formed in telophase. Analysis of DNA replication by incorporation of BrdU also detected asynchronous behavior during interphase. Quantification revealed that in about 32.5% of the S-phase trophozoites, the DNA was replicated asynchronously as demonstrated by asymmetry in fluorescence signals between the two nuclei. In 10% of the cells, only one of the two nuclei displayed the BrdU incorporation signal (Fig. 9).

Discussion

In many respects, the parasitic flagellate *G. intestinalis* represents an attractive model of the eukaryotic cell and of

the evolution of eukaryotes (Adam 2001; Svärd et al. 2003). However, despite the nearly completed genome sequencing project (McArthur et al. 2000), the knowledge on the exact number of *Giardia* chromosomes, their distribution between the two nuclei, and, with regard to karyotype, ploidy and homo- vs heterokaryosity, is still lacking. The major obstacle is that no preparative method is available that enables the separation of the two nuclei from each other. In this respect, cytogenetic methods can be helpful. As the first step toward understanding the organization and evolution of genomes of *Giardia* nuclei, we used conventional cytogenetic techniques in combination with light and immunofluorescence microscopy to obtain basic information as to karyotype of each of the two nuclei and chromosome behavior during mitotic division.

Observations on *Giardia* chromosomes during mitosis

In contrast to medically important unicellular parasites in which chromosomes do not condense during mitosis [e.g., trypanosomes (Ersfeld et al. 1999)] or are not rendered visible by conventional cytogenetic techniques [e.g., the

Fig. 9 The asynchronous DNA replication revealed by BrdU incorporation. The same intensity of signal in both nuclei (*two asterisks*), differences in signal intensity between the nuclei (*one asterisk*), and signal present only in one nucleus (*arrow*). *Bar* 6 μm
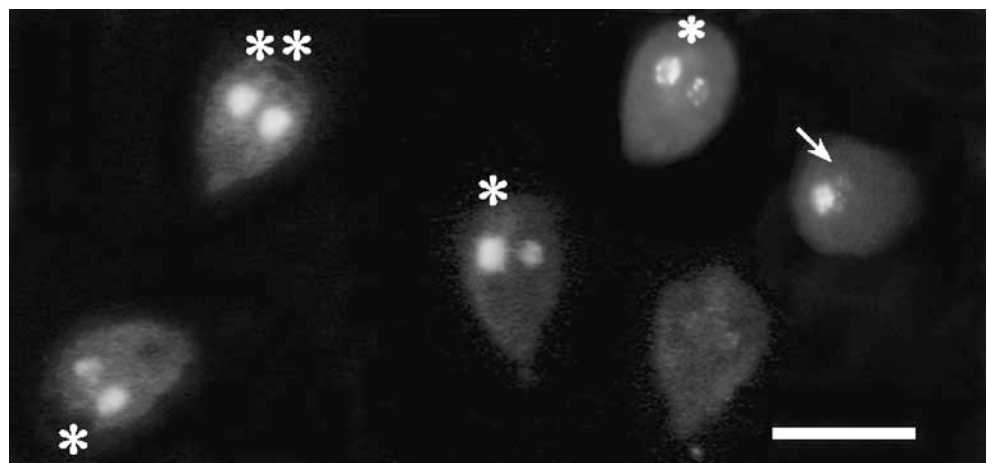
malaria parasite *Plasmodium falciparum* (Coppel and Black 2005)], chromosomes of *Giardia* readily condense and can be visualized. Condensation proceeds in both nuclei, and subsequent separation into chromatids and mitotic segregation to form daughter nuclei is in accord with typical scenario of eukaryotic chromosome behavior. However, *Giardia* chromosomes condense, separate, and segregate inside the largely intact nuclear membrane. Condensation proceeds in prophase; chromosomes do not visibly congress to spindle equator to form a metaphase plate. Chromatid alignment at anaphase, as well as clustering of intranuclear microtubules into bundles, is suggestive of a nonconventional mode of segregation, resembling the sliding model of minichromosomal segregation in *Trypanosoma brucei* (Gull et al. 1998). Absence of homologs of *Schizosaccharomyces pombe rad21* in the *Giardia* genome (Logsdon J and Schurko A, personal communication) could indicate that the atypical arrangement of chromatids might be a consequence of a modification of cohesin complex (Taylor et al. 2004). Despite the absence of visible constrictions, it is likely that giardial chromosomes are not holokinetic; the low number of microtubules entering the nucleus and possibly interacting with chromosomes indicates that the kinetic activity is restricted to a tiny area on the chromosome surface. But further studies are necessary to elucidate the molecular basis of chromosome behavior observed during *Giardia* mitosis.

Karyotypes of *Giardia* nuclei

It is interesting to note that in a single binucleated *Giardia* cell, chromosomes are not distributed symmetrically between nuclei. In four isolates studied, we found two dominant karyotype patterns in which the two nuclei differ in one and two chromosomes, respectively. Occurrence of minor karyotype variants in each *Giardia* isolate conforms to a usual frequency of artifacts of a spreading technique used for chromosome preparations (Gong et al. 2004; Rosenbusch 2004). Both statistical evaluation of karyotype distribution and approximately the same rate of variation in the isolates (three noncloned, geographically distinct isolates and the cloned line WB-1B) suggest that also in *Giardia*, the minor variants represent the artifacts. Of course, we cannot definitely exclude the possibility that some of the minor variants could be minor karyotypes suppressed under culture conditions. In vitro selection of distinct genotypes has been reported in multiple *Giardia* lines generated from a single patient, as well as during cloning and subcloning of particular *Giardia* isolates (Upcroft and Upcroft 1994; Le Blancq and Adam 1998). However, the differences found in those studies seem to relate more likely to changes in chromosome sizes than in copy number. Chromosome size heterogeneity caused in

part by frequent rearrangements in subtelomeric regions of homologous chromosomes is a feature of *Giardia* (Le Blancq and Adam 1998).

The findings that representatives of the two major genetic groups of *G. intestinalis* (Monis et al. 1996) differ in karyotypes could be of particular interest. Provided that it would be confirmed by evaluation of a significant number of isolates and clones, the distinct karyotype patterns may reflect species differences inside the *G. intestinalis* complex. Morphologically uniform *G. intestinalis* comprises seven groups that are genetically distinct enough to be considered separate species (Thompson and Monis 2004).

Ploidy

The level of ploidy of a binucleate *Giardia* cell is still unclear mainly because the current knowledge (Upcroft et al. 1996; Le Blancq and Adam 1998; Bernander et al. 2001) is based on chromosome composition of a cell, not of each nucleus. A variety of observations coming from electrophoretic karyotyping and FACS favor the tetraploid genome of a trophozoite with two diploid nuclei as a deduced consequence (Yang and Adam 1994, 1995; Hou et al. 1995; Upcroft et al. 1996; Le Blancq and Adam 1998; Bernander et al. 2001). Considering the five chromosome linkage groups (Le Blancq and Adam 1998), and a ploidy of two for each nucleus, the deduced chromosome number per single nucleus should be 10. This number falls into the range of chromosome numbers (9–11) observed in this study. However, our results run counter to the assumption that *Giardia* nuclei are simply diploid. Instead, asymmetrical distribution as well as odd chromosome numbers indicates that at least for some chromosome(s), either one or both nuclei are aneuploid. Moreover, if one copy of each of the five linkage groups is present in each nucleus [as demonstrated by fluorescence in situ hybridization (Yu et al. 2002)], the nucleus with nine chromosomes should be monosomic for one chromosome pair. Different ploidies for different chromosomes could account for the asymmetry observed in *Giardia*, but further work is definitely needed to understand how particular chromosomes are distributed in a particular nucleus. Indeed, a possible aneuploidy has already been suggested based on findings of at least three copies of three *Giardia* chromosomes by qualitative molecular analyses (Adam 1992; Yang and Adam 1994, 1995).

In some unicellular, clonally propagated organisms (e.g., *Leishmania*, *Trypanosoma cruzi*, and *Trichomitus batrachorum*), aneuploidy seems to be tolerated (Ravel et al. 1998; Gaunt et al. 2003; Raikov 1982). In *Giardia*, the stable occurrence of odd chromosome numbers and, thus, stable aneuploidy during both vegetative division and the passage through a cyst stage further support the assumption

that *Giardia* is also in principle asexual.Theoretically, the stable transmission of an aneuploid pattern can be possible only if meiosis is absent because a principal requirement for the first meiotic division, the presence of just two homologous copies of each chromosome, is not met. In *Giardia*, sexual reproduction has never been recognized during its life cycle (Adam 2001), and proposed predominant clonal propagation (Tibayrenc and Ayala 2002) has been supported by the rarity of transposable elements (Wickstead et al. 2003) and by the apparent lack of deleterious ones (Arkhipova and Morrison 2001). The organization of *Giardia* mitosis currently described in this study hampers chromatin interfusion between the nuclei during trophozoite division when each progeny receives one copy of each parent nucleus. Moreover, our results exclude chromatin interchange between different nuclei during karyokinesis in the cyst and acquisition of both copies of one parent nucleus by a single daughter cell during excystation. The stable occurrence of the karyotype asymmetry with nonpaired (odd) chromosomes and the type of mitosis strongly indicate that each nucleus behaves as a clonal lineage during the whole life cycle of *Giardia*. Consequently, each nucleus should undergo an independent accumulation of mutations. Thus, within each nucleus, homologous chromosomes could differentiate independently from each other during evolution by accumulation of rearrangements and nondisjunctions. But how the low level of allelic heterozygosity reported for *Giardia* genes (Baruch et al. 1996; Adam 2001) is retained in the cell if at least one copy of each chromosome is present in each nucleus (Yu et al. 2002) remains an enigmatic issue.

Recent findings of functional homologs of meiotic genes in the *Giardia* genome (Ramesh et al. 2005) do not mean that *Giardia* necessarily undergoes canonical meiosis (Birky 2005). A loss of meiosis cannot be excluded, and the genes might function in another processes, e.g., in mitotic recombination. A clonal theory proposed for some parasitic protozoa including *Giardia* does not state that sex is totally absent but rather that it is too rare to break a prevailing pattern of clonal population structure (Tibayrenc and Ayala 2002).

Cell-cycle-dependent nuclear asynchrony

In mitotic cells, asymmetries between karyotypes are accompanied by two short phases of asynchrony between otherwise synchronously dividing nuclei. The significance of these phenomena for the *Giardia* cell is unknown, although some benefits could be expected. Mitotic silencing of gene transcription seems to be ubiquitous among eukaryotic cells (Gottesfeld and Forbes 1997). Therefore, an early-prophase asynchrony might allow transcription from the slower progressing nucleus even if the partner nucleus has already

entered mitosis. It is interesting to note that the slower progressing *Giardia* nucleus was that with the higher chromosome number. Our data from LSC provide convincing evidence that the two *Giardia* nuclei are also asymmetric as to their DNA content. Surprisingly, variability in the DNA content does not correlate with a stable chromosome number. A possible explanation could come from asynchrony in DNA replication currently demonstrated by BrdU incorporation experiments. From the BrdU incorporation, we cannot determine the timing of the replication; however, it is obvious that in agreement with earlier studies (Wiesehahn et al. 1984), at least in one-third of interphase cells one nucleus starts replication earlier than the other one. Asynchrony during key phases of the *Giardia* cell cycle (S-phase, mitosis) indicates that despite the karyotype differences, both nuclei may complement for at least some basic functions, which might be a reason to keep the set of single-copy genes in each of them (Yu et al. 2002).

In summary, we have found that the binucleated *Giardia* cell possesses two asymmetrical nuclei as to their karyotypes and DNA content, which behave partly asynchronously during the S- and M-phases of the cell cycle. The karyotype differences may reflect evolutionary divergence between the nuclei. To what extent they are different and whether the differences allow the consideration of *Giardia* as an organism carrying two genomes need further studies.

References

Adam RD (1992) Chromosome-size variation in *Giardia lamblia*—the role of rDNA repeats. Nucleic Acids Res 20:3057–3061
Adam RD (2000) The *Giardia lamblia* genome. Int J Parasitol 20:475–484
Adam RD (2001) Biology of *Giardia lamblia*. Clin Microbiol Rev 14:447–475
Adam RD, Nash TE, Wellems TE (1988) The *Giardia lamblia* trophozoite contains sets of closely related chromosomes. Nucleic Acids Res 16:4555–4567
Ali SA, Hill DR (2003) *Giardia intestinalis*. Curr Opin Infect Dis 16:453–460
Arkhipova IR, Morrison HG (2001) Three retrotransposon families in the genome of *Giardia lamblia*: two telomeric, one dead. Proc Natl Acad Sci U S A 98:14497–14502
Baruch AC, Isaac-Renton J, Adam RD (1996) The molecular epidemiology of *Giardia lamblia*: a sequence-based approach. J Infect Dis 174:233–236

Bernander R, Palm JED, Svärd SG (2001) Genome ploidy in different stages of the *Giardia lamblia* life cycle. Cell Microbiol 3:55–62

Birky CW (2005) Sex: is *Giardia* doing it in the dark? Curr Biol 15:56–58

Brugerolle G (1975) Contribution à l′étude cytologique et phylétique des diplozoaires (Zoomastigophorea, Diplozoa, Dangeard 1910). V. Nouvelle interprétation de l′organisation cellulaire de *Giardia*. Protistologica 11:99–109

Brugerolle G (1991) Flagellar and cytoskeletal systems in amitochondrial flagellates: Archamoeba, Metamonada and Parabasala. Protoplasma 164:70–90

Cavalier-Smith T (1995) Cell cycles, diplokaryosis and the archezoan origin of sex. Arch Protistenkd 145:189–207

Červa L, Nohýnková E (1992) A light microscopic study of the course of cellular division of *Giardia intestinalis* trophozoites grown in vitro. Folia Parasitol 39:97–104

Coppel RL, Black CG (2005) Parasite genomes. Int J Parasitol 35:465–479

Elmendorf HG, Singer SM, Nash TE (2000) Targeting of proteins to the nuclei of *Giardia lamblia*. Mol Biochem Parasitol 106: 315–319

Elmendorf HG, Dawson SC, McCaffery JM (2003) The cytoskeleton of *Giardia lamblia*. Int J Parasitol 33:3–28

Erlandsen SL, Rasch EM (1994) The DNA content of trophozoites and cysts of *Giardia lamblia* by microdensitometric quantitation of Feulgen staining and examination by laser scanning confocal microscopy. J Histochem Cytochem 42:1413–1416

Ersfeld K, Melville SE, Gull K (1999) Nuclear and genome organization of *Trypanosoma brucei*. Parasitol Today 15:58–63

Fan JB, Korman SH, Cantor CR, Smith CL (1991) *Giardia lamblia*: haploid genome size determined by pulse field gel electrophoresis is less than 12 Mb. Nucleic Acids Res 19:1905–1908

Filice FP (1952) Studies on the cytology and life history of a *Giardia* from the laboratory rat. Univ Calif Publ Zool 57:53–146

Gaunt MW, Yeo M, Frame IA, Stothard JR, Carrasco HJ, Taylor MC, Mena SS, Veazey P, Miles GAJ, Acosta N, Arias AR, Miles MA (2003) Mechanism of genetic exchange in American trypanosomes. Nature 421:936–939

Gillin FD, Boucher SE, Rossi SS, Reiner DS (1989) *Giardia lamblia*: the roles of bile, lactic acid, and pH in the completion of the life cycle in vitro. Exp Parasitol 69:164-174

Gillin DF, Reiner DS, McCaffery JM (1996) Cell biology of the primitive eukaryote *Giardia lamblia*. Annu Rev Microbiol 50:679–705

Gong N, Yang H, Zhang G, Landau BJ, Guo X (2004) Chromosome inheritance in triploid Pacific oyster *Crassostrea gigas* Thunberg. Heredity 93:408–415

Gottesfeld JM, Forbes DJ (1997) Mitotic repression of the transcriptional machinery. Trends Biochem Sci 22:197–202

Gull K, Alsford S, Ersfeld K (1998) Segregation of minichromosomes in trypanosomes: implications for mitotic mechanisms. Trends Microbiol 6:319–323

Hou G, Le Blancq M, Yaping E, Zhu H, Lee MG (1995) Structure of a frequently rearranged rRNA-encoding chromosome in *Giardia lamblia*. Nucleic Acids Res 23:3310–3317

Kabnick KS, Peattie DA (1990) In situ analyses reveal that the two nuclei of *Giardia lamblia* are equivalent. J Cell Sci 95:353–360

Keister DB (1983) Axenic culture of *Giardia lamblia* in TYI-S-33 medium supplemented with bile. Trans R Soc Trop Med Hyg 77:487–488

Kofoid CA, Christiansen EB (1915) On binary and multiple fission in *Giardia muris* (Grassi). Univ Calif Publ Zool 16:30–54

Kolisko M, Cepicka I, Hampl V, Kulda J, Flegr J (2005) The phylogenetic position of enteromonads: a challenge for the present models of diplomonad evolution. Int J Syst Evol Microbiol 55:1729–1733

Le Blancq SM, Adam RD (1998) Structural basis for karyotype heterogeneity in *Giardia lamblia*. Mol Biochem Parasitol 97:199–208

Lloyd D, Harris JC (2002) *Giardia*: highly evolved parasite or early branching eukaryote? Trends Microbiol 10:122–127

McArthur AG, Morrison HG, Nixon JEJ, Passamaneck NQE, Kim U, Hinkle G, Crocker MK, Holder ME, Farr R, Reich CI et al (2000) The *Giardia* genome project database. FEMS Microbiol Lett 189:271–273

Monis PT, Mayerhofer G, Andrews RH, Homan WL, Limper L, Ey PL (1996) Molecular genetic analysis of *Giardia intestinalis* isolates at the glutamate dehydrogenase locus. Parasitology 112:1–12

Monis PT, Andrews RH, Mayerhofer G, Ey PL (2003) Genetic diversity within the morphological species *Giardia intestinalis* and its relationship to host origin. Infect Genet Evol 3:29–38

Nohýnková E, Dráber P, Reischig J, Kulda J (2000) Localization of gamma-tubulin in interphase and mitotic cells of a unicellular eukaryote, *Giardia intestinalis*. Eur J Cell Biol 79:438–445

Nohýnková E, Tůmová P, Kulda J (2006) Cell division of *Giardia intestinalis*: flagellar developmental cycle involves transformation and exchange of flagella between mastigonts of a diplomonad cell. Eukaryot Cell 5:753–761

Passarge E (1974) Analysis of chromosomes in mitosis and evaluation of cytogenetic data. In: Schwarzacher HG, Wolf U (eds) Methods in human cytogenetics. Springer, Berlin Heidelberg New York, pp 135–205

Prowazek S, Werner H (1914) Zur Kenntnis der sog. Flagellaten. Arch Schiffs Tropenhyg 18:311–326

Raikov IB (1982) The protozoan nucleus. Morphology and evolution. Springer Verlag, Wien, New York

Raikov IB (1994) The diversity of forms of mitosis in Protozoa: a comparative review. Eur J Protistol 30:253–269

Ramesh MA, Malik SB, Logsdon JM (2005) A phylogenetic inventory of meiotic genes: evidence for sex in *Giardia* and an early eukaryotic origin of meiosis. Curr Biol 15:185–191

Ravel C, Debussay P, Blackwell JM, Ivens AC, Bastien P (1998) The complete chromosomal organization of the reference strain of the *Leishmania* genome project, *L.major* 'Friedlin'. Parasitol Today 14:301–303

Rodenwaldt E (1912) Flagellaten (*Trichomonas*, *Lamblia*). In: von Prowazek S (ed) Handbuch der Pathogenen Protozoen. Barth, Leipzig

Roger AJ, Svärd SG, Tovar J, Clark CG, Smith MW, Gillin FD, Sogin ML (1998) A mitochondrial-like chaperonin 60 gene in *Giardia lamblia*: evidence that diplomonads once harbored an endosymbiont related to the progenitor of mitochondria. Proc Natl Acad Sci U S A 95:229–234

Rosenbusch B (2004) The incidence of aneuploidy in human oocytes assessed by conventional cytogenetic analysis. Hereditas 141: 97–105

Siddall ME, Hong H, Desser SS (1992) Phylogenetic analysis of the Diplomonadida (Wenyon, 1926) Brugerolle, 1975: evidence for heterochrony in protozoa and against *Giardia lamblia* as a "missing link". J Protozool 39:361–367

Sola L, Rossi AR, Iaselli V, Rasch EM, Monaco PJ (1992) Cytogenetics of bisexual/unisexual species of *Poecilia*. II. Analysis of heterochromatin and nucleolar organizer regions in *Poecilia mexicana mexicana* by C-banding and DAPI, quinacrine, chromomycin A3, and silver staining. Cytogenet Cell Genet 60:229–235

Sumner AT (1972) A simple technique for demonstrating centromeric heterochromatin. Exp Cell Res 75:304–306

Svärd SG, Hagblom P, Palm JED (2003) *Giardia lamblia*—a model organism for eukaryotic cell differentiation. FEMS Microbiol Lett 218:3–7

Šedinová J, Flegr J, Ey P, Kulda J (2003) Use of random amplified polymorphic DNA (RAPD) analysis for the identification of

Giardia intestinalis subtypes and phylogenetic tree construction. J Eukaryot Microbiol 50:198–203

Taylor SS, Scott MIF, Holland AJ (2004) The spindle checkpoint: a quality control mechanism which ensures accurate chromosome segregation. Chromosome Res 12:599–616

Thompson RCA, Monis PT (2004) Variation in *Giardia*: implications for taxonomy and epidemiology. Adv Parasitol 58:69–137

Tibayrenc M, Ayala FJ (2002) The clonal theory of parasitic protozoa: 12 years on. Trends Parasitol 18:405–410

Tovar J, Leon-Avila G, Sanchez LB, Šuták R, Tachezy J, Giezen N, Hernandez M, Miller M, Lucocq JM (2003) Mitochondrial remnant organelles of *Giardia intestinalis* function in iron sulphur protein maturation. Nature 426:172–174

Upcroft JA, Chen NH, Upcroft P (1996) Mapping variation in chromosome homologues of different *Giardia* strains. Mol Biochem Parasitol 76:135–143

Upcroft P, Upcroft JA (1994) Two distinct varieties of *Giardia* in a mixed infection from a single human patient. J Eukaryot Microbiol 41:189–194

Upcroft P, Upcroft JA (1999) Organization and structure of the *Giardia* genome. Protist 150:17–23

Upcroft JA, Abedinia M, Upcroft P (2005) Rearranged subtelomeric rRNA genes in *Giardia duodenalis*. Eukaryot Cell 4:484–486

Wickstead B, Ersfeld K, Gull K (2003) Repetitive elements in genomes of parasitic protozoa. Microbiol Mol Biol Rev 67:360–375

Wiesehahn GP, Jarroll EL, Lindmark DG, Meyer EA, Hallick LM (1984) *Giardia lamblia*: autoradiographic analysis of nuclear replication. Exp Parasitol 58:94–100

Yang YM, Adam RD (1994) Allele-specific expression of a variant-specific surface protein (VSP) of *Giardia lamblia*. Nucleic Acids Res 22:2102–2108

Yang YM, Adam RD (1995) A group of *Giardia lamblia* variant-specific surface protein (VSP) genes with nearly identical 5′ regions. Mol Biochem Parasitol 75:69–74

Yu LZ, Birky CW, Adam RD (2002) The two nuclei of *Giardia* each have complete copies of the genome and are partitioned equationally at cytokinesis. Eukaryot Cell 1:191–199

Giardia intestinalis: Aphidicolin influence on the trophozoite cell cycle

Klára Hofštetrová [a], Magdalena Uzlíková [a], Pavla Tůmová [a], Karin Troell [b], Staffan G. Svärd [b,c], Eva Nohýnková [a,*]

[a] 3rd Department of Infectious and Tropical Diseases, First Faculty of Medicine, Charles University in Prague and University Hospital Bulovka, Czech Republic
[b] Department of Cell and Molecular Biology, Uppsala University, SE-751 24 Uppsala, Sweden
[c] Microbiology and Tumor Biology Center, Karolinska Institute, SE-171 77 Stockholm, Sweden

ABSTRACT

This study is a thorough examination of the effects of the DNA polymerase inhibitor aphidicolin on the nuclear cycle and cell cycle progression characteristics, as well as their reversibility, in *Giardia intestinalis*. *Giardia* trophozoites are arrested in the G1/S-junction after aphidicolin treatment according to their DNA content. However, cell growth continues and trophozoites arrested with aphidicolin resemble cells in the G2 phase and trophozoites in ageing cultures. Extensive treatment with aphidicolin causes side effects and we detected positive signals for phosphorylated histone H2A, which, in mammalian cells, is involved in a signalling pathway triggered as a reaction to double stranded DNA breaks. These results suggest that aphidicolin causes dissociation of the nuclear and cytoplasmic cycles, a phenomenon that has also been described for other inhibitors in mammalian cell lines. Thus, if aphidicolin is used for synchronization of *Giardia* trophozoites, this fact must be accounted for, and treatment with aphidicolin must be minimal.

© 2009 Elsevier Inc. All rights reserved.

1. Introduction

Aphidicolin (APH) is a mycotoxin from a group of tetracyclic diterpenoids produced by the fungi *Cephalospora aphidicola* or *Nigrospora oryzae* (Spadari et al., 1982). It induces replication fork stalling and inhibition of DNA replication due to its competitive binding with dNTP to eukaryotic DNA α polymerase when applied to most eukaryotic organisms (Huberman, 1981; Spadari et al., 1982). Aphidicolin has been used more or less successfully as a tool for cell cycle synchronization in various cell lines, including plant and vertebrate cells (Samuels et al., 1998; Uzbekov et al., 1998; Kues et al., 2000). After aphidicolin treatment, cells are arrested at the G1/S phase border, and after being released from this block, they are supposed to move to S phase and G2 as a synchronized population. However, the level of synchronization is often significantly reduced after one cell cycle (O'Connor and Jacman, 1996).

Synchronized cell populations are needed when studying processes dependent on a specific cell cycle stage. However, it is necessary to be aware of the various negative side effects of the drugs employed for synchronization on cell structures and functions. Aphidicolin induces chromosomal gaps and DNA double strand breaks, especially at common fragile sites (Glover et al., 1984; Glover, 2006). Fragile sites in general are difficult to replicate,

and their slow replication is further exacerbated in the presence of aphidicolin: therefore many fragile sites remain unreplicated in G2 (Zlotorynski et al., 2003). Gaps and breaks on fragile sites may further lead to chromosome lesions, deletions and translocations, which are detected even in cells released from aphidicolin (Carme et al., 1999). There is also evidence that aphidicolin can cause dissociation of nuclear and cytoplasmic cycles (Urbani et al., 1995; Cooper, 2001), Aphidicolin has been used for studying the cell cycles of some parasitic protozoa. In a dose-dependent manner, it reversibly inhibits replication and cell division in two amoeba species, *Entamoeba histolytica* (Makioka et al., 1998) and *Entamoeba invadens* (Kumagai et al., 1998), the malaria parasite *Plasmodium falciparum* (Abu-Elheiga et al., 1990; Choi and Mikkelsen, 1991; Chavalitshewinkoon et al., 1993) and in *Trypanosoma brucei* (Ploubidou et al., 1999).

Recently, it has been used for synchronization of *Giardia* trophozoites (Reiner et al., 2008; Poxleitner et al., 2008). Reiner et al. (2008) used synchronization method with the effective aphidicolin concentration for the time equal to the duration of one cell cycle. Poxleitner et al. (2008) pretreated trophozoites with nocodazole, which blocked them in G2 phase and then treated the cells with aphidicolin also for the time corresponding to the duration of one cell cycle. *Giardia intestinalis* is a parasitic diplomonad that infects the small intestine of humans or other mammals and causes diarrhoea. Its life cycle comprises two stages: a binucleated flagellated trophozoite (the pathogenic stage) that multiplies by binary fission in the intestinal lumen and a quadrinucleated cyst (the

infectious stage) that is discharged with faeces (Thompson, 2004). Although our knowledge regarding this parasitic protist has increased in many aspects, including the completed genome project, cell cycle progression in *Giardia* has not yet been satisfactory described even on a structural basis. This appears to be an important task because identification of similarities or differences between *Giardia* and human cell cycles may lead to the possibility of parasite-unique cell cycle regulators as new drug targets (Hammarton et al., 2003).

The aim of this study is to examine the effect of the synchronization drug aphidicolin on individual cell characteristics during the cell cycle of *Giardia* trophozoites, in order to find out to what extent and for which parameters the population can be regarded as synchronized.

2. Materials and methods

2.1. Cell cultures

The HP-I line of the Portland-1 isolate of *G. intestinalis* (ATCC 30888), donated by E.A. Meyer (Oregon Health Sciences University, Portland, USA), was used in the study. Trophozoites were grown axenically in 13×100 mm screw cap tubes in a filter-sterilised TYI-S-33 medium supplemented with bovine bile (Keister, 1983) at 37 °C and sub-cultured twice a week.

2.2. Effect of aphidicolin on cell population growth and its reversibility

A stock solution of 1 mg/ml aphidicolin from *Nigrospora sphaerica* (Sigma) was prepared in sterile dimethyl sulphoxide (DMSO) (Sigma) and stored in aliquots at −20 °C. To study the effect of aphidicolin on cell population growth in *Giardia*, trophozoites were incubated with 5 or 10 µg/ml aphidicolin. Control cultures were grown without drug. These concentrations were chosen as optimal reversible (5 µg/ml) and irreversible aphidicolin (10 µg/ml) dose, according to preliminary experiments with various concentrations (data not shown). For experiments 1.0×10^4 trophozoites in 100 µl TYI-S-33 were inoculated per well into 96-well microplates (Costar) and incubated under anaerobic conditions (<1% O_2, 9–13% CO_2 generated by AnaeroGen Oxoid) in an Anaerobic Jar (Oxoid) at 37 °C in TYI-S-33 for 6, 12, 24 and 48 h. For testing the reversibility, medium with aphidicolin was replaced with fresh medium without drug after 6, 12, 24 and 48 h of incubation in the presence of the drug, and trophozoites were further incubated in the drug free medium for the next 12 or 24 h. Cells were harvested at each time interval and counted in a hemocytometer. Each interval count was done in triplicate and the average is shown.

2.3. Preparations for measuring cell size

Trophozoites were incubated in 24-well microplates (Costar) on coverslips under the same conditions and harvested in the same intervals as stated above. For measurement of cell size, wet mounts prepared from the attached cells were fixed in sublimate-alcohol and stained with the standard procedure by the Trichrom-Gömori (Gomori, 1953). Cell size (length and width) of 100 cells per each aphidicolin concentration and interval was measured and analysed using an Olympus BX40 light microscope and QuickPhoto Micro 2.2. and ImageJ software (NIH, USA).

2.4. Western blot

Protein lysates from the same number of aphidicolin-treated (5 µg/ml) and control cells at the intervals stated above, were prepared by mixing the washed pellet with sample buffer (30% glycerol/10% SDS/2-β-mercaptoethanol/0.05% Bromphenol blue/50 mM Tris–HCl, pH 6.8) and boiling the suspension for 5 min in a water bath. Proteins were separated on 12% SDS–PAGE and transferred onto nitrocellulose membrane. Blocking of the membrane was performed in 3% BSA/PBS for 1 h at RT. Primary antibody to cyclin B1 (Abcam) was diluted 1:5000 and the membrane was incubated with the antibody 1 h at RT. Following washes, the membrane was incubated with the secondary antibody anti-mouse IgG conjugated with alkaline phosphatase (Sigma) diluted 1:1000. Following washes, blots were developed using Sigma Fast™ BCIP/NBT (5-bromo-4-chloro-3-indolyl phosphate/Nitro blue tetrazolium) according to the manufacturer's instructions.

2.5. Immunofluorescence labelling

2.5.1. Median body

To determine the presence of a median body, immunofluorescence staining was carried out according to Nohynkova et al. (2000). Attached cells on coverslips were fixed with ice-cold methanol (at −20 °C for 5 min), permeabilised with ice-cold acetone (at −20 °C for next 5 min), re-hydrated in phosphate-buffer saline (PBS) at pH 7.2 (10 min) and blocked with 3% bovine serum albumin BSA/PBS (30 min). They were incubated with antibody against acetylated α-tubulin (6-11-B-1, Sigma) diluted 1:100 in 2% BSA/PBS for 1 h at room temperature (RT), washed three times with PBS pH 7.2 and incubated with secondary antibody diluted 1:100 in 2% BSA/PBS (anti-mouse IgG FITC, Sigma) for 1 h at RT, washed three times with PBS pH 7.2 and finally mounted in Vectashield mounting media with DAPI (Vector). Figures were captured with the same microscope as stated above as well as the camera Olympus DP 70 and the program DP Manager.

2.5.2. Detection of phosphorylated histone H2A in Giardia cells

To determine the occurrence of damaged DNA, we used an antibody against phosphorylated histone H2A, a DNA double strand break marker. Attached cells on coverslips were fixed with ice-cold methanol (at −20 °C for 5 min), permeabilised with ice-cold acetone (at −20 °C for the next 5 min), and air dried. The cells were re-hydrated with PBS, pH 7.2 for 10 min and then blocked with 5% goat serum albumin in PBS for 60 min. As the following step cells were incubated with primary antibody against phosphorylated Ser139 in human histone H2AX (AR-0149, LP BIO) diluted 1:250 in 2% BSA/0.1% Triton X-100/PBS for 90 min. After washing (three times with PBS, each 10 min), they were incubated with a secondary antibody (goat anti-rabbit IgG H&L/FITC, Abcam) diluted 1:200 with 2% BSA/0.1% Triton X-100/PBS for 60 min. The cells were washed three times and mounted in Vectashield mounting media with DAPI (Vector). The affected (signal in one or both nuclei) and unaffected nuclei were counted in a total of 200 cells per each examined condition.

2.5.3. Mitotic index

To count the mitotic index, cells attached on coverslips (after 12 and 24 h incubation with aphidicolin and 1, 2, 4, 6, 12 and 24 h after release from aphidicolin and incubation in fresh media without drug) were fixed with ice-cold methanol (at −20 °C for 5 min), permeabilised with ice-cold acetone (at −20 °C for the next 5 min), and air dried. Cells were then mounted in Vectashield mounting media with DAPI (Vector). The number of mitotic figures was counted in a total number of 500 cells per interval.

2.5.4. Detection of DNA synthesis

DNA synthesis was visualized using an immunofluorescence assay for the detection of 5-bromo-2′-deoxy-uridine (BrdU) incorporated into DNA (5-bromo-2′-deoxy-uridine Labeling and Detection Kit I, Roche). Trophozoites were processed according to the manu-

facturer's protocol in intervals of 6 and 24 h. Briefly, trophozoites were incubated with 10 mM BrdU labelling reagent in an anaerobic chamber (Červa and Nohýnková, 1992) for 50 min, rinsed three times in washing buffer and fixed in 70% ethanol/50 mM glycine–HCl (pH 2.0), −20 °C for 30 min. After rinsing with washing buffer the fixed cells were incubated with anti BrdU antibody (diluted 1:10 with 66 mM Tris/0.66 mM $MgCl_2$/2-mercaptoethanol) in a wet chamber (at 37 °C, 30 min), rinsed three times in washing buffer and incubated with secondary antibody conjugated with fluorescein (diluted 1:10 in washing buffer) at 37 °C, 30 min and finally rinsed three times with washing buffer and mounted in Vectashield with DAPI (Vector). The number of positive cells (signal in one or both nuclei) was counted in a total of 200 cells.

2.6. Flow cytometry analysis

For flow cytometry, trophozoites treated with 5 μg/ml of aphidicolin for 6, 12 and 24 h were fixed and stained according to Bernander et al. (2001). Briefly, for each interval, cells were harvested by centrifugation (900g), with a cell concentration of approximately 1×10^7 cells/ml. The pellet was resuspended in 50 μl fresh TYI-S-33 and 150 μl fixative (1% Triton X-100/40 mM citric acid/20 mM dibasic sodium phosphate/200 mM sucrose, pH 3.0) and fixed for 5 min at room temperature. Then 350 μl of diluent buffer (125 mM $MgCl_2$ in PBS, pH 7.4) was added, and samples were stored at 4 °C until measurement. Fixed cells were centrifuged (4000g/3 min), washed in PBS, then resuspended in 500 μl PBS with 1 μg RNAse A (Boehringer, Mannheim) and incubated at 37 °C for 30 min. Then, cells were centrifuged, resuspended in a 10 mM Tris/10 mM $MgCl_2$, 180 μg/ml mithramycin A and 4 μg/ml ethidium bromide solution (Skarstad et al., 1996) and stained for 30 min on ice. Flow cytometry was performed on an A40 Analyzer Flow Cytometer (Apoge Flow system, Hemel Hempstead, UK). The data were analysed using Apogee A40 Flow Cytometer v. 1.75 software.

3. Results

In different sets of experiments, we examined the effects of a reversible and irreversible aphidicolin concentrations on *Giardia* trophozoites, namely on their DNA synthesis, DNA damage and characteristics of cell cycle progression, i.e. cell population growth, mitotic index, cell size, level of cyclin B and presence of median bodies. We also studied the reversibility of these treatments.

3.1. Impact of 5 and 10 μg/ml aphidicolin after 6 h of treatment

Data from cell population growth expressed as a percentage of control growth showed that the propagation of cells treated with aphidicolin for 6 h dropped down to 87% (89% in cells treated with 10 μg/ml aphidicolin) (Fig. S1). No trophozoites going through mitosis were detected.

Flow cytometry analysis showed that in the aphidicolin-treated cells, the DNA content of a majority (almost 80%) of the cell population shifted to the G1/S phase junction, which led to a dramatic decrease in the number of cells with G2 + M DNA content (Fig. 1A). In comparison, the major part of the untreated population in logarithmic phase (approximately 70% cells) had a DNA content corresponding to cells in G2 + M (Fig. 1B). A positive signal for BrdU incorporation, representing the rate of the DNA synthesis, was detected in either one or both nuclei in 60% of cells treated with 5 μg/ml aphidicolin. However, this signal was much weaker than in control cells and appeared like single dots in the nuclei in comparison to the homogenous signal in the whole nuclei in control cells

(Fig. 2A and B). In cells treated with 10 μg/ml aphidicolin, no positive signal was detected (data not shown).

Phosphorylated H2A (either in one or both nuclei) was present in 55% (73% in cells treated with 10 μg/ml aphidicolin) of cells in comparison to controls where the fluorescence signal for phosphorylated H2A was detected in only 17% of trophozoites. In the
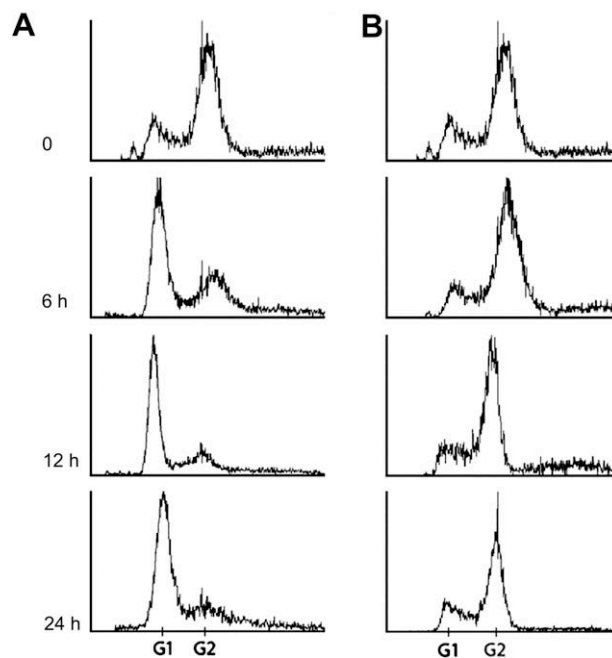

Fig. 1. Flow cytometric analysis of aphidicolin influence on the cell cycle of *Giardia intestinalis*. Trophozoites incubated with 5 μg/ml aphidicolin for 6, 12 and 24 h (A), and control trophozoites incubated without drug (B). Histograms represent DNA content.
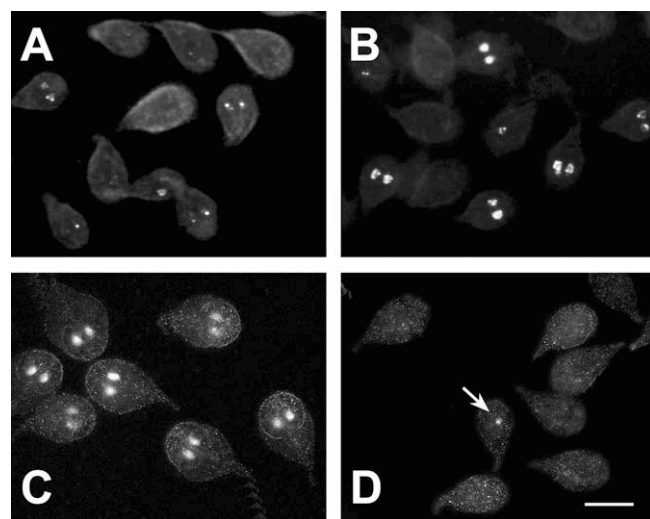

Fig. 2. Immunofluorescence detection of BrdU incorporation (A and B) and phosphorylation of histone H2A (C and D) in *Giardia* trophozoites. BrdU incorporation in cells treated with 5 μg/ml aphidicolin for 6 h is ceased so that the signal occurs only as few spots in the *Giardia* nuclei (A) in comparison with untreated cells where the strong fluorescence signal is evident (B). Trophozoites previously incubated with 5 μg/ml aphidicolin for 24 h show a positive staining for phosphorylated histone H2A in most cells and usually in bothe nuclei (C), whereas very few cells from the untreated population posses positive signals, usually single dots (arrow), only in one of the two nuclei (D). Bar represents 10 μm.

control cells, the positive signal was mostly in one of the two nuclei (Figs. 2C, D and 3A).

Treated trophozoites also showed differences in cell size; their lengths and widths were slightly larger in comparison to controls, and the size distribution was broader (Table S1). The presence of median bodies was slightly higher in aphidicolin-treated trophozoites, at 78% for 5 μg/ml, in comparison to 69% in the control population. There was no detectable difference in cyclin B levels in control and aphidicolin-treated cells (data not shown).

3.2. Impact of 5 and 10 μg/ml aphidicolin after 12 h of treatment

Trophozoite growth dropped further to 59% with 5 μg/ml aphidicolin treatment (43% in cells treated with 10 μg/ml) (Fig. S1). Cells treated with 5 μg/ml were still proliferating, although the growth almost fully stopped at a concentration of 10 μg/ml aphidicolin. The mitotic index was very low, at 0.2% for both concentrations (Fig. 4A).

The percentage of cells with a DNA content in the G1/S phase further increased after 12 h incubation (Fig. 1A). Phosphorylated H2A was detected in 74% of trophozoites treated with 5 μg/ml aphidicolin (87% with 10 μg/ml), and 69% of positively stained cells had positive signals in both nuclei at a concentration 5 μg/ml (75% for 10 μg/ml). In comparison, 14% of control cells showed a positive signal (Fig. 3B). Trophozoite size further increased in comparison to controls, by 13% in length and 15% in width for 5 μg/ml (Table S1). Median bodies were present in 98% for 5 μg/ml, in comparison to 59% in the control population. A slightly higher amount of cyclin B was detected in aphidicolin-treated cells (data not shown).

3.3. Impact of 5 and 10 μg/ml aphidicolin after 24 h of treatment

At this time point the impact on cells was more prominent in many aspects. Cell population growth dropped to 12% of control growth in trophozoites treated with 5 or 10 μg/ml aphidicolin (Fig. S1). The mitotic index remained very low at 0.2% (Fig. 4B).

A histogram of the DNA content showed a homogeneous population – 80% of cells displayed their DNA content in the G1/S phase (Fig. 1A). BrdU incorporation (even weaker signal than after 6 h) was detected in 69% of cells treated with 5 μg/ml aphidicolin (in cells treated with 10 μg/ml aphidicolin no positive signal was detected), and a full signal was present in 44% of control trophozoites. Phosphorylated H2A was detected in 99% of cells treated either with 5 or 10 μg/ml, with almost all of them in both nuclei, in comparison with controls where only 3% of trophozoites were positive (Fig. 3C).

The size of the trophozoites further increased in comparison to controls by 30% in cell length and 52% in cell width (for 5 μg/ml), and the size distribution was broader (Table S1). The presence of median bodies remained at 99% in the population treated with 5 μg/ml. Median bodies in aphidicolin-treated cells were larger in comparison to controls (Fig. 5). The control population had median bodies in 83% of the cells. The level of cyclin B in aphidicolin-treated cells was higher for this interval (data not shown).

3.4. Impact of 5 and 10 μg/ml aphidicolin after 48 h of treatment

Trophozoites after 48 h of incubation resembled trophozoites from the previous interval. Cell population growth dropped down to 8% (5 μg/ml) and 2% (10 μg/ml) of control growth (Fig. S1).
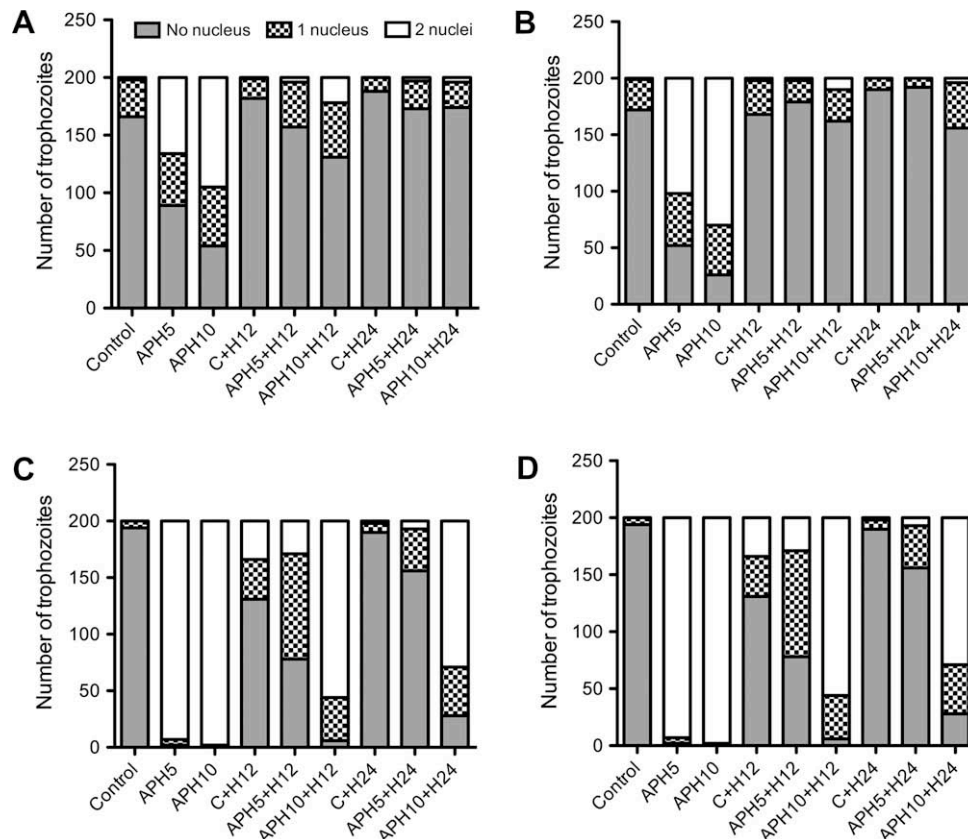

Fig. 3. Detection of phosphorylated histone H2A in *Giardia* trophozoites' nuclei. Trophozoites exposed to 5 (APH5) and 10 (APH10) μg/ml aphidicolin and control untreated cells incubated for 6 (A), 12 (B), 24 (C) and 48 (D) h, respectively, and the reversibility were followed in time intervals 12 (APH5 + H12; APH10 + H12; C + H12) and 24 (APH5 + H24; APH10 + H24; C + H24) h after release from aphidicolin. A positive signal was detected in either none, one or both nuclei. A total number of 200 trophozoites were counted per interval.
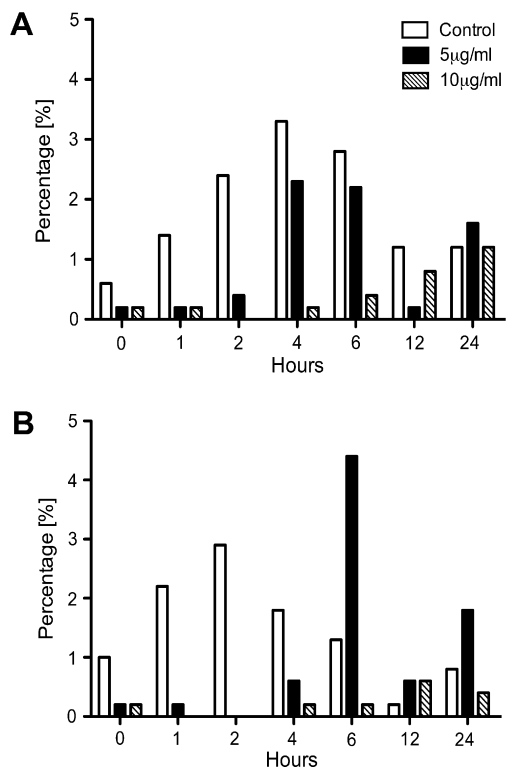
Fig. 4. Mitotic index. Percentage of trophozoites in mitosis during recovery from aphidicolin treatment. After initial incubation with aphidicolin for 12 (A) and 24 (B) h, the percentage of trophozoites undergoing mitosis is shown at intervals 1, 2, 4, 6, 12 and 24 h after release from aphidicolin block. Time interval 0 represents the moment of washing out media with aphidicolin. Total number of 500 trophozoites was counted for each interval.

Phosphorylated H2A was present in 99% of cells at 5 μg/ml, in 100% at 10 μg/ml (again in both nuclei) and in 4% of controls (Fig. 3D).

Trophozoites, however, did not stop to grow in cell size. The difference in cell size was significant in comparison to controls, and the size distribution of treated cells was still wider than that in control cells. Length was larger by 34% and width by 45% at 5 μg/ml, compared to controls (Table S1). A median body was present in 99% of aphidicolin-treated cells (for both concentrations) in comparison to 65% of controls and they were still much larger compared to controls.

3.5. Release after 6 h incubation with aphidicolin

The replacement of aphidicolin-containing medium resulted in increased cell population growth, although it was still slower than in controls (data not shown). The presence of a positive signal for phosphorylated H2A decreased significantly 12 h after release, from 55% to 21.5% in cells treated previously with 5 μg/ml (34.5% – 10 μg/ml; 9% – controls). After 24 h following aphidicolin replacement, phosphorylated H2A occurred in 13.5% cells treated previously with 5 μg/ml (13% – 10 μg/ml; 6% – controls) (Fig. 3A). However, we have also detected a positive signal for phosphorylated H2A in the dividing nuclei of trophozoites incubated previously with 10 μg/ml (Fig. S2).

Interestingly, the cell size was smaller in cells released from the aphidicolin block than in controls and the cell size distribution in these trophozoites was narrower, so it looks like these cells were more homogenous in cell size (Table S1). The presence of median bodies decreased in recovering cells (data not shown).

3.6. Release after 24 h of incubation with aphidicolin

Giardia trophozoites previously treated with 5 μg/ml were able to recover from this block, unlike cells treated with 10 μg/ml. The percentage of mitotic cells was the highest 6 h after medium replacement, at 4% in cells treated with 5 μg/ml aphidicolin, but stayed low in cells treated with 10 μg/ml aphidicolin (0.2%) (Fig. 4B).

The positive signal for phosphorylated H2A disappeared slower in comparison to the previous interval. It was present in 61.5% of cells treated with 5 μg/ml aphidicolin 12 h after media replacement (97% – 10 μg/ml; 35% – controls). After 24 h the positive signal was still detected in 22.5% of cells treated previously with 5 μg/ml (86% – 10 μg/ml; 5% – controls) (Fig. 3C). Again, a positive signal for phosphorylated H2A was detected in dividing nuclei in trophozoites incubated previously with 10 μg/ml aphidicolin. The cell size was variable and we could not detect any distinct changes.

4. Discussion

Until recently efficient tools for synchronization of *Giardia* trophozoites were absent. In order to perform experiments aimed at gene expression or studying cell cycle regulatory molecules, it is essential to work with a synchronized cell population. Two synchronizing methods for the *Giardia* population have been published and both of them used aphidicolin, either alone (Reiner et al., 2008) or in combination with the microtubule polymerization inhibitor nocodazole (Poxleitner et al., 2008). In our study, the effect of aphidicolin on *Giardia* trophozoites was tested in order to evaluate and better understand the consequences of these synchronization methods on individual *Giardia* trophozoites using an extended repertoire of cell biological characteristics.
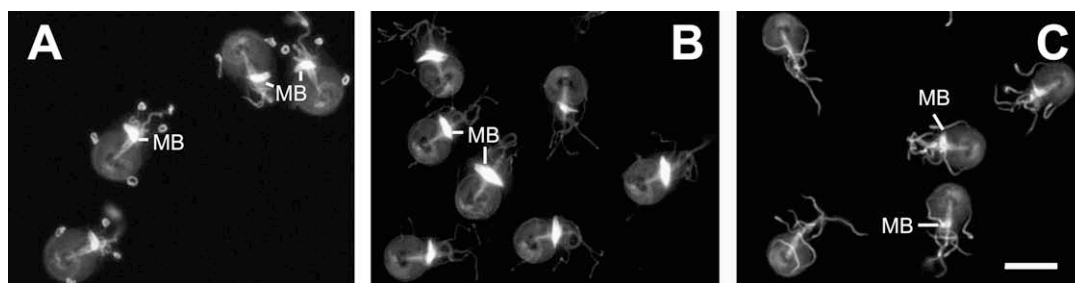

Fig. 5. Occurrence of median bodies. After 24-h incubation with 5 μg/ml aphidicolin, large median bodies are present in 99% trophozoites (A). Size and occurrence of the median bodies in the treated trophozoites are similar to those of untreated cells from ageing cultures after 72 h of cultivation (B). For comparison, control untreated trophozoites in log phase are included (C). MB: median body. Bar represents 10 μm.

4.1. The effect of aphidicolin on Giardia cell population growth

As already reported in Reiner et al. (2008) and Poxleitner et al. (2008), our study confirmed that the effect of aphidicolin on cell population growth in *Giardia* is highly concentration- and time-dependent, similar to other anaerobic protists, *E. histolytica* (Makioka et al., 1998) or *E. invadens* (Kumagai et al., 1998). However, the opinions differ on optimal (efficient but not harmful) drug concentrations in *Giardia*. Our results show that *Giardia* trophozoites can divide, grow and recover without abnormalities after up to 12 h of incubation with a concentration of 5 µg/ml aphidicolin. This is in agreement with Reiner et al. (2008), but in contrast to Poxleitner et al. (2008), who claimed that trophozoites cannot survive with aphidicolin concentrations higher than 6 µM (2.03 µg/ml). Indeed, there is a difference in the parasite isolate used in this study, but this cannot explain the different results of Reiner and Poxleitner since they used even the same clone (C6) of isolate WB. According to our results, irreversible influence on cell population growth is a consequence of a higher concentration (10 µg/ml aphidicolin); further, a very small population can divide even released from this concentration. However, the presence of phosphorylated H2A in the dividing nuclei in some of these cells indicates that they enter M phase without repairing damaged DNA. Defects in mitotic checkpoint can be also found in other anti-cancer drugs (Cheung et al., 2005) or in cancer cells (Michel et al., 2004).

4.2. DNA replication block due to aphidicolin treatment

It is widely accepted that aphidicolin inhibits DNA replication in eukaryotic cells and this effect is used for arresting cells at the G1/S phase border (Pedrali-Noy and Spadari, 1979; Patel et al., 1997; Speit and Schütz, 2008). Prolonged stalling of the DNA replication fork as a result of aphidicolin treatment may result in DNA damage and checkpoint activation in HeLa cells (Liu et al., 2003). Using two approaches – BrdU incorporation and flow cytometry analysis – to study DNA replication, we confirmed that DNA synthesis in *Giardia* trophozoites is stopped during aphidicolin treatment, similar to the *Xenopus* cell line XL2 (Uzbekov et al., 1998), the mouse C2C12 myoblast (Görisch et al., 2008) and other organisms and cell types. Flow cytometry analysis showed that the majority of *Giardia* cells treated with aphidicolin shifted to a peak corresponding to DNA content at the G1/S phase, as was also previously shown by Reiner et al. (2008) and Poxleitner et al. (2008); however, there is usually a small population (15%) of cells staying in G2.

4.3. DNA damage due to aphidicolin treatment

More recently, further effects of aphidicolin were revealed, e.g. inducing gaps and breaks and double strand breaks (DSB) on specific common fragile sites and delaying replication (Glover, 2006; Kurose et al., 2006; Liu et al., 2003). A phosphorylated variant of histone H2AX is involved in a signalling pathway triggered as a reaction to DSB in mammalian cells (Zhou and Elledge, 2000; Pilch et al., 2003; Kurose et al., 2006). *Giardia* has two copies of the core histone H2A (Wu et al., 2000; Yee et al., 2007). The sequences show clear similarity to histones known from other eukaryotes and near its C-terminus it contains the same SQ motif, which is characteristic for and phosphorylated in the variant H2AX in response to DNA damage (Chambers and Downs, 2007). We found that this post-translational modification of histone H2A is induced in *Giardia* exposed to aphidicolin We also demonstrated that phosphorylated forms of H2A occur naturally in *Giardia* cells during routine culture cultivation (mostly in only one of the two nuclei), especially in stationary phase cells. It is, however, rapidly induced and enhanced significantly under aphidicolin influence after short incubation times as early as 1 h (data not shown).

To our knowledge there is no direct evidence that the aphidicolin molecule itself causes DNA damage. DSB can also result from stalled and collapsed replication forks due to aphidicolin influence (Marusyk et al., 2007). As unrepaired or incorrectly repaired DNA lesions or chromosomal aberrations can lead to cancer or cell death (Zhou and Elledge, 2000), in response to such DNA disorders like DSB, cells have developed highly sophisticated systems to recognize DSB and arrest cell cycle until the lesions are corrected. In *Giardia* cells during replacement of the histone H2A after the release from aphidicolin trophozoites reenter cell division, which might indicate that DSB are repaired through DNA repair machinery. We suppose that this block of mitotic entry after aphidicolin-mediated DNA damage and following reentry into mitosis after the release from aphidicolin is a strong indication for the presence of a DNA damage checkpoint in *Giardia*. However, further studies are clearly needed to demonstrate whether components of a DNA damage checkpoint signalling cascade are activated in *Giardia* in response to exposure to aphidicolin.

Interestingly, we found that the phosphorylated form of H2A does not occur in both nuclei equally, with frequently only one nucleus found to be positive. As already described earlier, during DNA replication and mitosis (Tumová et al., 2007a; Wiesehahn et al., 1984), the two nuclei in *Giardia* do not start and replicate synchronously. The importance of such asynchronicity of *Giardia* nuclei within the cell cycle remains unclear.

4.4. Dissociation of nuclear and cytoplasmic cycles

Whereas DNA replication and entry into mitosis (cell population growth) in *Giardia* trophozoites has stopped as discussed above, other cell cycle processes continue. A gradually increasing cell size that becomes even bigger than that of untreated G2 trophozoites, together with significantly higher protein content in treated cells, suggests that the nuclear and cytoplasmic cycles are dissociated. Increasing cell size has already been documented in sea urchin embryos (Sluder and Lewis, 1987), *Paramecium caudatum* or bloodstream forms of *T. brucei* under aphidicolin influence (Sabaneyeva et al., 1999; Mutomba and Wang, 1996). An increased cell size has also been detected in senescent cells in mammalian cell cultures (Campisi et al., 1996), in mother cells of *Saccharomyces cerevisiae* when approaching the end of the replicative life span (Henderson and Gottschling, 2008) and in human fibroblasts treated with hydroxyurea, which are reminiscent of senescent cells in morphology and replicative potential (Yeo et al., 2000). Therefore, it seems that cells that cannot enter mitosis for some reason (activated checkpoint due to the presence of inhibitor, lack of nutrients, senescent cells) continue synthesizing proteins and increasing in cell size. Additionally we assume that, in *Giardia*, as a consequence of this continuing cytoplasmic cycle, a high percentage of aphidicolin-treated cells contains median bodies (almost 100% of cells), and that these median bodies are also bigger than those in controls are. The median body is a microtubular structure unique to the genus *Giardia*. It is composed from a bulk of short cytoplasmic microtubules that likely represent a pool of microtubules for assembly of new adhesive daughter disks, another organelle unique to *Giardia*, during cell division (Soloviev, 1963). Indeed, during the normal cell cycle, the organelle undergoes assembly and disassembly in parallel with cell cycle progression (Tumová et al., 2007b). In this respect, the median body can be considered a mark for cell (cytoplasmic) cycle progression in *Giardia* trophozoites. It seems that the process of microtubule polymerization in median bodies continues longer than under normal conditions because, due to DNA damage checkpoint activation, the mitosis is not started. Similarly, aphidicolin-treated cells

resemble stationary (senescent) trophozoites in that they posses median bodies (mainly large ones) in 98% of the trophozoites.

We found higher levels of mitotic cyclin B in cells treated with aphidicolin for 24 h in comparison with control cells. Higher transcriptional upregulation of cyclin B1 in aphidicolin-treated cells was also observed by Menges et al. (2005) in *Arabidopsis* cell cultures. Culligan et al. (2006) suggest that cyclin B1 might play an additional role in damage response. Kung et al. (1993) and Urbani et al. (1995) detected higher levels of cyclin B in Chinese hamster ovary cells and HeLa cells. This would support the idea that aphidicolin can cause dissociation of the nuclear and cytoplasmic cycles. In unperturbed cells, cyclin B appears at the end of S phase and reaches peak expression during G2 and M phase (Piaggio et al., 1995; Uzbekov et al., 1998).

4.5. Release from aphidicolin block

We found the effect of aphidicolin on *Giardia* trophozoites to be fully reversible after washing-off the drug, respective to incubation length and aphidicolin concentration. In accordance with Poxleitner et al. (2008) we detected the peak of mitotic entry at approximately 5 h after aphidicolin release. Surprisingly, we detected that a minority of released trophozoites are able to undergo mitosis even with damaged DNA, i.e. they override the DNA damage checkpoint. However, the viability of such trophozoites is not known.

To sum up the reaction of individual *Giardia* trophozoites to aphidicolin, cells treated with aphidicolin for 6 h decrease mitosis and cytokinesis and accumulate in G1/S. Phosphorylated H2A starts appearing, indicating DNA damage. Nevertheless, the cell size and presence of median bodies do not differ. After 12 h treatment, cell population growth continues to decrease and the population in G1 increases, as does the positivity for phosphorylated H2A, the larger cell size, and the occurrence and size of median bodies. After 24 h, cell population growth has almost completely ceased, and a major part of the cellular population stays in G1. Phosphorylated H2A is present in almost 100% of trophozoites, as are large median bodies and an even larger cell size. The mitotic index increases and the population grows again after washing-off aphidicolin. Positivity for phosphorylated H2A drops as well as the cell size and the percentage and size of median bodies.

Inhibitors used for synchronization of the cell cycle usually affect only a particular reaction or pathway in the complex cell cycle (Cooper 2001, 2003) and calling these cells synchronized is rather problematic, since they appear to be aligned solely according to one characteristic, in this case according to the DNA content. This shows that standard definition of a cell cycle phase based simply on DNA content is questionable. It also shows that drug treatment to obtain synchronized cells must be minimal, both concentration and time-wise.

Acknowledgments

Appendix A. Supplementary data

Supplementary data associated with this article can be found, in the online version, at doi:10.1016/j.exppara.2009.09.004.

References

Abu-Elheiga, L., Spira, D.T., Bachrach, U., 1990. *Plasmodium falciparum:* properties of an α-like DNA polymerase, the key enzyme in DNA synthesis. Experimental Parasitology 71, 21–26.

Bernander, R., Palm, J.E., Svard, S.G., 2001. Genome ploidy in different stages of the *Giardia lamblia* life cycle. Cell Microbiology 3, 55–62.

Campisi, J., Dimri, G.P., Nehlin, J.O., Testori, A., Yoshimoto, K., 1996. Coming of age in culture. Experimental Gerontology 31, 7–12.

Carme, F., Rosa, M., Josep, E., 1999. Chromosome aberrations induced by aphidicolin. Mutation Research 29, 47–53.

Červa, L., Nohýnková, E., 1992. A light microscopic study of the course of cellular division of *Giardia intestinalis* trophozoites grown in vitro. Folia Parasitologica 39, 97–104.

Chambers, A.L., Downs, J.A., 2007. The contribution of the budding yeast histone H2A C-terminal tail to DNA-damage responses. Biochemical Society Transactions 35, 1519–1524.

Chavalitshewinkoon, P., de Vries, E., Stam, J.G., Franssen, F.F., van der Vliet, P.C., Overdulve, J.P., 1993. Purification and characterization of DNA polymerases from *Plasmodium falciparum*. Molecular and Biochemical Parasitology 61, 43–53.

Cheung, H.W., Jin, D.Y., Ling, M.T., Wong, Y.C., Wang, Q., Tsao, S.W., Wang, X., 2005. Mitotic arrest deficient 2 expression induces chemosensitization to a DNA-damaging agent, cisplatin, in nasopharyngeal carcinoma cells. Cancer Research 65, 1450–1458.

Choi, I., Mikkelsen, R.B., 1991. Cell cycle-dependent biosynthesis of *Plasmodium falciparum* DNA polymerase-α. Experimental Parasitology 73, 93–100.

Cooper, S., 2001. Revisiting the relationship of the mammalian G1 phase to cell differentiation. Journal of Theoretical Biology 208, 399–402.

Cooper, S., 2003. Rethinking synchronization of mammalian cells for cell cycle analysis. Cellular and Molecular Life Science 60, 1099–1106.

Culligan, K.M., Robertson, C.E., Foreman, J., Doerner, P., Britt, A.B., 2006. ATR and ATM play both distinct and additive roles in response to ionizing radiation. The Plant Journal 48, 947–961.

Glover, T.W., Berger, C., Coyle, J., Echo, B., 1984. DNA polymerase alpha inhibition by aphidicolin induces gaps and breaks at common fragile sites in human chromosomes. Human Genetics 67, 136–142.

Glover, T.W., 2006. Common fragile sites. Cancer Letters 232, 4–12.

Gomori, G., 1953. Microscopic Histochemistry. Principles and Practice. The University of Chicago Press, Chicago. Vydavatelství DVPZ, Brno. ISBN 80-7013-239-6.

Görisch, S.M., Sporbert, A., Stear, J.H., Grunewald, I., Nowak, D., Warbrick, E., Leonhardt, H., Cardoso, M.C., 2008. Uncoupling the replication machinery: replication fork progression in the absence of processive DNA synthesis. Cell Cycle 7, 1983–1990.

Hammarton, T.C., Mottram, J.C., Doerig, C., 2003. The cell cycle of parasitic protozoa: potential for chemotherapeutic exploitation. Progress in Cell Cycle Research 5, 91–101.

Henderson, K.A., Gottschling, D.E., 2008. A mother's sacrifice: what is she keeping for herself? Current Opinion in Cell Biology 20, 723–728.

Huberman, J.A., 1981. New views of the biochemistry of eucaryotic DNA replication revealed by aphidicolin, an unusual inhibitor of DNA polymerase alpha. Cell 23, 647–648.

Keister, D.B., 1983. Axenice culture of *Giardia lamblia* in TYI-S-33 medium supplemented with bile. Transactions of the Royal Society of Tropical Medicine and Hygiene 77, 487–488.

Kues, W.A., Anger, M., Carnwath, J.W., Paul, D., Motlik, J., Niemann, H., 2000. Cell cycle synchronization of porcine fetal fibroblasts: effects of serum deprivation and reversible cell cycle inhibitors. Biology of Reproduction 62, 412–419.

Kumagai, M., Makioka, A., Ohtomo, H., Kobayashi, S., Takeuchi, T., 1998. *Entamoeba invadens*: reversible effects of aphidicolin on the growth and encystation. Experimental Parasitology 90, 294–297.

Kung, A.L., Sherwood, S.W., Schimk, R.T., 1993. Differences in the regulation of protein synthesis, cyclin B accumulation, and cellular growth in response to the inhibition of DNA synthesis in chinese hamster ovary and HeLa 53 cells. The Journal of Biological Chemistry 268, 23072–23080.

Kurose, A., Tanaka, T., Huang, X., Traganos, F., Darzynkiewicz, Z., 2006. Synchronization in the cell cycle by inhibitors of DNA replication induces histone H2AX phosphorylation: an indication of DNA damage. Cell Proliferation 39, 231–240.

Liu, J.S., Kuo, S.R., Melendy, T., 2003. Comparison of checkpoint responses triggered by DNA polymerase inhibition versus DNA damaging agents. Mutation Research 532, 215–226.

Marusyk, A., Wheeler, L.J., Mathews, C.K., DeGregori, J., 2007. p53 mediates senescence-like arrest induced by chronic replicational stress. Molecular and Cellular Biology 27, 5336–5351.

Makioka, A., Ohtomo, H., Kobayashi, S., Takeuchi, T., 1998. Effects of aphidicolin on *Entamoeba histolytica* growth and DNA synthesis. Tokai Journal of Experimental and Clinical Medicine 23, 417–422.

Menges, M., de Jager, S.M., Gruissem, W., Murray, J.A., 2005. Global analysis of the core cell cycle regulators of *Arabidopsis* identifies novel genes, reveals multiple and highly specific profiles of expression and provides a coherent model for plant cell cycle control. The Plant Journal 41, 546–566.

Michel, L., Benezra, R., Diaz-Rodriguez, E., 2004. MAD2 dependent mitotic checkpoint defects in tumorigenesis and tumor cell death: a double edged sword. Cell cycle 3, 990–992.

Mutomba, M.C., Wang, C.C., 1996. Effects of aphidicolin and hydroxyurea on the cell cycle and differentiation of *Trypanosoma brucei* bloodstream forms. Molecular and Biochemical Parasitology 80, 89–102.

Nohynkova, E., Draber, P., Reischig, J., Kulda, J., 2000. Localization of gamma-tubulin in interphase and mitotic cells of a unicellular eukaryote, *Giardia intestinalis*. European Journal of Cell Biology 79, 438–445.

O'Connor, P.M., Jacman, J., 1996. Synchronization of mammalian cells. In: Pagano, M. (Ed.), Cell Cycle-Materials and Methods. Springer-Verlag, Berlin, Heidelberg, pp. 63–74.

Patel, R., Wright, E.M., Whitaker, M., 1997. Caffeine overrides the S-phase cell cycle block in sea urchin embryos. Zygote 5, 127–138.

Pedrali-Noy, G., Spadari, S., 1979. Effect of aphidicolin on viral and human DNA polymerases. Biochemical and Biophysical Research Communication 88, 1994–2002.

Piaggio, G., Farina, A., Perrotti, D., Manni, I., Fuschi, P., Sacchi, A., Gaetano, C., 1995. Structure and growth-dependent regulation of the human cyclin B1 promoter. Experimental Cell Research 216, 396–402.

Pilch, D.R., Sedelnikova, O.A., Redon, Ch., Celeste, A., Nussenzweig, A., Bonner, W.M., 2003. Characteristics of γ-H2AX foci at DNA double-strand breaks sites. Biochemistry and Cell Biology 81, 123–129.

Ploubidou, A., Robinson, D.R., Docherty, R.C., Ogbadoyi, E.O., Gull, K., 1999. Evidence for novel cell cycle checkpoints in trypanosomes: kinetoplast segregation and cytokinesis in the absence of mitosis. Journal of Cell Science 112, 4641–4650.

Poxleitner, M.K., Dawson, S.C., Cande, W.Z., 2008. Cell cycle synchrony in *Giardia intestinalis* cultures achieved by using nocodazole and aphidicolin. Eukaryotic Cell 7, 569–574.

Reiner, D.S., Ankarklev, J., Troell, K., Palm, D., Bernander, R., Gillin, F.D., Andersson, J.O., Svärd, S.G., 2008. Synchronisation of *Giardia lamblia*: identification of cell cycle stage-specific genes and a differentiation restriction point. International Journal of Parasitology 38, 935–944.

Sabaneyeva, E., Tao, W., Verbelen, J.P., 1999. Aphidicolin inhibits DNA replication in the micronucleus and blocks cytokinesis in *Paramecium caudatum*. Cell Biology International 23, 859–862.

Samuels, A.L., Meehl, J., Lipe, M., Staehelin, L.A., 1998. Optimizing conditions for tobacco BY-2 cell cycle synchronization. Protoplasma 202, 232–236.

Skarstad, K., Bernander, R., Wold, S., Steen, H.B., Boye, E., 1996. Cell cycle analysis of microorganisms. In: Al-Rubeai, Emery.A.N. (Ed.), Flow Cytometry Applications in Cell Culture. Marcel Dekker, New York, pp. 241–255.

Sluder, G., Lewis, K., 1987. Relationship between nuclear DNA synthesis and centrosome reproduction in sea urchin eggs. Journal of Experimental Zoology 244, 9–100.

Soloviev, M.M., 1963. Studies on division of *Lamblia duodenalis* in cultures. Meditsinskaya Parazitologiya i Parazitamye Bolezni 32, 96–101.

Spadari, S., Sala, F., Pedrali-Noy, G., 1982. Aphidicolin: a specific inhibitor of nuclear DNA replication in eukaryotes. Trends in Biochemical Sciences 7, 29–30.

Speit, G., Schütz, P., 2008. The effect of inhibited replication on DNA migration in the comet assay in relation to cytotoxicity and clastogenicity. Mutation Research 655, 22–27.

Thompson, R.C., 2004. The zoonotic significance and molecular epidemiology of *Giardia* and giardiasis. Veterinary Parasitology 126, 15–35.

Tůmová, P., Hofštetrová, K., Nohýnková, E., Hovorka, O., Král, J., 2007a. Cytogenetic evidence for heterogeneity of two *Giardia* nuclei. Chromosoma 116, 65–78.

Tůmová, P., Kulda, J., Nohýnková, E., 2007b. Cell division of *Giardia intestinalis*: assembly of the adhesive disc, and the cytokinesis. Cell Motility and the Cytoskeleton 64, 288–298.

Urbani, L., Sherwood, S.W., Schimke, R.T., 1995. Dissociation of nuclear and cytoplasmic cell cycle progression by drugs employed in cell synchronization. Experimental Cell Research 219, 159–168.

Uzbekov, R., Chartrain, I., Philippe, M., Arlot-Bonnemains, Y., 1998. Cell cycle analysis and synchronization of the *Xenopus* cell line XL2. Experimental Cell Research 242, 60–68.

Wiesehahn, G.P., Jarroll, E.L., Lindmark, D.G., Meyer, E.A., Hallick, L.M., 1984. *Giardia lamblia*: autoradiographic analysis of nuclear replication. Experimental Parasitology 58, 94–100.

Wu, G., McArthur, A.G., Fiser, A., Šali, A., Sogin, M.L., Müller, M., 2000. Core histones of the amitochondriate protist, *Giardia lamblia*. Molecular Biology and Evolution 17, 1156–1163.

Yee, J., Tang, A., Lau, W.L., Ritter, H., Delport, D., Page, M., Adam, R.D., Müller, M., Wu, G., 2007. Core histone genes of *Giardia intestinalis*: genomic organization, promoter structure, and expression. BMC Molecular Biology 8, 26.

Yeo, E.J., Hwang, Y.C., Kang, C.M., Kim, I.H., Kim, D.I., Parka, J.S., Choy, H.E., Park, W.Y., Park, S.C., 2000. Senescence-like changes induced by hydroxyurea in human diploid fibroblasts. Experimental Gerontology 35, 553–571.

Zhou, B.B., Elledge, S.J., 2000. The DNA damage response: putting checkpoints in perspective. Nature 408, 433–439.

Zlotorynski, E., Rahat, A., Skaug, J., Ben-Porat, N., Ozeri, E., Hershberg, R., Levi, A., Scherer, S.W., Margalit, H., Kerem, B., 2003. Molecular basis for expression of common and rare fragile sites. Molecular and Cellular Biology 23, 7143–7151.

Protist

ORIGINAL PAPER

How Nuclei of *Giardia* Pass through Cell Differentiation: Semi-open Mitosis Followed by Nuclear Interconnection

Klára Jiráková[a], Jaroslav Kulda[b], and Eva Nohýnková[a,1]

[a]Department of Tropical Medicine, 1st Faculty of Medicine, Charles University in Prague and Faculty Hospital
  Bulovka, Studnickova 7, Prague 2, 128 00, Czech Republic
[b]Department of Parasitology, Faculty of Science, Charles University in Prague, Vinicna 7, Prague 2, 124 08,
  Czech Republic

Differentiation into infectious cysts (encystation) and multiplication of pathogenic trophozoites after hatching from the cyst (excystation) are fundamental processes in the life cycle of the human intestinal parasite *Giardia intestinalis*. During encystation, a bi-nucleated trophozoite transforms to a dormant tetra-nucleated cyst enveloped by a protective cyst wall. Nuclear division during encystation is not followed by cytokinesis. In contrast to the well-studied mechanism of cyst wall formation, information on nuclei behavior is incomplete and basic cytological data are lacking. Here we present evidence that (1) the nuclei divide by semi-open mitosis during early encystment; (2) the daughter nuclei coming from different parent nuclei are always arranged in pairs; (3) in both pairs, the nuclei are interconnected via bridges formed by fusion of their nuclear envelopes; (4) each interconnected nuclear pair is associated with one basal body tetrad of the undivided diplomonad mastigont; and (5) the interconnection between nuclei persists through the cyst stage being a characteristic feature of encysted *Giardia*. Based on the presented results, a model of nuclei behavior during *Giardia* differentiation is proposed.
© 2011 Elsevier GmbH. All rights reserved.

Key words: *Giardia*; encystation; precyst; excystation; excyzoite; semi-open mitosis; nuclear interconnection; membrane fusion.

Introduction

The parasitic protist *Giardia intestinalis* is a cause of diarrhea in humans worldwide. The life cycle of this parasite includes two stages, a proliferative, pathogenic form, known as the trophozoite, which colonizes the upper small intestine of its host, and a dormant, infective form, the cyst, which is expelled in the feces.

The trophozoite is bi-nucleated and possesses two complex mastigonts organized in two-fold rotational symmetry. Each mastigont bears four flagella originating in two tetrads of basal bodies and other cytoskeletal appendages anchored in the area of the basal bodies. A unique structure of the trophozoite is the ventral disc, an attachment organelle that is reinforced with a spirally wound layer of interconnected microtubules and giardin microribbons along the full length of each microtubule (Elmendorf et al. 2003; Holberton 1973). The mature trophozoites also possess the median body, a bundle of microtubules bearing short

[1]Corresponding author; fax +420 224 968 525
e-mail enohy@lf1.cuni.cz (E. Nohýnková).

microribbons (Brugerolle 1975). Immunostaining of the median body with antibodies against tubulin and β-giardin (Crossley et al. 1986), as well as its absence in cells freshly released from cytokinesis, suggest that it may serve as a store of pre-polymerized material for the assembly of daughter ventral discs during cytokinesis.

The cyst stage is enveloped by a thick wall enabling survival of the parasite in adverse conditions outside the host. The encysted cell is tetra-nucleated and contains internalized flagella, other mastigont structures, the median body and the fragmented skeleton of the ventral disc. The structure and chemical components of the cyst wall, as well as biochemical and secretory processes related to cyst wall formation, have been defined in numerous studies (Hehl and Marti 2004; Karr and Jarroll 2004; Konrad et al. 2010; Luján et al. 1995, 1997; Macechko et al. 1992; Stefanic et al. 2009). Significantly less information is available regarding the behavior of nuclei within the cyst and during encystation and excystation.

According to a model by Bernander et al. (2001), which is supported by experimental data, the *Giardia* life cycle includes two periods of genome replication, followed by different types of nuclear and cell division. The bi-nucleated trophozoite goes through a canonical cell cycle alternating between 4N (2x2N) and 8N (2x4N) cellular genome ploidy. Exit from this cycle to differentiate into a cyst takes place in the G2 phase (Bernander et al. 2001; Reiner et al. 2008). The G2 phase is the longest phase of the *Giardia* cell cycle (Hofštetrová et al. 2010; Reiner et al. 2008). During encystation, the two nuclei divide without intervening cytokinesis to form 4-nucleated cysts with 8N (4x2N) cellular ploidy. Another round of DNA replication brings the genome ploidy of mature cysts to 16N (4x4N). The steps that occur after excystation are poorly understood. Light and electron microscopic observations show that the excyzoite has 4 nuclei (Bernander et al. 2001; Chávez-Munguía et al. 2004; Filice 1952). Flow cytometry and fluorescence microscopic observation suggest the occurrence of two rapid, subsequent divisions which produce bi-nucleated trophozoites with basic cellular ploidy. It is assumed that the four 4N excyzoite nuclei are sorted to form two bi-nucleated daughter cells in the first division, while the second division is probably mitotic, but proceeds without previous DNA replication (Bernander et al. 2001). However, direct evidence of these processes is lacking. How and when the two nuclei of the trophozoite divide into the four nuclei of the cyst also remains unresolved.

The excystation of *Giardia intestinalis* was documented with scanning electron microscopy (Buchel et al. 1987) and transmission electron microscopy (Hetsko et al. 1998). Scanning electron microscopy cannot provide information about nuclei distribution and cytoskeleton reorganization during division of the excyzoite. Transmission electron microscopy provides detailed information about the ultrastructure of particular cell organelles but not about the cell morphology. Moreover, a morphological description of the excyzoite based on light microscopic observation has not been published.

The recent prediction of sex in *Giardia* (Birky 2010; Cooper et al. 2007; Logsdon 2008; Schurko and Logsdon 2008) brought the cyst nuclei into focus. Poxleitner et al. (2008) proposed a parasexual process of karyogamy called diplomixis. These authors reported nuclear fusion in 30% of examined cysts and provided cytological evidence for the exchange of genetic material between cyst nuclei with the aid of episomal plasmids. Besides partial achievements, the knowledge on precyst, cyst and excyzoite nuclei is still incomplete and even some basic morphological data are lacking.

Here we present new observations regarding nuclear division during encystation, arrangements of nuclei within the cyst and in the excyzoite, internuclear bridges and fusion and basic morphology of the excyzoite.

Results

Nuclear Division and DNA Replication during Encystation

First, we sought to characterize the timing and mechanism of nuclear division during *Giardia* differentiation. To visualize DNA replication in the cyst nuclei we used incorporation of bromodeoxyuridine (BrdU). To check whether, during encystation, karyokinesis proceeds with the aid of the mitotic spindle, we exposed encysting cells to albendazole, a microtubule inhibitor known to block assembly of mitotic spindles in *Giardia* trophozoites (Nohýnková et al. 2000). Incorporation of BrdU into the newly replicated DNA confirmed that in encysting cells nuclear division occurs before DNA replication, as indicated earlier (Bernander et al. 2001). In tetra-nucleated cysts, the incorporation of BrdU showed that DNA replication occurred in each of four cyst nuclei (Fig. 1B), which was confirmed with flow cytometry measurement of the DNA content in the cysts (Fig. 1A). About 36% of cysts stained
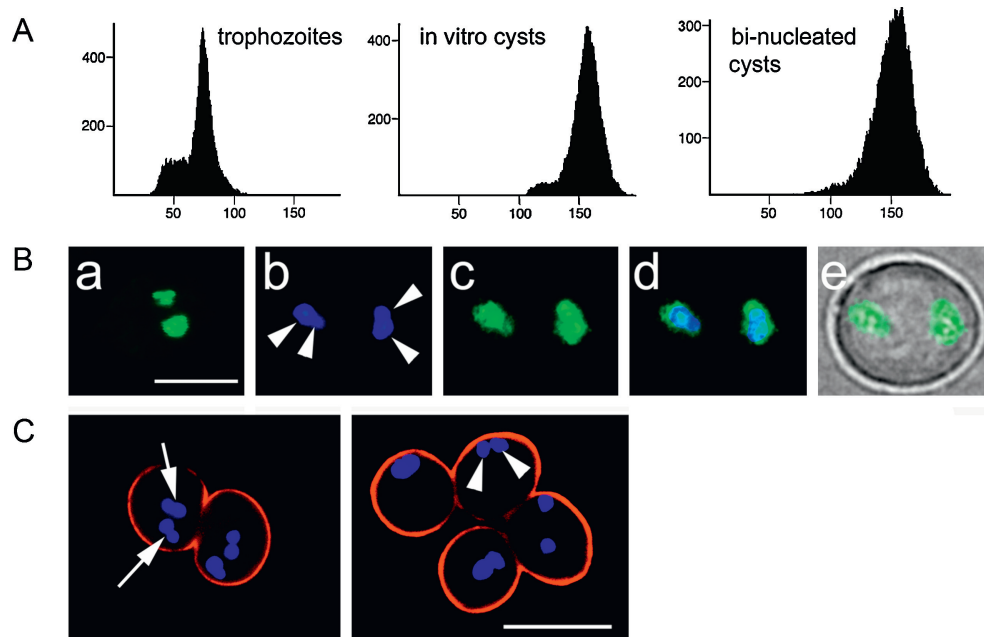
Figure 1. A. Flow cytometry analysis of the DNA content distributions of trophozoites, tetra-nucleated, in vitro generated cysts and bi-nucleated cysts formed in the presence of albendazole to show DNA replication in cysts. **B.** Replication of DNA visualized by BrdU incorporation and detected by immunofluorescence staining. **(a)** Fluorescence signals from two nuclei of trophozoites. **(b-e)** Fluorescence signals from four cyst nuclei. The BrdU signal (green) is co-localized to four DAPI (blue) stained nuclei (arrowheads) and merged with a brightfield image of a cyst. **C.** Encystation in the presence of albendazole. Note: cysts with two undivided nuclei (arrowheads); control cysts with four nuclei (arrows). Immunofluorescence staining: nuclei (blue); cyst wall (red). Scale: 5 μm (**B**); 10 μm (**C**).

positive for BrdU, and in all positive cysts, all four nuclei showed the BrdU signal.

Exposure to albendazole inhibited nuclear division, thus indicating involvement of the mitotic spindle in nuclear division during encystation. In the presence of albendazole, water-resistant cysts were formed which possessed only two nuclei (Fig. 1C). Interestingly, in non-divided nuclei, another round of DNA replication occurred, and the bi-nucleated cysts possessed the same amount of DNA as the control cysts with four nuclei (Fig. 1A).

Next, we investigated division of nuclei in different stages of encystation using light and electron microscopy.

Antibodies known to detect mitotic spindles in trophozoites (Tůmová et al. 2007a) did not detect spindles in any differentiating *Giardia*, though more than a hundred cells were analyzed. However, staining with anti-centrin antibody and DAPI revealed gradual separation of basal body tetrads and chromosome condensation in precysts (Fig. 2C, D) indicative of upcoming mitosis. Detailed analysis of the ultrastructure of the differentiating cells revealed that the two trophozoite nuclei

underwent division during the early phase of encystation, in the precysts. Mitotic nuclei were found only in non-adherent, glycogen-rich rounded cells with an expanded endoplasmic reticulum (ER)-like tubulo-vesicular network forming irregular lagoons or vesicles (Fig. 3A, C). These vesicles corresponded to nascent encystation specific vesicles (ESVs), which are the earliest morphological change during encystation (McCaffery and Gillin 1994). The formation of small, rounded vesicles of uniform size was also consistent with the initiation of encystation (Fig. 3B). The cytoskeleton of the ventral disc was not yet fragmented and no visible layer covering externally plasma membrane was formed in these cells.

Semi-open Mitosis in Precysts

The nuclei divided by semi-open mitosis (Fig. 3), which is consistent with canonical karyokinesis in proliferating, actively growing trophozoites (Sagolla et al. 2006; Tůmová et al. 2007a). Like the mitotic nuclei of the trophozoites, the nuclei in differentiating cells divided without nuclear envelope
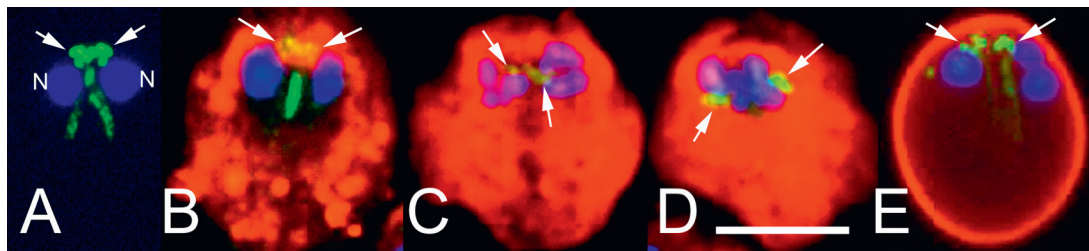
Figure 2. Arrangement of basal bodies during *Giardia* encystation. Fluorescence signal from basal bodies visualized using anti-centrin antibody (green) is merged with a signal from a cyst wall protein (red). Nuclei (DNA) are stained with DAPI (blue). **A**. In interphase cell, two basal body tetrads (arrows) are localized in between anterior ends of nuclei (N). Note four centrin dots in each tetrad. **B – D.** In precysts filled with cyst wall protein vesicles (red), chromosomes condense (**C, D**) and two basal body tetrads (arrows) gradually separate (**D**). **E.** In the mature cyst surrounded by the cyst wall (red), two basal body tetrads (arrows) in a typical "interphase" arrangement (see **A**) are seen between two nuclear pairs (N, N). Two overlapping nuclei of the left pair form a single cluster. Scale: 5 μm.

breakdown. Each mitotic spindle was formed by extra- and intranuclear microtubules. Extranuclear microtubules formed a single-layered cage enclosing the dividing nucleus; intranuclear microtubules perforated the nuclear envelope at the nuclear poles and entered the nucleoplasm (Fig. 3E-G). The poles of the mitotic spindles, where both extranuclear and intranuclear spindle microtubules were focused, were situated in the cytoplasm in close proximity to one of basal bodies, as indicated in Figure 3F and G. Only stages corresponding to metaphase spindles were detected by TEM. Within a rounded precyst, the positioning of the two spindles was impossible to determine accurately but they were clearly not parallel to each other as they are during mitosis in trophozoites (Sagolla et al. 2006; Tůmová et al. 2007a).

Nuclear division resulted in the formation of four daughter nuclei arranged in two opposite pairs. In each pair, the nuclei were localized close together such that parts of their envelopes were in close proximity (Fig. 3D). In this phase of encystation, the spiral microtubular array of the ventral disc cytoskeleton was fragmented into several pieces composed of disc microtubules with adjacent microribbons as described in early fine structural observations (Sheffield and Bjorvatn 1977). As detected by immunofluorescence staining, fragmentation of the disc during encystation was not accompanied by phosphorylation, including that of Aurora kinase (data not shown), in contrast to disassembly of the parent disc during division of trophozoites (Davids et al. 2008). The disc fragments were located in the cytoplasm, along with glycogen granules, large irregular ESVs and small rounded vesicles. No cyst wall material was visibly exported to the cell surface at this stage (Fig. 3D).

The shapes of the dividing as well as the segregated daughter nuclei were irregular due to folded nuclear envelopes (NE) and tubular projections continuing as the tubulo-vesicular network of the ER. Tubules from the ER, extending from the NE, were seen to pass between the extranuclear spindle microtubules. Lobular nuclei were also found in early cysts, i.e., in encysting cells with an assembled cyst wall (Fig. 4A, B). However, most cyst nuclei were rounded (Fig. 4D-F), in agreement with a decrease of the expansion of the ER and the absence of ESVs in mature cysts.

Interconnection of Nuclei during *Giardia* Encystation

The paired nuclei were linked with inter-nuclear bridges. On ultrathin sections, one, two, or three short bridges, dissimilar in width, were observed between nuclear doublets (Fig. 4B, D-H). Interconnection occurred shortly after karyokinesis as indicated by the low number (less than 10%) of precysts possessing four paired, but unlinked nuclei. The bridges were formed by fusion of adjacent nuclear envelopes. Likely, a two-step fusion occurred in *Giardia:* outer nuclear membranes fused first (Fig. 5A), so that the contents of the lumina of the NEs became continuous, followed by fusion of the inner nuclear membranes allowing continuity of the nuclear contents (Fig. 5B). To determine whether the bridges were transient structures limited to the early phase of the encystation process, in vitro-formed, water-resistant cysts and wild-type cysts of human origin were analyzed by TEM. The inter-nuclear bridges were found in cysts of any origin (Fig. 4), indicating that, from mitotic
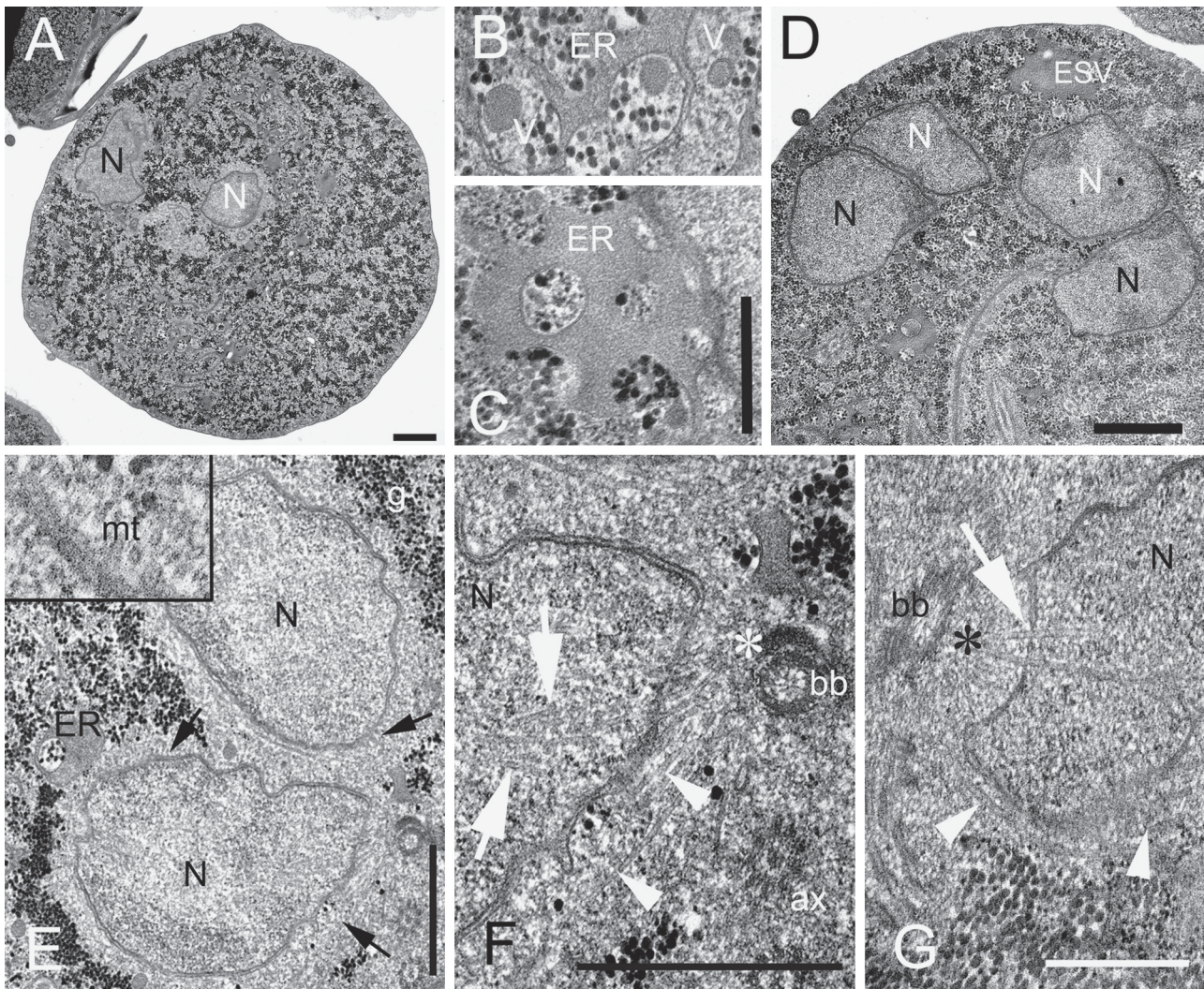
Figure 3. Semi-open mitosis in precysts of *Giardia intestinalis*. **A**. A typical ultrastructure of an encysting *Giardia* cell in which nuclear division occurs. No cyst wall is assembled on the surface of a rounded precyst; the cytoplasm is filled with an expanded network of endoplasmic reticulum and glycogen granules. **B – C.** Details of the tubulo-vesicular endoplasmic reticulum (ER) and the small rounded vesicles (v), which are characteristic of early encystation. **D.** Four nuclei resulting from mitosis in a precyst. The nuclei form two pairs. Note the absence of a cyst wall on the precyst surface; ESV - encystation specific vesicle. **E.** Two dividing nuclei in a precyst. The arrows point to microtubules of mitotic spindles externally to the envelope of each nucleus as shown in detail in the **inset** (mt - spindle microtubules). **F.** Semi-open mitosis. A detail of a mitotic spindle of the lower nucleus shown in **E**. Note that the spindle is formed from extranuclear (arrowheads) and intranuclear (arrows) microtubules. The pole of the mitotic spindle (asterisk) is situated close to the basal body (bb) of the flagellar axoneme. **G.** Entry of intranuclear spindle microtubules (arrow) into the nucleoplasm from the cytoplasm through pores of the intact nuclear envelope. Extranuclear spindle microtubules (arrowheads) in parallel with the nuclear envelope; spindle pole (asterisk); basal body (bb). N – nucleus. Scale: 1 μm (**A, D, E, F**), 500 nm (**B, C, G**).
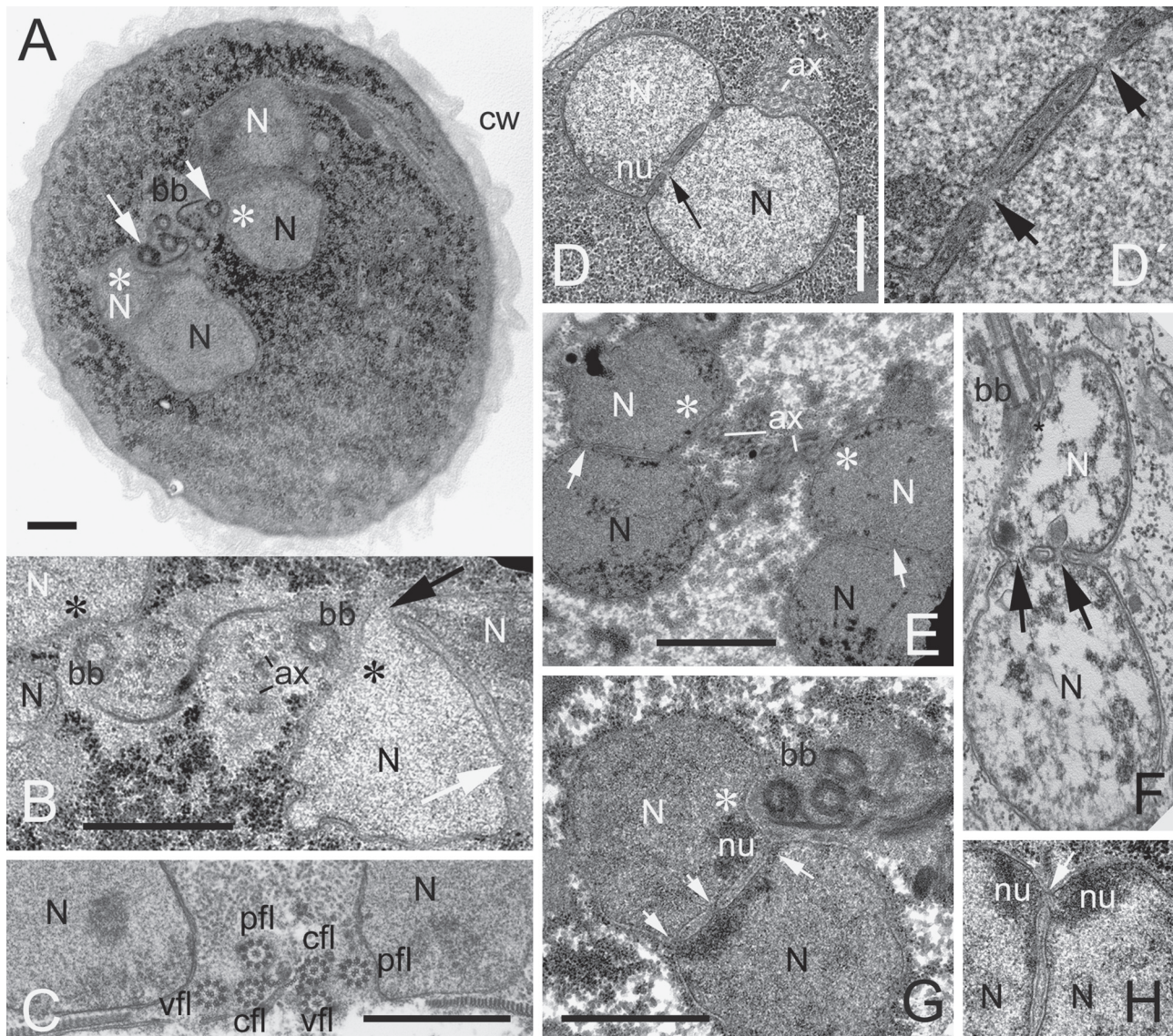
Figure 4. Interconnected nuclear pairs and their association with basal bodies. **A.** Ultrastructure of an early cyst with an assembled cyst wall (cw) showing two nuclear pairs in a typical arrangement left and right of two basal body tetrads (due to transverse section through a basal body region, only three basal bodies of the tetrad are visible). Note the position of a lateral basal body (arrows) of each tetrad is close to an envelope of one nucleus from the pair and a shallow pit in the envelope (asterisk). N – nucleus. **B.** Arrangement of the basal body tetrads/axonemes and two pairs of interconnected nuclei in a cyst copies that of axonemes and nuclei in a trophozoite (**C**). Arrow points to a link between paired nuclei (N); asterisk marks a site of contact between the nuclear envelope and the basal body (bb). Note the irregular shape of the nuclei. ax – axoneme; vfl – axoneme of ventral flagellum; pfl – axoneme of posteriolateral flagellum; cfl – axoneme of caudal flagellum. **D.** Two bridges (arrows) between a pair of cyst nuclei (N) shown in **D′** in detail. ax – axonemes; nu - nucleolus. **E.** Transverse section through two pairs of interconnected cyst nuclei (N) demonstrating that the nuclei are linked in both pairs (arrows). Note the same arrangement of axonemes (ax) as in the trophozoite (**C**). **F.** Longitudinal section through a pair of nuclei (N) in a cyst demonstrates two internuclear bridges (arrows). The upper nucleus is in close proximity to the basal body (bb) of the anteriolateral flagellum. **G.** Transversal section through a pair of cyst nuclei linked with three internuclear bridges (arrows) showing position of nucleoli (nu) next to the bridge. Asterisk marks a depression in the envelope, which is in contact with a basal body tetrad (bb). **H.** Positions of nucleoli (nu) of two interconnected nuclei (N). Arrow points to a bridge between the nuclei. Scale: 1 μm.
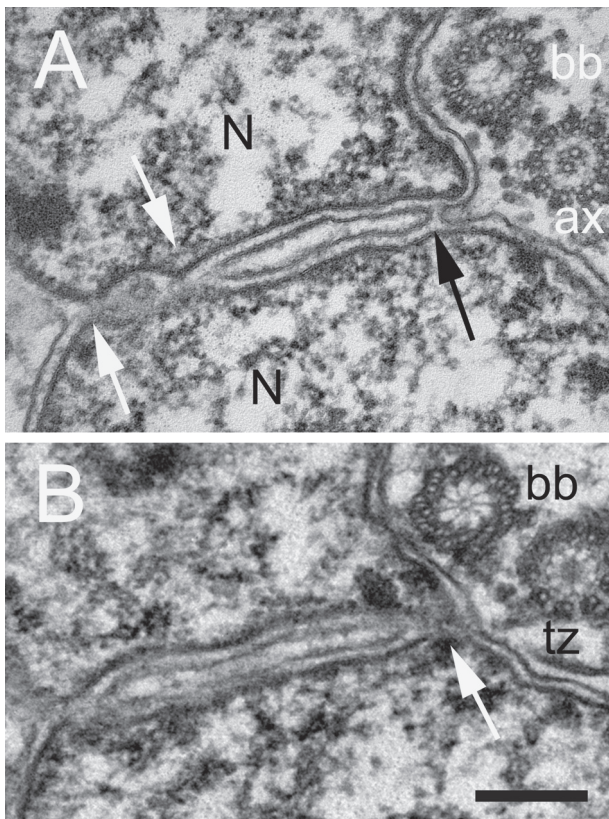
Figure 5. Fusion of envelopes (NE) of paired cyst nuclei. Two serial ultrathin sections, of thickness between 60-90 nm, demonstrate that fusion of the outer NE precedes fusion of the inner NE. **A**. Three sites of outer NE fusion (white and black arrows). Black arrow points to a site where continuity of NE lumen is evident. bb - basal body; ax - axoneme. **B**. On this serial section, both outer and inner NEs are already fused forming an internuclear bridge (white arrow). Note a contact between the nucleoplasm of the paired nuclei through the bridge. bb -basal body; tz-transitional zone between basal body and axoneme. Scale: 0.2 μm.

segregation in precysts onwards, the paired nuclei became interconnected.

Association of Nuclear Doublets with Basal Bodies/Axonemes

During the whole process of encystation, i.e., from precysts to cysts, only a single flagellar apparatus comprising axonemes of four pairs of flagella with basal bodies was present within the cell, consistent with earlier observations in cysts (Sheffield and Bjorvatn 1977). Confocal microscopy using an anti-acetylated tubulin antibody showed that, in principle, arrangement of the flagellar apparatus was the same as that in interphase cells in the majority of water-resistant cysts (Fig. 6). The pairs of cyst nuclei were situated close to the basal body tetrads. However, in the pair, each nucleus was located at different focal plane, indicating that one nucleus was closer to the basal bodies/axonemes than the other (Fig. 6). Localization of pairs of closely apposed nuclei near the flagellar basal bodies at one pole of the cyst was confirmed in 99.4% (156/157) of wild-type cysts stained with Gömöri trichrome. Ultrastructural analysis then showed that (1) the basal body tetrads were arranged and localized between pairs of daughter nuclei in the same manner as in trophozoites (Fig. 4A-C, E), (2) each nuclear pair was associated with a basal body tetrad, and (3) the association occurred with one nucleus from the pair (Fig. 4B, D-F). Comparative analysis suggested that the pertinent nucleus was next to the ventral or the posteriolateral basal body (Fig. 4B, C).

Excystation and Morphology of *Giardia intestinalis* Excyzoite

As already shown by scanning electron microscopy (Buchel et al. 1987), the excyzoite of *Giardia* emerged from the cyst by posterior end through a single polar opening in the cyst wall. Six flagella directed backward in the interphase cell, namely the caudal, posteriolateral and ventral flagella, protruded first (Fig. 7A, B). The cell then squeezed through the opening, with the anteriolateral flagella left in the cyst as last (Fig. 7B, C). The cytoskeleton of the rounded excyzoite comprised a single flagellar apparatus (Fig. 7D) and two duplicated microtubular structures as shown by immunostaining (Fig. 8A, B). The basal bodies/axonemes of the eight *Giardia* flagella were arranged the same way as in the interphase trophozoite except that the ventral and posteriolateral flagella emerged from the posterior end of the cell next to the caudal flagella (Fig. 7D). Two microtubular arcs, located to the left or right of the backward-directed axonemes, represented the fragmented skeleton of the ventral disc (Figs 7D, E; 8A, B), as reported earlier (Palm et al. 2005). They disappeared when the excyzoite started to divide (data not shown). Two other microtubular bundles were situated more or less symmetrically along the caudal axonemes (longitudinal cell axis) (Figs 7B, D; 8B). These structures, which have not been reported previously, likely corresponded to median bodies. They also disappeared in the dividing excyzoites.

A pair of nuclei was situated at each side, left and right, of the complex of basal bodies
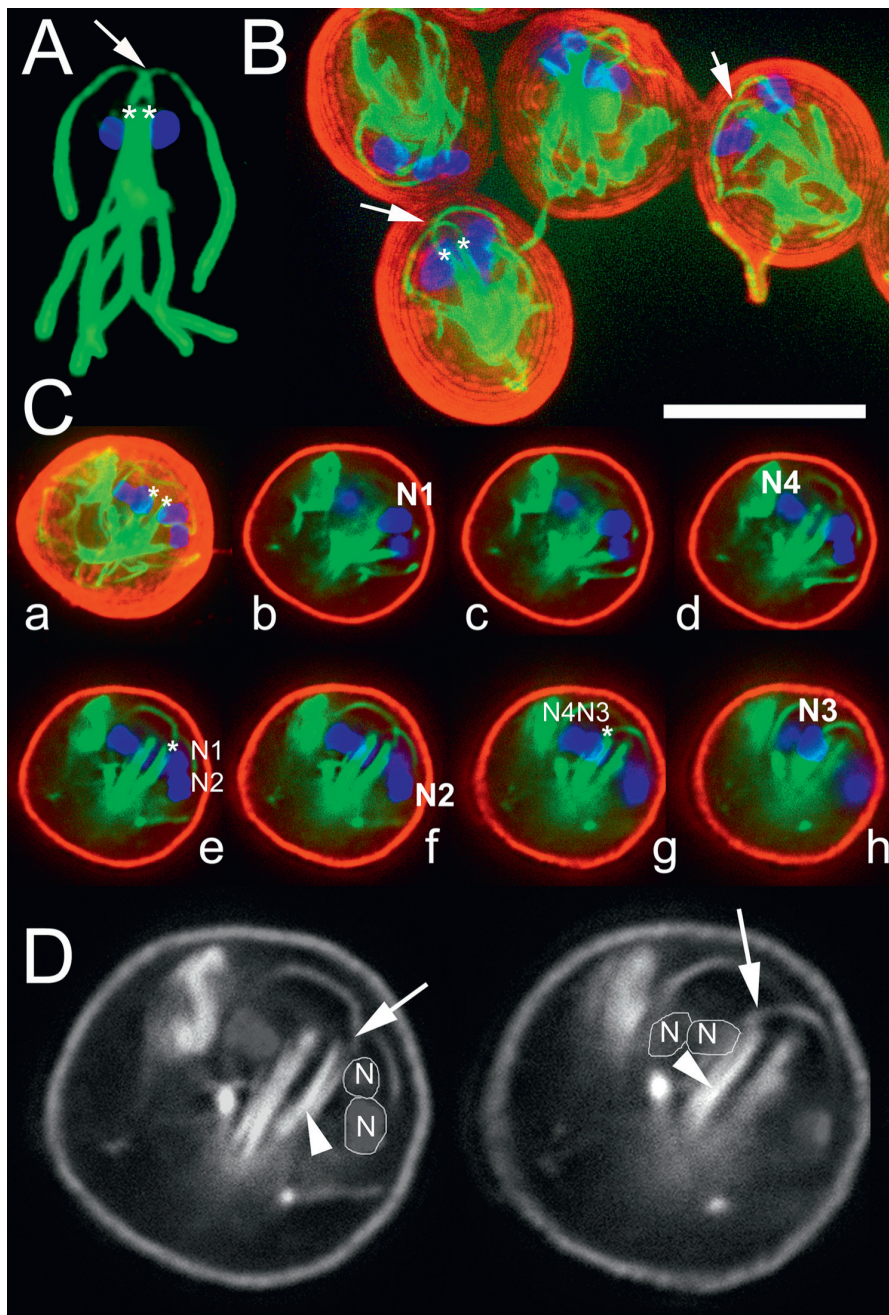
Figure 6. Arrangement of the *Giardia* flagellar apparatus and its relationship with paired cyst nuclei detected by immunofluorescence staining. **B, C.** Fluorescence signal from a cyst wall protein (red) is merged with a signal from DAPI (blue) stained nuclei co-localized with microtubular structures (green) visualized using anti-acetylated tubulin antibody. The same antibody is used to visualize flagellar apparatus of the trophozoite (**A**). **A, B.** Note a typical crossing of curved axonemes of anteriolateral flagella and a position of basal body tetrads (asterisks) in the trophozoite and the cysts. **C.** Optical sections taking through a cyst shows a close proximity of one nucleus of each nuclear pair, namely, nucleus N1 from a nuclear pair marked N1/N2 and nucleus N3 from the second nuclear pair (N3/N4) to basal bodies (asterisk in **e** and **g**). **D.** Enlarged images of the sections **Ce** and **Cg** converted to grayscale show in detail association of nuclear pairs (N/N) with basal bodies (proximal parts of axonemes) in each mastigont. Arrows point to basal bodies of axonemes of the anteriolateral flagella; arrowheads point to axonemes of the posteriorly directed flagella; outlines of nuclei are highlighted. Scale: 10 μm (**A-C**).
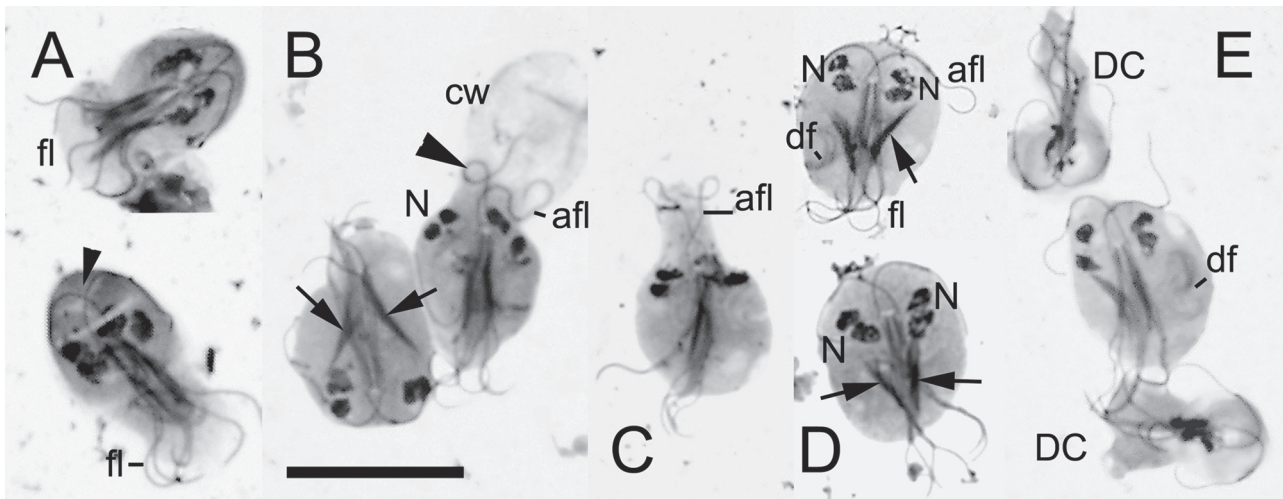
Figure 7. Light microscopic morphology of the *Giardia* excyzoite with Giemsa-Romanowski staining. **A.** Early excystation. Six flagella directed backward (fl) emerge first from the cyst opening. Axonemes of the anteriolateral flagella inside the cyst wall form a typical crossing (arrowhead). **B.** *Right*: excyzoite just before emerging from the cyst shelter, which is left behind (cw). Note the anteriolateral flagella (afl) still inside the cyst. N - nuclear pair. *Left*: Excyzoite with pronounced microtubular structures (arrows) arranged symmetrically along the longitudinal axis of the body. **C.** The excyzoite just released from the cyst. Note the deformation of the anterior body end with tapering anteriolateral flagella (afl). **D.** Two excyzoites demonstrating the basic morphology of the cell. An oval cell without a ventral disc comprises a single flagellar apparatus and two pairs of nuclei; each nuclear pair (N) is situated next to flagellar basal bodies. Fragments of disc cytoskeleton (df) and symmetrical microtubular bundles (arrows) localize in the cytoplasm. Flagellar axonemes are arranged exactly as in *Giardia* trophozoites. Note that exits of six posteriorly-directed flagella (fl) are situated close together. **E.** Comparison of excyzoite and two daughter cells (DC) resulting from the first cell division of the excyzoite after excystation. df - fragments of ventral disc cytoskeleton. Scale: 10 μm.

(Figs 7B, D; 8C, D). When excyzoites started to divide, the basal body tetrads segregated and appeared to position in between nuclei of a given pair (Fig. 8D), which next formed two nuclei in progeny (Fig. 8E). Due to fast division of the excyzoites and low number of cells in early division phase, reorganization of flagellar apparatus was not possible to follow. Cytokinesis proceeded the same way as in trophozoites (Tůmová et al. 2007b) resulting in small bi-nucleated daughter cells with four pairs of flagella, a ventral disc and no median body (Figs 7E; 8F, G).

then interconnects with one progeny coming from the second parent nucleus to form a pair of non-sister nuclei. Interconnection is achieved through focal fusion of nuclear envelopes forming transmembrane bridges. Each nuclear pair is associated with one mastigont from the undivided flagellar apparatus of the encysting trophozoite. The interconnection of both nuclear pairs persists in the mature cyst up to the excyzoite stage. During division of the excyzoite, each progeny receives one pair of non-sister nuclei.

A Model of Nuclei Behavior during *Giardia* Differentiation

Based on electron and light microscopy observations and published data (Poxleitner et al. 2008), we propose a model of nuclei behavior during *Giardia* encystation and excystation (Fig. 9). Two trophozoite nuclei divide shortly after the cell enters encystation, in the precyst. Each nucleus divides separately by semi-open mitosis, in synchrony with one another. One progeny of each parent nucleus

Discussion

In this report, we document several new observations regarding the differentiation of *Giardia intestinalis*: (1) semi-open mitosis in precysts, (2) pairing of daughter nuclei, (3) permanent interconnection between the paired cyst nuclei, and (4) association of nuclear pairs with basal bodies. We also describe, for the first time, basic light microscopic morphology of the *G. intestinalis* excyzoite.
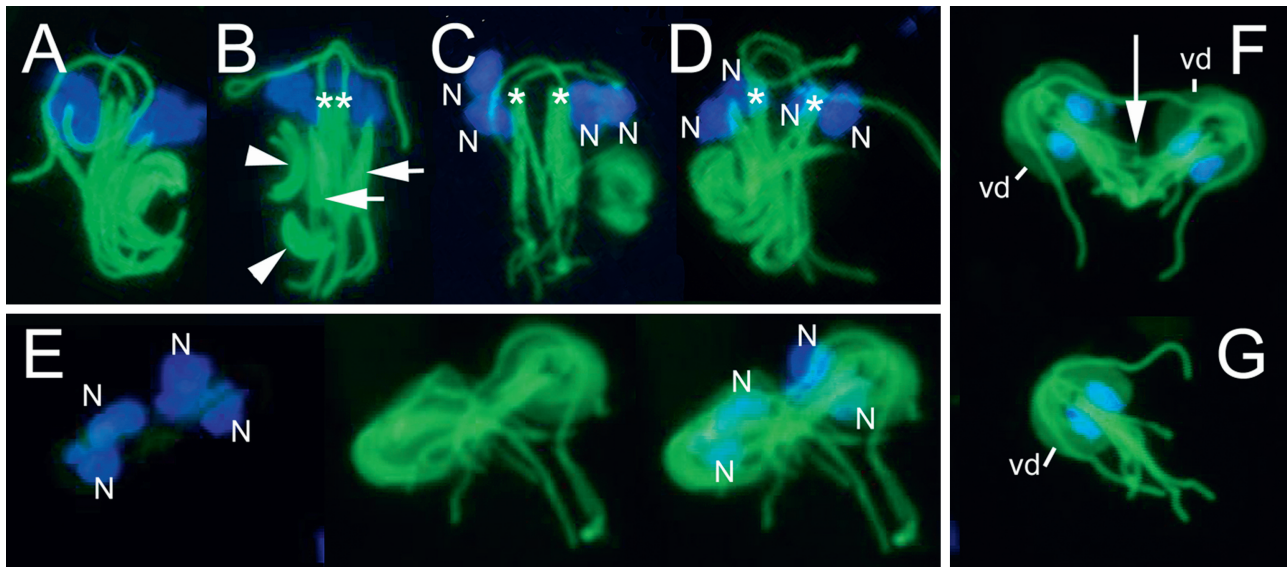
Figure 8. Microtubular structures of excyzoites detected by monoclonal antibody to acetylated alpha tubulin 6-11B-1 in immunofluorescence (green). Nuclei (N) are stained with DAPI (blue). **A-D.** The excyzoites. Doubled microtubular structures are shown: fragments of ventral disc cytoskeleton (arrowheads) and microtubular bundles (arrows). Asterisks in B, C and D mark two basal body tetrads. Note gradual segregation of the tetrads. **E-G.** Division of the excyzoite. Fluorescence signals from four DAPI (blue) stained nuclei (N) are co-localized to microtubular structures (green) of a dividing excyzoite. **F.** Two daughter cells before terminal phase of cytokinesis (arrow) of the excyzoite. Note the presence of a ventral disc (vd) in each progeny. **G.** A bi-nucleated daughter cell with four flagella pairs and a ventral disc (vd). Scale: 5 μm.

Semi-open Mitosis in Precysts

Nuclear division during *Giardia* differentiation is a poorly understood aspect of the life cycle of this pathogen. It is common knowledge that the *Giardia* trophozoite is bi-nucleated, whereas the cyst is tetra-nucleated. However, karyokinesis during encystment has not been documented. Here we provide direct evidence of nuclear division that takes place in the precyst. The mode of nuclear division corresponds to that in a trophozoite. The two nuclei divide by semi-open mitosis, a variant of closed mitosis, and two spindles are formed from extra- and intranuclear microtubules (Sagolla et al. 2006; Tůmová et al. 2007a). The nuclear genomes thus segregate separately but in synchrony with each other, in both stages of the *Giardia* life cycle. However, in relation to other cell cycle processes, there is a basic difference between nuclear division in the trophozoite and in the precyst. In the trophozoite, nuclear division is tightly coupled to cell division, involving profound mitotic reorganization of the cytoskeleton with complicated duplication of the flagellar apparatus, and cytokinesis (Nohýnková et al. 2006; Tůmová et al. 2007b). As in other eukaryotic cells (Barr and Gruneberg 2007), the plane of *Giardia* cytokinesis is

perpendicular to the segregation of chromosomes between progeny. Therefore, in the trophozoite both mitotic spindles positioned in the upper part of the cell are parallel to each other and perpendicular to the cleavage plane (Sagolla et al. 2006; Tůmová et al. 2007a). In contrast, nuclear division in the precyst is independent of cell division. Neither duplication of the flagellar apparatus, nor cytokinesis, occur during encystment. Nuclei divide in a non-dividing cell with a single flagellar apparatus, which conforms to that of an interphase trophozoite; no new basal bodies/axonemes are formed and no cleavage furrow is induced. In contrast to trophozoites, the relative position of the mitotic spindles seems to be less strict as indicated by the orientation of the spindles.

Because of a limited number of mitotic precysts that was found using light and immunofluorescence microscopy, some important questions still remain unanswered. First, it is unclear how the single flagellar apparatus is arranged during mitosis in the precyst. Understanding of this arrangement could explain why the two mitotic spindles are not oriented parallel one another. Second, the microtubule organization centers (MTOCs) for the spindle microtubules are unknown. In semi-open mitosis of trophozoite nuclei, spindle microtubules
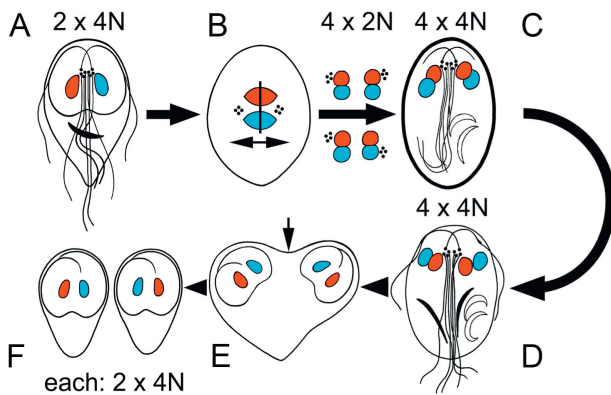
Figure 9. A model of *Giardia intestinalis* differentiation combining presented results with published data of Bernander et al. (2001) and Poxleitner et al. (2008). **A.** A binucleated trophozoite in G2 phase of cell cycle (genome ploidy 2x4N) enters encystation. **B.** In a precyst, both nuclei (red and blue) divide by semi-open mitosis (double-arrow indicates direction of nuclear segregation). During mitosis basal body tetrads (each black dot represents a basal body) separate, migrate to spindle poles but do not duplicate. Resulting four daughter nuclei (genome ploidy 4x2N) interconnect by nuclear membrane bridges forming two non-sister pairs. In each pair, one nucleus associates with one basal body tetrad: two possibilities are indicated. The interconnected nuclear pairs associated with the tetrads persist in a cyst (**C**), during excystation and in an excyzoite (**D**). DNA replication takes place in the cyst (**C**) resulting in 4x4N genome ploidy of the mature cyst and the excyzoite (**D**). The mutual position of nuclear pairs, basal bodies, and flagellar axonemes in the cyst and the excyzoite corresponds in principle to organization of the karyomastigont of the trophozoite. **E, F.** During excyzoite division (arrow indicates direction of cytokinesis) each daughter cell receives one pair of non-sister nuclei and the adhesive disc is formed. How is the full mastigont reconstructed is not known. Each daughter cell, having genome ploidy 2x4N, is ready for regular mitotic division.

emanate from regions neighboring segregated pairs of basal body tetrads (Tůmová et al. 2007a). Third, the extent to which mitotic spindles elongate is unknown. During telophase in the trophozoite, extranuclear spindle microtubules grow to direct daughter nuclei into forming daughter cells. Spindles in the precyst seem to be rather short as no daughter cells are formed.

Karyomastigonts of Encysted *Giardia*

Despite nuclear division in the precyst, the topological arrangements of mastigonts of the tetranucleated cyst correspond to that in trophozoites

(Sheffield and Bjorvatn 1977). The two karyomastigonts are linked to a pertinent tetrad of basal bodies positioned side by side between the nuclei. Instead of the two nuclei in trophozoites, there are two pairs of interconnected nuclei in cysts.

Pairing of Daughter Nuclei in Cysts

It is obvious that a single nuclear pair is formed from non-sister nuclei. Though the identity of the individual nuclei was not addressed here, the localization of episomes in only one nucleus per pair (Poxleitner et al. 2008) clearly confirms that each of the paired nuclei originates from a different parent nucleus. In a bi-nucleated *Giardia* trophozoite, stably transfected plasmids (episomes) establish only in one nucleus and, during mitosis, segregate between daughters. Thus, episomes can be used as a marker of one of the two *Giardia* nuclei and its progeny (Ghosh et al. 2001; Yu et al. 2002). In the results of a study of karyotypes (Tůmová et al. 2007a), the authors show that lines of *Giardia* trophozoites with different numbers of chromosomes in each nucleus maintain the pattern before and after encystment, indicating pairing of non-sister nuclei in cysts.

Interconnection of Cyst Nuclei

Solari et al. (2003) were the first to document the interconnection between paired cyst nuclei by transmission electron microscopy. They interpreted this phenomenon as incomplete nuclear division. Poxleitner et al. (2008) indicated the nuclear bridges may function to exchange genetic material between nuclei, but the authors considered the interconnections of the nuclei to be transient, occurring at a frequency of one nuclear pair in less than 30% of cysts. As is apparent from our observations, nuclei in both pairs are interconnected through most of the encysted stage of the *Giardia* life cycle. Moreover, the nuclear bridges also persist during excystation and in the excyzoite after emergence from the cyst envelope, as seen on published electron micrographs (Hetsko et al. 1998; fig. 1G, Chávez-Munguía et al. 2004, fig. 6). Thus, interconnection of non-sister nuclei is a regular feature of *Giardia* differentiation. The extent to which the *Giardia* nuclei are linked is unclear. However, it seems that they do not fuse completely, as is the case during karyogamy in mating yeast (Melloy et al. 2007). One to three membrane bridges were usually seen on ultrathin, non-serial sections through nuclei whether they were cut transversally or longitudinally. This is understandable only if, within a pair, the relative position of the two nuclei is not

fixed and, in a limited fashion, one nucleus can glide over the other. Indeed, some movement of nuclei within a pair was observed in live, acridine orange-stained cysts (Poxleitner et al. 2008). Focal fusions can occur between nuclei if their envelopes come into close proximity.

Why Are Cyst Nuclei Linked?

If nuclear pairing and interconnection are characteristics of *Giardia* differentiation, then the question why this is the case remains. According to a recent hypothesis (Poxleitner et al. 2008), nuclear fusion is a part of the parasexual process, called diplomixis, used by *Giardia* to maintain a low level of allelic heterozygosity. Exchange of genetic material between the non-sister nuclei, followed by somatic homologous recombination, represents a mechanism of diplomixis. Low levels of allelic heterozygosity in asexual *Giardia* possessing two nuclei, which do not mix during mitosis in trophozoites (Sagolla et al. 2006; Tůmová et al. 2007a), has been a puzzle over the last decade (Yu et al. 2002) and led to a search for sex in *Giardia* (Birky 2010). Recently, molecular evidence of sexual behavior was reported (Cooper et al. 2007; Lasek-Nesselquist et al. 2009), but the time during the life cycle when *Giardia* has sex is still unclear. Internuclear bridges between cyst nuclei do allow nuclear content to communicate. However, the restriction of the transfer of episomes to only one of two nuclear pairs per cyst (Poxleitner et al. 2008), indicates limited movement of plasmid DNA between nuclei. Ultrastructural analysis showed that electron dense materials, consistent with the structure of nucleoli (Fig. 3G, H), are often located next to the bridge. Thus, the nucleolus might act as a barrier to DNA movement as has been suggested in mammalian cells (Chubb et al. 2002).

The observations of the behavior of nuclei during encystation/excystation reported here, suggest an additional function for the internuclear bridges. These interconnections could act as structural components of the karyomastigont, ensuring that the nucleus, which is not near the basal bodies, is, nevertheless, associated with mastigont. This could be particularly important when the excyzoite emerges through the opening in the cyst wall during excystation, and is likely important for keeping paired, non-sister nuclei together when the excyzoite nuclei are segregated between progeny. Though we did not follow excystation by TEM, it is evident from two publications (Chávez-Munguía et al. 2004; Hetsko et al. 1998) that interconnections between paired nuclei persist during excystation. Although the

authors either did not comment (Chávez-Munguía et al. 2004), or reported the interconnected nuclei as division (Hetsko et al. 1998), the figures presented in their works clearly demonstrate links between paired nuclei and association of pairs with a single basal body complex.

Methods

Cell cultures and encystation in vitro: The line HP-1 of the isolate Portland-1 of *Giardia intestinalis* (ATCC 30888), donated by E. A. Meyer (Oregon Health Sciences University, Portland, USA), was used in the study. Trophozoites were grown axenically in 13 x 100 mm screw cap tubes in a filter-sterilized TYI-S-33 medium, pH 6.8, supplemented with bovine bile (Keister 1983) at 37 °C and sub-cultured twice a week. Encystation was induced by a two-step encystation protocol adapted from McCaffery and Gillin (1994) and Hausen et al. (2009). In the first step, cells were incubated in encystation medium TYE-GS3, pH 7.8, enriched with bovine bile (5 mg/ml) and calcium L-lactate (0.5 mg/ml) for 18 hrs; in the second step, encystation medium was replaced with growth medium TYI-S-33, pH 6.8. Cysts were harvested after 7 hrs and incubated overnight in distilled water at 4 °C to lyse trophozoites and incompletely formed cysts. Water-resistant cysts were further processed according to a particular method.

Purification of cysts from stool samples and excystation in vitro: To purify cysts from feces, the protocol from Bingham et al. (1979) was used. Briefly, stool samples of sheep or human origin were suspended in cold distilled water, passed through gauze and the suspensions were centrifuged (1000 x g for 10 min). Supernatant was discarded and the pellet was washed in three changes of cold, distilled water. The final suspension was placed on a 1 M sucrose gradient and the cysts were separated by centrifugation in the interlayer between the water/sucrose phases. Cysts were transferred to cold distilled water, centrifuged and washed several times. Purified cysts were stored in distilled water at 4 °C and were used within 14 days. Excystation was induced using a two-step protocol adapted by Hetsko et al. (1998). Cysts were first resuspended in a freshly prepared low-pH solution (pH 4.0) containing reduced glutathione and L-cysteine HCl in Hank's balanced salt solution (Sigma), and incubated at 37 °C for 20 min. After centrifugation (3500 x g for 5 min), the cyst pellet was resuspended in an alkaline solution (pH 8.0), containing trypsin and taurocholic acid in Tyrode's salt solution (Sigma), and incubated at 37 °C for 45 min. The cysts were then spun and inoculated into pre-warmed TYI-S-33 growth medium containing antibiotics (penicillin 2500 I.U./ml and amikacin 250 μg/ml). Excysting trophozoites were collected during 30 min of incubation in growth medium. Trophozoites were harvested by centrifugation and further processed for immunofluorescence or Giemsa staining.

Inhibition experiments: A stock solution of 750 μg/ml albendazole (Sigma) in DMSO was stored at 4 °C and diluted immediately before use with a medium to a final concentration 0.1 μg/ml. In two step encystations, the inhibitors were added to either the first step medium or the second step medium, or to both.

Immunofluorescence labeling (*Single labeling in trophozoites and excyzoites*): Immunofluorescence staining was carried out according to Nohýnková et al. (2000). Cells adhered on cover slips were fixed with ice-cold methanol (at -20 °C,

5 min) and permeabilized with ice-cold acetone (at -20 °C for next 5 min). The next steps were done at room temperature. The cells were rehydrated in phosphate-buffered saline (PBS, pH 7.2) for 10 min, blocked with 3% bovine serum albumin (BSA)/PBS (30 min), incubated with primary antibody diluted in 2% BSA/0.1% Triton-X-100/PBS for 1 hr, washed 3 times with PBS, then incubated with fluorescein-conjugated secondary antibody (anti-mouse IgG FITC, Sigma) diluted 1:100 in 2% BSA/0.1% Triton-X-100/PBS for 1 hr, washed 3 times with PBS and mounted in Vectashield mounting medium with DAPI (Vector). The primary antibodies used were the following: monoclonal antibody against tyrosylated tubulin (clone TUB-1A2, Sigma); monoclonal antibody against acetylated α-tubulin (clone 6-11B-1, Sigma); polyclonal antibody against phosphorylated Aurora A (T288, Abcam); monoclonal antibody BAS 6.8 against centrin (from Dr. K. Lechtreck, University of Cologne, Germany). The figures were captured on an Olympus BX51 fluorescence microscope with the Olympus DP 70 camera, the QuickPhoto Micro 2.2. program and the ImageJ image processing software (NIH, USA).

(*Single labeling in encysting cells and cysts*): Cysts and encysting cells were harvested by centrifugation (2000 x g for 10 min), washed in PBS, spread on cover slips and air-dried. Cells were then fixed with 4% paraformaldehyde (30 min; RT), washed with 100 mM glycine/PBS (5 min; RT), quenched with 2% BSA/PBS (30 min; RT) and incubated with Cy3 conjugated antibody against cyst wall protein 1 (A300; Waterborne) diluted 1:80 in 2% BSA/0.1% Triton-X-100/PBS (30 min at 37 °C), then washed, mounted and processed for microscopy as above.

Immunofluorescence labeling (*Double labeling*): Air-dried cysts on cover slips were fixed and labeled with primary antibody followed by FITC-conjugated secondary antibody as above. After washing with PBS, they were post-fixed in 4% paraformaldehyde for 30 min at RT and labeled with the second primary antibody according to the protocol for single labeling of cysts (above). Figures of double-labeled cysts were captured with an Olympus IX81 fluorescence microscope, photographed with an IX2-UCB camera and processed using CellÂR software (Olympus).

Detection of DNA synthesis: DNA synthesis was visualized using an immunofluorescence assay for the detection of 5-bromo-2′-deoxy-uridine (BrdU) incorporated into DNA (5-Bromo-2′-deoxy-uridine Labeling and Detection Kit I, Roche) according to the manufacturer's protocol. Encysting cells (20 hrs of encystation) were incubated in 10 mM BrdU labeling reagent (at 37 °C, 50 min), harvested by centrifugation (2000 x g for 10 min), rinsed in washing buffer, centrifuged and fixed in a solution of 70% ethanol/50 mM glycine-HCl (pH 2.0) at −20 °C for 30 min. After centrifugation and rinsing with washing buffer, a suspension of the fixed cells was spread on cover slip and air dried. The slides were incubated with anti-BrdU antibody (diluted 1:10 with 66 mM Tris/0.66 mM MgCl$_2$/2-mercaptoethanol) in a wet chamber (at 37 °C, 30 min), rinsed 3 times in washing buffer and incubated with secondary antibody conjugated with fluorescein (diluted 1:10 in washing buffer) (at 37 °C, 30 min), rinsed 3 times with washing buffer and mounted in Vectashield with DAPI (Vector).

Transmission electron microscopy: Non-adherent encysting cells (18 hours in encystation medium TYE-GS3), in vitro formed cysts and wild-type cysts of human origin were processed for TEM using a method routinely used in laboratory (Nohýnková et al. 2006). Briefly, cell suspensions were spun (2000 x g for 10 min), pellets were immediately resuspended in 10 volumes of freshly prepared, cold fixative (2.5% glutaraldehyde/5 mM CaCl$_2$/0.1 M cacodylate buffer, pH 7.4) and fixed overnight at 4 °C. Fixed cells were washed three-times

with cold PBS, pH 7.2, post-fixed in OsO$_4$/0.8% potassium ferricyanide/5 mM CaCl$_2$/0.1 M cacodylate buffer, pH 7.4 (15-20 min/4 °C), thoroughly washed with 3 changes of excess volumes of cold PBS, pH 7.2, dehydrated in acetone, and embedded in Epon (Poly/Bed 812, Polysciences). After staining with uranyl acetate/lead citrate, ultrathin sections were examined with a JOEL 1010 electron microscope.

Flow cytometry analysis: For flow cytometry, trophozoites or water-treated cysts were fixed according to Bernander et al. (2001). Briefly, in each interval, cells were harvested by centrifugation (900 x g), and the cell concentration was approximately 1 x 10^7 cells/ml. The pellet was resuspended in 50 μl fresh TYI-S-33 and 150 μl fixative (1% Triton X-100/40 mM citric acid/20 mM dibasic sodium phosphate/200 mM sucrose, pH 3.0) and fixed for 5 min at room temperature. Then, 350 μl of diluent buffer (125 mM MgCl$_2$ in PBS, pH 7.4) was added and the samples were stored at 4 °C until analysis. Fixed cells were centrifuged (4000 x g /3 min), washed in PBS, then cells were resuspended in 500 μl PBS with 1 μg RNAse A (Fermentas) and incubated at 37 °C for 30 min. Next, cells were centrifuged, resuspended in 10 mM Tris/10 mM MgCl$_2$ with 10 μg/ml propidium iodide (Sigma) and stained for 30 min. Flow cytometry was performed on FACS Canto II (BD Biosciences). The data were analyzed using BD FACSDiva^{TM} software.

References

Barr FA, Gruneberg U (2007) Cytokinesis: Placing and making the final cut. Cell **131**:847–857

Bernander R, Palm JE, Svard SG (2001) Genome ploidy in different stages of the *Giardia lamblia* life cycle. Cell Microbiol **3**:55–62

Bingham A, Jarroll EL, Meyer EA, Radulescu S (1979) Induction of *Giardia* Excystation and the Effect of Temperature on Cyst Viability as Compared by Eosin-exclusion and in vitro Excystation. In Jakubowski W, Hoff JC (eds) Waterborne Transmission of Giardiasis. U.S. Environmental Protect Agency, Cincinnati, Ohio, pp 217–229

Birky Jr CW (2010) *Giardia* sex? Yes, but how and how much? Trends Parasitol **26**:70–74

Brugerolle G (1975) Contribution a l'étude cytologique et phylétique des diplozoaires (Zoomastigophorea, Diplozoa, Dangeard 1910). V. Nouvelle interprétation de l'organisation cellulaire de *Giardia*. Protistologica **XI**: 99–109

Buchel LA, Gorenflot A, Chochillon C, Savel J, Gobert JG (1987) In vitro excystation of *Giardia* from humans: a scanning electron microscopy study. J Parasitol **73**:487–493

Chávez-Munguía B, Cedillo-Rivera R, Martínez-Palomo A (2004) The ultrastructure of the cyst wall of *Giardia lamblia*. J Eukaryot Microbiol **51**:220–226

Chubb JR, Boyle S, Perry P, Bickmore WA (2002) Chromatin motion is constrained by association with nuclear compartments in human cells. Curr Biol **12**:439–445

Cooper MA, Adam RD, Worobey M, Sterling CR (2007) Population genetics provides evidence for recombination in *Giardia*. Curr Biol **17**:1984–1988

Crossley R, Marshall J, Clark JT, Holberton DV (1986) Immunocytochemical differentiation of microtubules in the cytoskeleton of *Giardia lamblia* using monoclonal antibodies to alpha-tubulin and polyclonal antibodies to associated low molecular weight proteins. J Cell Sci **80**:233–252

Davids BJ, Williams S, Lauwaet T, Palanca T, Gillin FD (2008) G*iardia lamblia* aurora kinase: a regulator of mitosis in a binucleate parasite. Curr Opin Microbiol **10**:555–559

Elmendorf HG, Dawson SC, McCaffery JM (2003) The cytoskeleton of *Giardia lamblia*. Int J Parasitol **33**:3–28

Filice FP (1952) Studies on the cytology and life history of a *Giardia* from the laboratory rat. Univ Calif Publ Zool **57**: 53–146

Ghosh S, Frisardi M, Rogers R, Samuelson J (2001) How *Giardia* swim and divide. Infect Immun **69**:7866–7872

Hausen MA, de Oliveira RP, Gadelha AP, Campanati L, de Carvalho JJ, de Carvalho L, Barbosa HS (2009) *Giardia lamblia:* a report of drug effects under cell differentiation. Parasitol Res **105**:789–796

Hehl AB, Marti M (2004) Secretory protein trafficking in *Giardia intestinalis*. Mol Microbiol **53**:19–28

Hetsko ML, McCaffery JM, Svärd SG, Meng TC, Que X, Gillin FD (1998) Cellular and transcriptional changes during excystation of *Giardia lamblia* in vitro. Exp Parasitol **88**:172–183

Hofštetrová K, Uzlíková M, Tůmová P, Troell K, Svärd SG, Nohýnková E (2010) *Giardia intestinalis:* aphidicolin influence on the trophozoite cell cycle. Exp Parasitol **124**:159–166

Holberton DV (1973) Fine structure of the ventral disc apparatus and the mechanism of attachment in the flagellate *Giardia muris*. J Cell Sci **13**:11–41

Karr CD, Jarroll EL (2004) Cyst wall synthese: N-acetygalactosaminyltransferase aktivity is induced to form the novel N-acetylgalactosamine polysacharide in the *Giardia* cyst wall. Microbiology **150**:1237–1243

Keister DB (1983) Axenic culture of *Giardia lamblia* in TYI-S-33 medium supplemented with bile. Trans Roy Soc Trop Med Hygien **77**:487–488

Konrad C, Spycher C, Hehl AB (2010) Selective condensation drives partitioning and sequential secretion of cyst wall proteins in differentiating *Giardia lamblia*. PloS Pathog **6(4):**e1000835

Lasek-Nesselquist E, Welch DM, Thompson RC, Steuart RF, Sogin ML (2009) Genetic exchange within and between assemblages of *Giardia duodenalis*. J Eukaryot Microbiol **56**:504–518

Logsdon Jr JM (2008) Evolutionary genetics: sex happens in *Giardia*. Curr Biol **18**:R66–R68

Luján HD, Mowatt MR, Nash TE (1997) Mechanisms of *Giardia lamblia* differentiation into cysts. Microbiol Mol Biol Rev **61**:294–304

Luján HD, Marotta A, Mowatt MR, Sciaky N, Lippincott-Schwartz J, Nash TE (1995) Developmental induction of Golgi structure and function in the primitive eukaryote *Giardia lamblia*. J Biol Chem **270**:4612–4618

Macechko PT, Steimle PA, Lindmark DG, Erlandsen SL, Jarroll EL (1992) Galactosamine-synthesizing enzymes are induced when *Giardia* encyst. Mol Biochem Parasitol **56**:301–309

McCaffery JM, Gillin FD (1994) Giardia lamblia: Ultrastructural basis of protein transport during growth and encystations. Exp Parasitol **79**:220–235

Melloy P, Shen S, White E, McIntosh JR, Rose MD (2007) Nuclear fusion during yeast mating occurs by a three-step pathway. J Cell Biol **179**:659–670

Nohýnková E, Tůmová P, Kulda J (2006) Cell division of *Giardia intestinalis*: flagellar developmental cycle involves transformation and exchange of flagella between mastigonts of a diplomonad cell. Eukaryot Cell **5**:753–761

Nohýnková E, Dráber P, Reischig J, Kulda J (2000) Localization of gamma-tubulin in interphase and mitotic cells of a unicellular eukaryote, *Giardia intestinalis*. Eur J Cell Biol **79**:438–445

Palm D, Weiland M, McArthur AG, Winiecka-Krusnell J, Cipriano MJ, Birkeland SR, Pacocha SE, Davids B, Gillin F, Linder E, Svärd S (2005) Developmental changes in the adhesive disk during *Giardia* differentiation. Mol Biochem Parasitol **141**:199–207

Poxleitner MK, Carpenter ML, Mancuso JJ, Wang CJ, Dawson SC, Cande WZ (2008) Evidence for karyogamy and exchange of genetic material in the binucleate intestinal parasite *Giardia intestinalis*. Science **319**:1530–1533

Reiner DS, Ankarklev J, Troell K, Palm D, Bernander R, Gillin FD, Andersson JO, Svärd SG (2008) Synchronisation of *Giardia lamblia*: identification of cell cycle stage-specific genes and a differentiation restriction point. Int J Parasitol **38**:935–944

Sagolla MS, Dawson SC, Mancuso JJ, Cande WZ (2006) Three-dimensional analysis of mitosis and cytokinesis in the binucleate parasite *Giardia intestinalis*. J Cell Sci **119**:4889–4900

Schurko AM, Logsdon Jr JM (2008) Using a meiosis detection toolkit to investigate ancient asexual "scandals" and the evolution of sex. Bioessays **30**:579–589

Sheffield HG, Bjorvatn B (1977) Ultrastructure of the cyst of *Giardia lamblia*. Am J Trop Med Hyg **26**:23–30

Solari AJ, Rahn M, Saura A, Lujan HD (2003) A unique mechanism of nuclear division in *Giardia lamblia* involves components of the ventral disc and the nuclear envelope. Biocell **27**:329–346

Stefanic S, Morf L, Kulangara C, Regös A, Sonda S, Schraner E, Spycher C, Wild P, Hehl AB (2009) Neogenesis and maturation of transient Golgi-like cisternae in a simple eukaryote. J Cell Sci **122**:2846–2856

Tůmová P, Hofštetrová K, Nohýnková E, Hovorka O, Král J (2007a) Cytogenetic evidence for heterogeneity of two *Giardia* nuclei. Chromosoma **116**:65–78

Tůmová P, Kulda J, Nohýnková E (2007b) Cell division of *Giardia intestinalis*: assembly and disassembly of the adhesive disc, and the cytokinesis. Cell Motility Cytoskeleton **64**: 288–298

Yu LZ, Birky Jr CW, Adam RD (2002) The two nuclei of *Giardia* each have complete copies of the genome and are partitioned equationally at cytokinesis. Eukaryot Cell **1**:191–199

Available online at www.sciencedirect.com

SciVerse ScienceDirect

Mitotic checkpoints in a binucleated protozoan parasite *Giardia intestinalis*

Running title: Control of *Giardia* mitosis

Kristyna Markova[1], Klara Jirakova[1], Magdalena Uzlikova[1], Pavla Tumova[1],

Jaroslav Kulda[2], and Eva Nohynkova[1*]

Department of Tropical Medicine, 1st Faculty of Medicine, Charles University in

Prague, Studnickova 7, Prague 2, Czech Republic[1]; Department of Parasitology,

Faculty of Science, Charles University in Prague, Prague, Czech Republic[2]

* Corresponding author. Mailing address: Department of Tropical Diseases,

Studnickova 7, Prague 2, Czech Republic, Phone: +420 224968525. Fax: +420

224968525. Email: enohy@lf1.cuni.cz

Key words: *Giardia*, cytokinesis without mitosis, mitotic checkpoints, spindle

assembly checkpoint, Mad-2, albendazole, epoxomicin

Abstract

Spindle assembly checkpoint (SAC) is a regulatory mechanism that maintains genome integrity by preventing chromosome missegregation, and it has been documented across model eukaryotes. Despite its significance, little is known about the origin and evolution of this mechanism. Herein, SAC in *Giardia intestinalis*, a binucleated protozoan parasite that causes intestinal infections worldwide and is unrelated to all classical model organisms was examined using albendazole, which inhibits mitotic spindle assembly by preventing microtubule polymerization, and epoxomicin, which inhibits the proteasome. It has been shown that only limited regulation of cell division occurs in *Giardia* that carry out cell division even in the absence of a mitotic spindle and chromosome segregation. Moreover, *Giardia* cells perform a second round of DNA synthesis without chromosome segregation, thereby overriding mitotic and G1/S checkpoints. Accordingly, a genome search showed that there is only limited DNA replication machinery and poor support for several SAC members. Overexpression of the essential SAC component, Mad-2, did not result in metaphase-anaphase block, growth retardation or aneuploidy, as has been documented in fission yeast and mice. Similarly, any accumulation of cyclin-B, which is characteristic of cells arrested by SAC, was not observed in albendazole treated cells. However, mitotic exit network genes were identified. Additionally, an accumulation of doublets of interconnected cells in late cytokinesis in response to albendazole treatment was observed. We conclude that *Giardia* does not possess a conventional SAC, and that its mitosis is regulated in a different manner than in budding yeast and mammalian models.

INTRODUCTION

Variations of cell cycle control have been found among protozoan parasites, such as those responsible for malaria or sleeping sickness (23, 27) indicating that control mechanisms may be modified in lower unicellular eukaryotes. Whether the variations relate to parasitic lifestyle or represent steps in development of control mechanisms in eukaryotic cell is currently unknown.

Giardia intestinalis is a unicellular parasitic eukaryote that causes intestinal infections in humans and animals worldwide. Flagellated trophozoites (~ 12 x 6 µm) colonize the upper small intestine where they multiply, resulting in pathology. *Giardia* belongs to diplomonads, a group of protists with double sets of cell organelles including nuclei: their interphase cells have two nuclei of similar size and appearance in a single cell (2). Each nucleus contains a complete copy of the genome (64). The presence of four-fold content of haploid genome size (1C = 12Mb) in a *Giardia* cell proposed by FACS (5) and four variants of chromosome 1 estimated by PFGE (37) led to suggestions that each nucleus is diploid. Cytogenetic studies showed that, within a single cell, the two nuclei differ slightly in chromosome number indicating aneuploidy (59).

The binucleated *Giardia* trophozoite undergoes canonical cell cycle (G1/S/G2/M): a G1 cell (DNA content 4C, two nuclei) proceeds to the S phase, which is followed by G2 (DNA content 8C, two nuclei), a dominant phase of the *Giardia* cell cycle (5, 60). Under standard conditions, G2 trophozoites enter M phase with a rapid karyokinesis of both nuclei (3 minutes) followed by a slow cytokinesis (10). The two

nuclei of the trophozoite replicate and divide in parallel with slight asynchrony (33, 62). They divide by semi-open mitosis so that each mitotic spindle is composed from intra- and extra- nuclear microtubules, and a nuclear envelope is largely intact. *Giardia* mitosis seems to display unusual features such as the absence of a metaphase plate and premature chromatid separation (55, 62) : therefore, a non-conventional mode of chromatid segregation has been suggested (62). Cell division in *Giardia* requires the transformation of parent basal bodies/flagella, decomposition of the parent adhesive disc and assembly of two daughter discs resulting in freely swimming dividing cells which adhere again to finish cytokinesis, an extremely long process (up to 1 hour) when compared to mitosis (50, 63).

Based on our previous findings, we hypothesize that rapid and perhaps atypical chromosome segregation and the presence of two nuclei may involve specific modifications of the general scheme of mitotic control including deviations already found in some parasitic protists (17, 26). In a eukaryotic cell, cell cycle transitions are monitored by checkpoints that ensure the completion of required processes before initiating the following step. In *Giardia*, a functional DNA damage and replication checkpoint has been proposed under DNA defective conditions (treatment with the DNA polymerase inhibitor aphidicolin) (30). Here, we focus on mitotic checkpoints in *Giardia*: the spindle assembly checkpoint (SAC), a safety mechanism that inhibits progression from metaphase to anaphase, and the mitotic exit network (MEN) that regulates telophase and cytokinesis. Even when a single kinetochore is not attached to spindle microtubules or lacks tension across two kinetochores, SAC stays active. Its core Mad1-Mad2 tetramer complex forms at the kinetochore and initiates Cdc-20 binding and the subsequent inhibition of the ubiquitin ligase complex required for mitosis (APC/C - anaphase promoting complex/cyclosome) (1, 47). The checkpoint

signal is extinguished by proper chromosome alignment, and the subsequently formed APC/C/Cdc-20 and Cdh-1 complexes degrade anaphase inhibitors such as securin or cyclin-B (61). Similarly, if chromosomes fail to segregate, MEN halts cell in anaphase. A key component of MEN, Cdc-14 phosphatase, dephosphorylates Cdh-1, which mediates the degradation of Cdc-20, aurora-B, polo-like kinase and others (38). When failure of chromosome segregation occurs, the Cdc-14 activating factor Tem-1 is deactivated, and Cdc-14 is trapped in a nucleolus and causes anaphase arrest (53). In this paper, we examine the presence or absence of mitotic checkpoints by preventing spindle formation and inhibiting degradation of essential molecules in mitotic control. We screened for the presence of SAC members in the *Giardia* genome and analyzed their expression and localization in control, albendazole- and epoxomicin-treated cells.

We found that *Giardia* cells with inhibited assembly of mitotic spindles did not arrest their cell cycle. On the contrary, they divided further and reduplicated their DNA. In the *Giardia* genome database, we found only a limited homology of SAC members in contrast to a high homology of MEN factors. Despite its proposed function in a functional SAC, in *Giardia*, the expression of Mad-2 decreased, and cyclin-B did not accumulate in the arrested cells. Furthermore, localization of Mad-2 was mainly along caudal flagella but never within nuclei. We conclude that *Giardia* does not possess a conventional spindle assembly checkpoint, and that its cell division is regulated in a different manner than in conventional models.

MATERIALS AND METHODS

Strain, media, growth conditions, inhibitory tests

The HP-1 line of Portland-1 isolate of *Giardia intestinalis* (ATCC 30888), donated by E. A. Meyer (Oregon Health Sciences University, Portland, USA), was used in

this study. Trophozoites were cultivated axenically in 13×100 mm screw cap glass tubes in TYI-S-33 medium supplemented with bovine bile (34) (pH 6.8, supplemented with penicillin and amikacin) at 37°C and sub-cultured twice a week. After reaching 70% confluence, the medium was replaced with pre-warmed 100 ng/ml albendazole or 10 ng/ml nocodazole containing TYI-S-33 medium, and the cells were incubated at 37°C for the specified period of time. Cells were harvested via incubation on ice for 15 min followed by centrifugation at $900 \times g$ for 10 min. The harvested cells were the initial material for subsequent isolations. Glass slides for immunostaining were prepared by briefly air drying or immediately fixing smears.

Alternatively, *Giardia* cells were incubated for 6, 12 or 24 hours in 5 μM epoxomicin in TYI-S-33. Cultures of trophozoites were enriched by mitotic cells when required. Cells were exposed to albendazole (100 ng/ml) for 7 hours, and detached cells were decanted. Remaining attached trophozoites were covered with albendazole-free medium, and the onset of mitotic cells was observed under a microscope. Cells were harvested and fixed immediately.

Chromosome spreads

The samples were prepared from cultured trophozoites that were hypotonized, repeatedly fixed in methanol/acetic acid, dropped on glass slides and stained with DAPI as described previously (62). Preparations were observed using an Olympus BX51 fluorescence microscope.

Immunostaining

The following antibodies were used at the following defined dilutions (diluted in 2%BSA, 0.01% Tween 20 in PBS): anti-cyclin B (Abcam, ab2631) 1:500, aurora kinase A (Abcam, ab12875) 1:300, aurora kinase A phosphoT288 (Abcam, ab18318)

1:300, and acetylated α-tubulin (Sigma, 6-11B-1) 1:500. Briefly, dried smears of cells were fixed for 7 min in ice-cold methanol followed by permeabilization in acetone (5 min) at -20°C. Slides were air dried, rehydrated for 10 min with PBS and processed as described previously (30). Double staining was performed for cyclin B and acetylated α-tubulin. Cyclin-B antibody was applied first and then samples were fixed for 15 min in 4% paraformaldehyde in PBS and washed in PBS. A second round of staining (anti-acetylated α-tubulin) was performed without modification.

RT PCR and qRT PCR

Total RNA was isolated from *Giardia* control trophozoites and trophozoites after 1, 7, 12 or 24 hours of incubation in albendazole using a High Pure RNA isolation kit (Roche). Total RNA (500 ng) was converted into cDNA using a RevertAid First Strand cDNA synthesis kit (Fermentas). Primers for qRT PCR (product length ~120 bp) were designed using open-source PerlPrimer software (version 1.1.14; Marshall OJ, PerlPrimer [http://perlprimer.sourceforge.net/]). qRT PCR was performed using a SYBR green PCR master kit (Roche) and LC480 platform (Roche). Glycyl-tRNA synthetase and glutamate dehydrogenase were used as the endogenous controls, and primer-pair efficiencies were determined using serial dilutions of corresponding PCR products. All experiments were done in triplicate. The accession numbers of analyzed *Giardia* genes are as follows (EuPathDB Bioinformatics Resource Center, University of Pennsylvania, Philadelphia [www.giardiadb.org)] (3): aurora kinase (GL50803_5358), cyclin-A (GL50803_14488), cyclin-B (GL50803_3977), Cdc-14 (GL50803_9270), glutamate dehydrogenase (GL50803_21942), glycyl-tRNA synthetase (GL50803_9011), mad-2 (GL50803_100955).

Western blot analysis

Cell lysates prepared in RIPA buffer with a protease inhibitor mix were quantified by a BCA assay. Then, gels were loaded with 40 µg per line and then proteins transferred onto a nitrocellulose membrane. *Giardia* cyclin B was detected using an anti-cyclin-B1 antibody (Abcam, ab2631) at a 1:5000 dilution at 4°C overnight. Ubiquitinylated proteins were identified using an anti-ubiquitin antibody (Abcam, ab19247) at a 1:1000 dilution for 2 hours at room temperature (RT). Detection based on alkaline phosphatase conjugated to a secondary antibody and NBT/BCIP substrate (Sigma) was used.

Detection of DNA synthesis

DNA synthesis was visualized using an immunofluorescence assay for the detection of 5-bromo-20-deoxy-uridine (BrdU) incorporated into DNA (5-bromo-20-deoxy-uridine Labeling and Detection Kit I, Roche). Trophozoites were processed according to the manufacturer´s instructions.

Flow cytometry analysis

For flow cytometry, untreated or albendazole-treated (100 ng/ml) trophozoites for 3, 7 and 24 hours were fixed as described previously (5). Briefly, cells were harvested by centrifugation ($900 \times g$) with a cell concentration of approximately 1×10^7 cells/ml. The pellet was resuspended in 50 µl fresh TYI-S-33 medium and 150 µl fixative (1% Triton X-100/40 mM citric acid/20 mM dibasic sodium phosphate/200 mM sucrose, pH 3.0) for 5 min at RT. Then, 350 µl of the diluent buffer (125 mM $MgCl_2$ in PBS, pH 7.4) was added, and samples were stored at 4ºC until measurement. Fixed cells were centrifuged ($4000 \times g$, 3 min), washed in PBS, resuspended in 500 µl PBS with 1µg RNAse A (Fermentas) and incubated at 37ºC for 30 min. Then, the cells were centrifuged, resuspended in 10 mM Tris/10 mM $MgCl_2$ with 10 µg/ml propidium iodide (Sigma) and stained for 30 min. Flow

cytometry was performed on FACS Canto II (BD Biosciences). The data were analyzed using BD FACSDiva[TM] software.

Mad-2-HA transfected trophozoites

The Mad-2 homolog (GL50803_100955) was cloned from trophozoite cDNA using the following primers: Mad-2F (GAATTCC CATATGGCTACCCAGACCAAGAATGC), and Mad-2R (GCG GGATCC CAGCGCTTCCTCTCCAGACTT). The full-length sequence was cloned into the pOndra plasmid under the control of a GDH promoter and flanked at the C-terminus by an HA-tag. Ampicillin and G418 resistance were encoded by the plasmid. Approximately 1×10^7 of trophozoites (300 µl) were incubated for 15 min with 30 µg of plasmid on ice and electroporated with 350 V for 175 ms. Cells were grown in 7 ml glass tubes for 24 hours after transfection without selection. The medium containing G418 (150 µg/ml) was replaced daily the following 4 days and then increased to 600 µg/ml and exchanged every other day. The stable transfection was established in 2-3 weeks. The expression of the cloned gene (Mad-2) was controlled and quantified by qRT PCR and a western blot analysis. Transformants were sub-cloned (a single cell gave rise to a new population) and harvested for RNA isolation, and slides with fixed cells were alternatively prepared for immunolocalization. Mad2-HA cells were exposed to albendazole treatment as described above and compared to control cells.

RESULTS

Cell division proceeds independently of mitosis: albendazole treatment

When *Giardia* trophozoites were exposed to 100 ng/ml albendazole, karyokinesis was fully blocked in 100% of cells 9 hours later (corresponding to the generation time of the isolate) due to the inhibition of mitotic spindle assembly (Fig. 1).

Nevertheless, the cells continued to divide. As a consequence of the albendazole treatment, two undivided parental nuclei with G2 content persisted in dividing cells. At M-phase entry, the nuclei were released from a complex of basal bodies (Fig. 1A). Cytokinesis was completed in 80% of these cells (Fig. 1). During cytokinesis, the two nuclei were randomly distributed between the daughter cells, resulting in a population of aberrant trophozoites with one, two, or no G2 nuclei at all (Fig. 1) . Remaining 20% of albendazole-treated cells started, but did not complete cytokinesis: the progeny were interconnected by their caudal parts, forming binucleated "doublets". Notably, basal bodies (bb) and flagellar axonemes were not affected (Fig. 1), as cell division proceeded with an undisturbed pattern of parent bb/flagella reorganization and *de novo* assembly of complementary bb/axonemes (50). In contrast, *de novo* assembly of daughter adhesive discs was inhibited in progeny, precluding the adhesion to substrate.

The effect of epoxomicin on *Giardia* cells with respect to mitosis

Epoxomicin inhibits proteasome function by covalently binding to its catalytic subunits (42). Epoxomicin leads to potential cell cycle progression disturbances because cell cycle regulation is dependent on proteasome-mediated protein degradation in a majority of organisms. We demonstrated that epoxomicin is a potent inhibitor of *Giardia* proteasomes. As seen in Fig. 2B, a significant accumulation of ubiquitinylated proteins in whole cell lysates of epoxomicin-treated trophozoites was found in response to the decreased degradation. Moreover, we showed that after 24 hours of trophozoite exposure to epoxomicin, aberrant trophozoites containing atypical number and positioning of nuclei appeared (Fig. 2A). This disturbance in karyokinesis was likely caused by the proteasome inhibition during interphase since mitotic cells exposed to the epoxomicin did not manifest any aberrations (Fig. 2A).

We observed near-equal levels of the dominant B-like cyclin in albendazole- and epoxomicin-treated cells when compared to unaffected cells. The molecular weight of approximately 44 kDa corresponded roughly (possibly due to posttranslational modification) to the expected 40 kDa based on the sequence of the annotated *Giardia* G2/M cyclin (GL50803_3977). Cyclin-B belongs to a group of proteins whose regulation by ubiquitinylation and subsequent degradation is required to exit from mitosis. Thus, accumulation of cyclin-B under a proteasome-defective condition would be expected, but this was not observed in this case.

Mitotic checkpoint genes in *Giardia intestinalis*

We found orthologues of most core SAC genes in the genome of *Giardia intestinalis*. However, when sequences were compared, mad-1, mad-3 and cdc-20 were poorly conserved. Securin, which is not generally associated with genes of conservative sequence, was not identified. Notably, mad-1 has been shown to be a binding partner of mad-2 during the process of cdc-20 sequestration (41). The homolog of the crucial gene mad-2 was found (GL_50803_100955), and it contained, accordingly, a conserved HORMA domain, a chromatin recognition domain (E-value $2e^{-45}$), and a general identity to human mad-2A of 43% (64% positivity). The analysis of putative *Giardia* cdc-20 (GL_50803_33762, the closest match to budding yeast and human cdc-20) revealed that a WD40 domain is present (E-value $5e^{-54}$), but the region required for direct interaction with mad-2 immediately upstream of the WD40 repeats (58) did not resemble any of the described patterns (57). However, none of the *Giardia* WD40 genes fit the cdc-20 profile with greater identity. The overall homology to cdc-20 from human (25% identity, E value $3.4e^{-09}$) and budding yeast (24% identity, E value e^{-10}) was very low. These results indicate that the gene set for the conventional spindle assembly checkpoint might be incomplete or insufficiently

conserved. Nevertheless, mad-2 (a crucial component of the SAC), bub-3, aurora kinase, cenp-E (spindle kinesin involved in the SAC), and a huge repertoire of NEK-like kinases were present. Unlike the SAC, the MEN members bub-2, cdc-14 and tem-1 were identified as conserved homologs to human or budding yeast genes as was previously noted by Morrison and colleagues (45). This suggests that the second branch of the mitotic regulation may be conserved and may influence the response to albendazole, a karyokinesis-inhibiting treatment.

Spindle checkpoint molecules in albendazole-affected cells

To proceed to anaphase and beyond, eukaryotic cells usually require APC/C^{Cdc20} -mediated degradation of several prometaphase proteins such as securin or mitotic cyclin-B. The SAC protein Mad-2 inhibits degradation of the prometaphase proteins and arrests cells in metaphase until proper conditions are established. These changes may also be reflected at the mRNA level. To evaluate the changes in expression of SAC and associated genes in albendazole-treated cells, RT-PCR analysis of mad-2, cyclin-B, cyclin-A, bub-3, aurora kinase and cdc-14 was conducted. Cells exposed for 7 hrs to albendazole demonstrated significantly decreased levels of mad-2, cyclin-A and cyclin-B as determined by RT-PCR analysis (Fig. 3C). qRT-PCR revealed an almost five-fold decrease in mad-2, cyclin-B and cdc-14 after 24 hrs of albendazole treatment (compared to a three-fold decrease after 7 hours; Fig. 2B). The expression of cyclin B-like protein, which is associated with basal bodies during the *Giardia* cell cycle, was most intense signal during mitosis but did not show any accumulation corresponding to mitotic arrest by immunostaining (Fig. 3A). Similarly, aurora kinase (AK) immunostaining showed no notable differences between treated and control cells, both for the active and inactive forms (Fig. 3B). Though AK is a necessary component of the SAC, especially during SAC complex

assembly at the kinetochores, we did not observe any prominent changes caused by the treatment and eventual SAC activation. Western blot analysis confirmed a lack of cyclin-B accumulation and showed a steady cyclin-B level in albendazole-treated cells when compared to controls (Fig. 3). The antibody identified one major band but three additional weak bands were observed. These likely correspond to other cyclin-like proteins encoded in the *Giardia* genome. The protein levels of the additional bands oscillated, but the trends were similar for control and albendazole-treated cells. Moreover, the general ubiquitinylation of proteins was compared, but no difference between control and albendazole-treated cells was found (Fig. 2B). These observations at the mRNA and/or protein levels suggested that Mad-2 is not utilized during albendazole treatment. Further, the accumulation of cyclin-B was not observed.

Mad-2 overexpression does not affect *Giardia* trophozoites

Using a strong GDH promoter, we achieved 13-times-greater expression of Mad-2 than the endogenous level. Mad-2 was detected via an HA tag fused to the C-terminus. Mad-2 localization was restricted in interphase as well as in mitotic cells in the region of the caudal flagella and the median body, but never in the nuclei (Fig. 4A). Rarely, we found a strong signal in the whole cell, which we considered an artifact of strong expression and a product of subsequent degradation. However, this cytoplasmic localization could be also attributed to cytoplasmic pool of Mad-2. Trophozoites overexpressing Mad-2 did not show any division abnormalities, and the karyotype was also constant. Their general morphology was not affected (Fig. 4), nor was the DNA profile of the population or their ability to encyst (data not shown). They responded to albendazole treatment similar to the control cells, and qRT PCR

analysis showed no notable changes in expression of selected mitotic and SAC genes (data not shown).

DNA reduplication in cells without mitosis

Flow cytometric analysis of cellular DNA content of populations of trophozoites exposed to albendazole (different durations of treatment) and controls revealed DNA re-replication in cells that did not undergo mitosis (Fig. 1C). Control cells from the logarithmic phase of growth formed two major subpopulations (peaks): a minor G1 peak (cell DNA content 4C; two nuclei with a basic set of unreplicated DNA) and a dominant G2 peak that corresponds to 8C DNA content (each nucleus with replicated DNA). With shorter incubation intervals (3 hours albendazole), the DNA content of the treated population resembled that of the control cells without albendazole (data not shown). After 7 hrs of incubation with albendazole, the notably larger first peak corresponded to the G1/S phase, and a new peak with DNA content higher than 8C started to appear. After 24 hrs of incubation with albendazole, three distinctive peaks were formed, one corresponding to G1, one corresponding approximately to G2 and one falling between 8C and 16C DNA content. The FACS results together with the morphological profiles of the albendazole-treated population (see above) allowed us to define three cell sub-populations: (i) cells with one G2 nucleus corresponding to G1 peak; (ii) cells with either two G2 nuclei, or with one G2 nucleus with re-replicated DNA, both corresponding to the G2 peak and (iii) cells with two nuclei that have proceeded to another round of replication; this sub-population, covering both single cells and doublets, formed the third peak in the flow cytometry histogram. Note that after 7 hrs of incubation there was an increased signal between the second and third peak, indicating that DNA synthesis was occurring. The second round of DNA replication in the nuclei that did not undergo karyokinesis was further

documented with BrdU incorporation and chromosomal spreads (Figs. 1D, E). After 12 hours of incubation with albendazole, BrdU was detected in the nuclei of both single cells and doublets, and chromosomal spreads showed as many as twenty condensed chromosomes per nucleus in a significant portion of cells after 24 hrs.

DISCUSSION

Cytokinesis without nuclear division in *Giardia intestinalis* exposed to mitotic poisons

The *Giardia* genome analysis revealed that the tools for key cellular processes are minimal. Nevertheless, protein kinases form the single largest protein class (45), magnifying the importance of a complex signal transduction network and thus the requirement of multi-level regulation. Mitotic checkpoints are potent regulatory mechanisms that prevent aneuploidies caused, for example, by imprecise chromosome segregation, across the eukaryotic kingdom in yeast (11), human cells (47) and plants (9). Mitotic checkpoints influence progress to the G1 phase at different levels, such as preventing separation of MTOCs when spindle assembly is defective (31). Our results showed that none of these mechanisms seemed to be fully functional in *Giardia*, which proceeded to cytokinesis in spite of incomplete mitosis. The results with albendazole treatment are in accordance with epoxomicin or nocodazole, thus excluding the possibility that the observed changes are artifacts of total inhibition of spindle assembly. Even though several crucial members of these checkpoints are relatively well conserved, they are incapable of arresting cells exposed to mitotic poison. The lack of mitotic arrest could be connected to the fact that the APC/C subunits usually required for targeted polyubiquitination of cyclin-B cannot be easily identified in the genome of *Giardia intestinalis*. However, other ubiquitin ligation systems have been described in *Giardia* (21), and ubiquitin-mediated proteolysis other

than APC/C can take place to regulate mitosis such as oscillating ubiquitinylation of putative cyclins (Fig. 3). In addition, a ubiquitinylation system utilizing HECT ubiquitin ligase has been shown to positively regulate the spindle checkpoint (59), and its homologues have been identified in *Giardia* (21). Furthermore, the observed accumulation of trophozoite doublets is an indication of MEN, whose crucial members were identified in the *Giardia* genome. These trophozoites interconnected by their caudal parts constituted 20% of the total population after 9 hours of treatment. Nevertheless, the presence of doublets might also correspond to possible defective cytokinesis caused by loss of adhesion due to treatment as the terminal phase of *Giardia* cytokinesis was considered to be adhesion dependent (63).

The dysfunction or absence of mitotic checkpoints does not seem to be unique within parasitic protozoa. *Trypanosoma brucei*, the causative agent of sleeping sickness, was shown to undergo cytokinesis even when mitosis was inhibited by rhizoxin, suggesting that the normal mitosis to cytokinesis checkpoint is missing (54). The absence of a checkpoint was also demonstrated in the malaria parasite, *Plasmodium falciparum*, where mitotic failure neither inhibited cytokinesis nor DNA synthesis (56), which is consistent with our findings. The absence of sudden checkpoints in parasitic protozoa might be an adaptation to specific life cycles (17). In the apicomplexan *Toxoplasma gondii*, an experimental disruption of microtubules leads to budding and nuclear division uncoupling. Subsequently, a low level of regulation was suggested (46), but these results were challenged with mutant analysis and genetic complementation, which revealed the presence of many checkpoints. Thus, the former conclusion was thought to be the result of a loss of strict physical context by the treatment (24). Nevertheless, this is not the case for experiments with *Giardia intestinalis* because our results with albendazole treatment are congruent with those from epoxomicin

treatment. In addition, it has been shown that *Giardia* strains and isolates differ in karyotypes, as e.g. the two nuclei of cells of the P15 isolate contain mostly 10+11 chromosomes while those of HP-1 contain 9+11 (62) compared to most probably original 10+10 pattern observed in some isolates from non-A assemblages (data not shown). Based on our data, it is possible that such an instability and unequal chromosome counts between nuclei in the cell might be a consequence of limited regulation of chromosome segregation naturally present in *Giardia*.

Giardia was previously regarded as early diverging eukaryote (25, 28). Later, its position on eukaryotic tree has been revised (36). Due to the presence of features resembling primitive organisms as well as advanced eukaryotes, hypothesizing the origin of specific cellular processes such as cell cycle regulation is highly problematic. The absence of specific genes, structures or pathways might be seen from different points of view: (i) they are not yet present (original condition), (ii) they were not developed in the lineage due to its inutility or even disutility, (iii) they were secondarily lost due to parasitism, or (iv) they were substituted by an alternative, but unrelated, element. Yet another possible reason for the absence of mitotic arrest in *Giardia* emerges from the hypothesis of premature chromatid separation: it might be explained by the presence of separated chromatids at the beginning of mitosis, well in advance of their segregation and putative attachment to spindle microtubules (62). This unusual progression through mitosis would make SAC inadequate for regulation of chromosome segregation.

The role of Mad-2 in *Giardia* and spindle checkpoint

Here, we report that Mad-2 overexpression had no significant effect on *Giardia* trophozoites although multiple effects such as metaphase-anaphase arrest (*S. pombe*) (29) and/or accumulation of aneuploidy and tumorigenesis (48) have been described

elsewhere. The increase in single and triple-nucleated cells in some Mad-2 overexpressing clones was not statistically significant (data not shown). Moreover, Mad-2 localization did not correspond with the proposed function. However, the specifically labeled caudal flagellar pair plays a crucial role in the assembly and orientation of daughter discs in telophase (50). Privileged caudal basal bodies drive the nucleation of spiral MT arrays that form the basis of the ventral adhesive disc (14). Thus, we can speculate that the observed oscillations at the transcript level reach their maximum level in mitosis (complete data not shown), suggesting that Mad-2 plays a part in controlling late-stage mitotic events such as disc distribution. These actions must be well coordinated with cytokinesis.

The decrease in mad-2 with albendazole treatment was accompanied by a decrease in cyclin B-like as well as cyclin A-like transcripts reconcilable with observed stable protein levels when compared to control cells. The exponentially growing *Giardia* population (control cells) consists of a dominant G2 sub-population with mitotic cells representing the smallest percentage (1-2%). Thus the observed transcript/protein levels agree with the inactive checkpoint. An active checkpoint would arrest cells in mitosis leading to a dramatic increase of mitosis specific components such as cyclin-B compared to controls with sporadically occurring mitotic cells. Finally, in contrast to other reported cases, the mad2-null fruit fly mutant (SAC inactivation) is viable and has proper chromosome segregation. This suggests that mitotic systems, which do not need mad-2 functionality in regulatory complexes at kinetochores, exist even among metazoans (8).

Dissociation of nuclear and centrosomal cycles

Duplication of the centrosome (a super-organelle containing centrioles) in animals is coordinated with DNA replication. Therefore, it occurs in S phase, and there are

regulatory factors that limit the centrosome duplication to once per cell cycle (15). In contrast, *Giardia* duplicates basal bodies (centriole homologs in flagellated cells) during mitosis (50) and it has been shown that even if mitosis is halted, basal body duplication is not affected. This suggests that not only cytokinesis but also basal body duplication is mitosis-independent. It seems that nuclear and centrosomal cycles are disconnected in *Giardia* and we can speculate that *Giardia* division may be regulated via the centrosomal cycle which seems to drive cytokinesis even in the absence of nuclear division. Moreover, basal bodies of *Giardia* trophozoites are known to co-localize with numerous proteins required for both cellular and nuclear division such as aurora kinase (13), centrin (4, 43), gamma tubulin (49) and cyclin B-like proteins, which demonstrates the essential role of basal bodies for every phase of *Giardia* division.

Does proteasome-mediated degradation play a role in *Giardia* cell cycle regulation?

Our results showed that epoxomicin-inhibition of the proteasome gave rise to aneuploid cells in *Giardia*. It is interesting to note that when the drug was added to mitotic cells, these cells completed mitosis and cytokinesis properly, suggesting that the progression through mitosis might be proteasome-independent. Thus, it seems that specific factors such as CDK inhibitors are degraded before mitosis. Few studies have been published on proteasome function in *Giardia* to date, and its role in cell cycle regulation has not been studied before. The *Giardia* genome encodes a single gene for ubiquitin, multiple protein ubiquitin ligase systems (21) and the typical eukaryotic complex proteasome 20S (20, 21, 52). The presence of this machinery together with our data supports its important regulatory function. Nevertheless, the problem of

19

which steps in the cell cycle are regulated via specific phosphorylation, expression changes or targeted proteasomal degradation remains to be solved.

DNA reduplication is not blocked in *Giardia* trophozoites with aberrant mitosis

Licensing of DNA replication in G1 (loading of inactive helicase) and initialization in S phase, as triggered by CDKs while the APC/C is inactive, work as a two-step control mechanism preventing reduplication (6, 16). Here, we define reduplication in *Giardia* trophozoites that have completed cytokinesis without mitosis and the excessive round of DNA replication results in duplicated G2 nuclei.

As described in various eukaryotes, the assembly of pre-replication complexes (pre-RC) requires the S-phase licensing factors Cdt-1 and Cdc-6, which recruit a MCM2-7 complex with helicase activity. Additional factors such as MCM-10 and Cdc-45 secure the loading of polymerases and conversion of a pre-replication complex to a replication fork that is tightly bound to S phase CDK and DDK activity (i.e. CDC7 kinase and DBF4) (19, 44). Reduplication might occur when new pre-RC are assembled prematurely. The oscillation of APC/C activity is essential: (i) a high rate in late mitosis/G1 allows pre-RC formation and (ii) a low rate in S/G2 prevents their assembly and therefore reduplication (16). In the majority of eukaryotic species examined, Cdt-1, a critical regulator of replication licensing, is degraded at START by ubiquitin-mediated proteolysis to prevent the reassembly of pre-RC (35). In *Giardia*, only the basal machinery of the replication complexes is present (39). The genome codes for a single subunit of the origin recognition complex (orc1/cdc6) and mcm2-7, but other components such as cdc-45 and more importantly cdt-1 and dbf-4 are missing. Similar findings were also described in other protozoans. *Trypanosoma brucei* (22) possesses cdc-45 but lacks cdt-1 and dbf-4, as does *Entamoeba histolytica* (12), and *Plasmodium falciparum* lacks cdt-1, dbf-4 and also

cdc-45 (51). When compared to *E. histolytica*, the *Giardia* genome codes for a cdc-7 homolog and possibly mcm-10 while cdc-45, mcm-8 and mcm-9 are missing. In contrast, *E. histolytica* lacks cdc-7 but contains cdc-45, mcm-8 and mcm-9 and is known to undergo a variable number of endo-reduplicative cycles, perhaps as a result of a lack of regulatory mechanisms (12, 40). These examples demonstrate that replication regulation varies across protozoa, and a comparison of individual protozoans offers a model of gradual addition of regulatory subunits during, in this respect, rapid evolution. Of particular note is the high variability in pre-RC regulation even within the single genus *Saccharomyces*, where Cdc-6 was shown to be regulated in fundamentally different ways depending on the species (18). Lack of reduplication regulation can be seen as a primitive condition, but endoreduplication has also been described as an effective modification of the cell cycle commonly seen in plants (32) and metazoan tissues with high metabolic activity (7).

ACKNOWLEDGEMENTS

REFERENCES

1.   **Acquaviva, C., and J. Pines**. 2006. The anaphase-promoting complex/cyclosome: APC/C. J. Cell Sci. **119**:2401-2404.

2.   **Adam, R. D.** 2001. Biology of Giardia lamblia. Clin. Microbiol. Rev. **3**:447-475.

3.   **Aurrecoechea, C., J. Brestelli, B. P. Brunk, J. M. Carlton, J. Dommer, S. Fischer, B. Gajria, X. Gao, A. Gingle, G. Grant, O. S. Harb, M. Heiges, F. Innamorato, J. Iodice, J. C. Kissinger, E. Kraemer, W. Li, J. A. Miller, H. G. Morrison, V. Nayak, C. Pennington, D. F. Pinney, D. S. Roos, C. Ross, C. J. Stoeckert, Jr., S. Sullivan, C. Treatman, and H. Wang**. 2009. GiardiaDB and TrichDB: integrated genomic resources for the eukaryotic protist pathogens Giardia lamblia and Trichomonas vaginalis. Nucleic Acids Res. **37**:D526-530.

4.   **Belhadri, A.** 1995. Presence of centrin in the human parasite Giardia: a further indication of its ubiquity in eukaryotes. Biochem. Biophys. Res. Commun. **214**:597-601.

5.   **Bernander, R., J. E. Palm, and S. G. Svard**. 2001. Genome ploidy in different stages of the Giardia lamblia life cycle. Cell. Microbiol. **3**:55-62.

6.   **Blow, J. J., and A. Dutta**. 2005. Preventing re-replication of chromosomal DNA. Nat. Rev. Mol. Cell. Biol. **6**:476-486.

7.   **Brodsky, W. Y., and I. V. Uryvaeva**. 1977. Cell polyploidy: its relation to tissue growth and function. Int. Rev. Cytol. **50**:275-332.

8.   **Buffin, E., D. Emre, and R. E. Karess**. 2007. Flies without a spindle checkpoint. Nat. Cell. Biol. **9**:565-572.

9.   **Caillaud, M. C., L. Paganelli, P. Lecomte, L. Deslandes, M. Quentin, Y. Pecrix, M. Le Bris, N. Marfaing, P. Abad, and B. Favery**. 2009. Spindle assembly checkpoint protein dynamics reveal conserved and unsuspected roles in plant cell division. PLoS One **4**:e6757.

10.   **Cerva, L., and E. Nohynkova**. 1992. A light microscopic study of the course of cellular division of Giardia intestinalis trophozoites grown in vitro. Folia Parasitol. (Praha) **39**:97-104.

11.   **Clarke, D. J., and J. Bachant**. 2008. Kinetochore structure and spindle assembly checkpoint signaling in the budding yeast, Saccharomyces cerevisiae. Front. Biosci. **13**:6787-6819.

12.   **Das, S., and A. Lohia**. 2002. Delinking of S phase and cytokinesis in the protozoan parasite Entamoeba histolytica. Cell. Microbiol. **4**:55-60.

13.   **Davids, B. J., S. Williams, T. Lauwaet, T. Palanca, and F. D. Gillin**. 2008. Giardia lamblia aurora kinase: a regulator of mitosis in a binucleate parasite. Int. J. Parasitol. **38**:353-369.

14.   **Dawson, S. C., and S. A. House**. Life with eight flagella: flagellar assembly and division in Giardia. Curr. Opin. Microbiol. **13**:480-490.

15.   **Delattre, M., and P. Gonczy**. 2004. The arithmetic of centrosome biogenesis. J. Cell. Sci. **117**:1619-1630.

16.   **Diffley, J. F.** 2004. Regulation of early events in chromosome replication. Curr. Biol. **14**:R778-786.

17.   **Doerig, C., D. Chakrabarti, B. Kappes, and K. Matthews**. 2000. The cell cycle in protozoan parasites. Prog. Cell Cycle Res. **4**:163-183.

18.   **Drury, L. S., and J. F. Diffley**. 2009. Factors affecting the diversity of DNA replication licensing control in eukaryotes. Curr. Biol. **19**:530-535.

19.   **Early, A., L. S. Drury, and J. F. Diffley**. 2004. Mechanisms involved in regulating DNA replication origins during the cell cycle and in response to DNA damage. Philos. Trans. R. Soc. Lond. B Biol. Sci. **359**:31-38.

20.   **Emmerlich, V., Scholze, H., Gillin, F. D., Bakker-Grunwald, T.** 2001. Characterization of a proteasome alpha-chain from Giardia lamblia. Parasitol. Res. **87**:112-115.

21.   **Gallego, E., Alvarado, M., Wasserman, M.** 2007. Identification and expression of the protein ubiquitination system in Giardia intestinalis. Parasitol. Res. **101**:1-7.

22.   **Godoy, P. D., L. A. Nogueira-Junior, L. S. Paes, A. Cornejo, R. M. Martins, A. M. Silber, S. Schenkman, and M. C. Elias**. 2009. Trypanosome prereplication machinery contains a single functional orc1/cdc6 protein, which is typical of archaea. Eukaryot. Cell **8**:1592-1603.

23.   **Grant, K. M.** 2008. Targeting the cell cycle in the pursuit of novel chemotherapies against parasitic protozoa. Curr. Pharm. Des. **14**:917-924.

24.   **Gubbels, M. J., M. Lehmann, M. Muthalagi, M. E. Jerome, C. F. Brooks, T. Szatanek, J. Flynn, B. Parrot, J. Radke, B. Striepen, and M. W. White**. 2008. Forward genetic analysis of the apicomplexan cell division cycle in Toxoplasma gondii. PLoS Pathog. **4**:e36.

25.   **Gupta, R. S., K. Aitken, M. Falah, and B. Singh**. 1994. Cloning of Giardia lamblia heat shock protein HSP70 homologs: implications regarding origin of eukaryotic cells and of endoplasmic reticulum. Proc. Natl. Acad. Sci. U S A **91**:2895-2899.

26.   **Hammarton, T. C.** 2007. Cell cycle regulation in Trypanosoma brucei. Mol. Biochem. Parasitol. **153**:1-8.

27.   **Hammarton, T. C., J. C. Mottram, and C. Doerig**. 2003. The cell cycle of parasitic protozoa: potential for chemotherapeutic exploitation. Prog. Cell. Cycle. Res. **5**:91-101.

28.   **Hashimoto, T., Y. Nakamura, T. Kamaishi, F. Nakamura, J. Adachi, K. Okamoto, and M. Hasegawa**. 1995. Phylogenetic place of mitochondrion-lacking protozoan, Giardia lamblia, inferred from amino acid sequences of elongation factor 2. Mol. Biol. Evol. **12**:782-793.

29.   **He, X., T. E. Patterson, and S. Sazer**. 1997. The Schizosaccharomyces pombe spindle checkpoint protein mad2p blocks anaphase and genetically interacts with the anaphase-promoting complex. Proc. Natl. Acad. Sci. U S A **94**:7965-7970.

30.   **Hofstetrova, K., M. Uzlikova, P. Tumova, K. Troell, S. G. Svard, and E. Nohynkova**. 2010. Giardia intestinalis: aphidicolin influence on the trophozoite cell cycle. Exp. Parasitol. **124**:159-166.

31.   **Chiroli, E., G. Rancati, I. Catusi, G. Lucchini, and S. Piatti**. 2009. Cdc14 inhibition by the spindle assembly checkpoint prevents unscheduled centrosome separation in budding yeast. Mol. Biol. Cell. **20**:2626-2637.

32.   **Joubes, J., and C. Chevalier**. 2000. Endoreduplication in higher plants. Plant. Mol. Biol. **43**:735-745.

33.   **Kabnick, K. S., Peattie, D. A.** 1990. In situ analysis reveal that the two nuclei of Giardia lamblia are equivalent. J. Cell Sci. **Pt 3**:353-360.

34.   **Keister, D. B.** 1983. Axenic culture of Giardia lamblia in TYI-S-33 medium supplemented with bile. Trans. R. Soc. Trop. Med. Hyg. **77**:487-488.

35.   **Kim, Y., and E. T. Kipreos**. 2007. Cdt1 degradation to prevent DNA re-replication: conserved and non-conserved pathways. Cell Div. **2**:18.

36.   **Kolisko, M., I. Cepicka, V. Hampl, J. Leigh, A. J. Roger, J. Kulda, A. G. Simpson, and J. Flegr**. 2008. Molecular phylogeny of diplomonads and enteromonads based on SSU rRNA, alpha-tubulin and HSP90 genes: implications for the evolutionary history of the double karyomastigont of diplomonads. BMC Evol. Biol. **8**:205.

37.   **Le Blancq, S. M., and R. D. Adam**. 1998. Structural basis of karyotype heterogeneity in Giardia lamblia. Mol. Biochem. Parasitol. **97**:199-208.

38.   **Li, M., and P. Zhang**. 2009. The function of APC/CCdh1 in cell cycle and beyond. Cell Div. **4**:2.

39.   **Liu, Y., T. A. Richards, and S. J. Aves**. 2009. Ancient diversification of eukaryotic MCM DNA replication proteins. BMC Evol. Biol. **9**:60.

40.   **Lohia, A., C. Mukherjee, S. Majumder, and P. G. Dastidar**. 2007. Genome re-duplication and irregular segregation occur during the cell cycle of Entamoeba histolytica. Biosci. Rep. **27**:373-384.

41.   **Luo, X., Z. Tang, J. Rizo, and H. Yu**. 2002. The Mad2 spindle checkpoint protein undergoes similar major conformational changes upon binding to either Mad1 or Cdc20. Mol. Cell. **9**:59-71.

42.   **Meng, L., R. Mohan, B. H. Kwok, M. Elofsson, N. Sin, and C. M. Crews**. 1999. Epoxomicin, a potent and selective proteasome inhibitor, exhibits in vivo antiinflammatory activity. Proc. Natl. Acad. Sci. U S A **96**:10403-10408.

43.   **Meng, T. C., S. B. Aley, S. G. Svard, M. W. Smith, B. Huang, J. Kim, and F. D. Gillin**. 1996. Immunolocalization and sequence of caltractin/centrin from the early branching eukaryote Giardia lamblia. Mol. Biochem. Parasitol. **79**:103-108.

44.   **Mimura, S., T. Seki, S. Tanaka, and J. F. Diffley**. 2004. Phosphorylation-dependent binding of mitotic cyclins to Cdc6 contributes to DNA replication control. Nature **431**:1118-1123.

45.   **Morrison, H. G., A. G. McArthur, F. D. Gillin, S. B. Aley, R. D. Adam, G. J. Olsen, A. A. Best, W. Z. Cande, F. Chen, M. J. Cipriano, B. J. Davids, S. C. Dawson, H. G. Elmendorf, A. B. Hehl, M. E. Holder, S. M. Huse, U. U. Kim, E. Lasek-Nesselquist, G. Manning, A. Nigam, J. E. Nixon, D. Palm, N. E. Passamaneck, A. Prabhu, C. I. Reich, D. S. Reiner, J. Samuelson, S. G. Svard, and M. L. Sogin**. 2007. Genomic minimalism in the early diverging intestinal parasite Giardia lamblia. Science **317**:1921-1926.

46.   **Morrissette, N. S., Sibley, L. D.** 2002. Disruption of microtubules uncouples budding and nuclear division in Toxoplasma gondii. J. Cell Sci. **115**:1017-1025.

47.   **Musacchio, A., and E. D. Salmon**. 2007. The spindle-assembly checkpoint in space and time. Nat. Rev. Mol. Cell Biol. **8**:379-393.

48.   **Niault, T., K. Hached, R. Sotillo, P. K. Sorger, B. Maro, R. Benezra, and K. Wassmann**. 2007. Changing Mad2 levels affects chromosome segregation and spindle assembly checkpoint control in female mouse meiosis I. PLoS One **2**:e1165.

49.   **Nohynkova, E., P. Draber, J. Reischig, and J. Kulda**. 2000. Localization of gamma-tubulin in interphase and mitotic cells of a unicellular eukaryote, Giardia intestinalis. Eur. J. Cell Biol. **79**:438-445.

50.   **Nohynkova, E., P. Tumova, and J. Kulda**. 2006. Cell division of Giardia intestinalis: flagellar developmental cycle involves transformation and exchange of flagella between mastigonts of a diplomonad cell. Eukaryot. Cell **5**:753-761.

51.   **Patterson, S., C. Robert, C. Whittle, R. Chakrabarti, C. Doerig, and D. Chakrabarti**. 2006. Pre-replication complex organization in the atypical DNA replication cycle of Plasmodium falciparum: characterization of the mini-chromosome maintenance (MCM) complex formation. Mol. Biochem. Parasitol. **145**:50-59.

52.   **Paugam, A., Bulteau, A. L., Dupouy-Camet, J., Creuzet, C., Friguet, B.** 2003. Characterization and role of protozoan parasite proteasomes. Trends Parasitol. **12**:55-59.

53.   **Pereira, G., C. Manson, J. Grindlay, and E. Schiebel**. 2002. Regulation of the Bfa1p-Bub2p complex at spindle pole bodies by the cell cycle phosphatase Cdc14p. J. Cell Biol. **157**:367-379.

54.   **Ploubidou, A., D. R. Robinson, R. C. Docherty, E. O. Ogbadoyi, and K. Gull**. 1999. Evidence for novel cell cycle checkpoints in trypanosomes: kinetoplast segregation and cytokinesis in the absence of mitosis. J. Cell Sci. **112 (Pt 24)**:4641-4650.

55.   **Sagolla, M. S., S. C. Dawson, J. J. Mancuso, and W. Z. Cande**. 2006. Three-dimensional analysis of mitosis and cytokinesis in the binucleate parasite Giardia intestinalis. J. Cell Sci. **119**:4889-4900.

56.   **Sinou, V., Y. Boulard, P. Grellier, and J. Schrevel**. 1998. Host cell and malarial targets for docetaxel (Taxotere) during the erythrocytic development of Plasmodium falciparum. J. Eukaryot. Microbiol .**45**:171-183.

57.   **Sironi, L., M. Mapelli, S. Knapp, A. De Antoni, K. T. Jeang, and A. Musacchio**. 2002. Crystal structure of the tetrameric Mad1-Mad2 core complex: implications of a 'safety belt' binding mechanism for the spindle checkpoint. EMBO J. **21**:2496-2506.

58.   **Sironi, L., M. Melixetian, M. Faretta, E. Prosperini, K. Helin, and A. Musacchio**. 2001. Mad2 binding to Mad1 and Cdc20, rather than oligomerization, is required for the spindle checkpoint. EMBO J. **20**:6371-6382.

59.   **smundson, E. C., D. Ray, F. E. Moore, Q. Gao, G. H. Thomsen, and H. Kiyokawa**. 2008. The HECT E3 ligase Smurf2 is required for Mad2-dependent spindle assembly checkpoint. J. Cell Biol. **183**:267-277.

60.   **Svard, S. G., P. Hagblom, and J. E. Palm**. 2003. Giardia lamblia -- a model organism for eukaryotic cell differentiation. FEMS Microbiol. Lett. **218**:3-7.

61.   **Taylor, S. S., M. I. Scott, and A. J. Holland**. 2004. The spindle checkpoint: a quality control mechanism which ensures accurate chromosome segregation. Chromosome Res. **12**:599-616.

62.   **Tumova, P., K. Hofstetrova, E. Nohynkova, O. Hovorka, and J. Kral**. 2007. Cytogenetic evidence for diversity of two nuclei within a single diplomonad cell of Giardia. Chromosoma **116**:65-78.

63.   **Tumova, P., J. Kulda, and E. Nohynkova**. 2007. Cell division of Giardia intestinalis: assembly and disassembly of the adhesive disc, and the cytokinesis. Cell Motil. Cytoskeleton **64**:288-298.

64.   **Yu, L. Z., C. W. Birky, Jr., and R. D. Adam**. 2002. The two nuclei of Giardia each have complete copies of the genome and are partitioned equationally at cytokinesis. Eukaryot. Cell **1**:191-199.

Figure legend

Fig. 1 Albendazole-treated *Giardia* cells re-replicate DNA without preceding proper chromosome segregation

(A) A control trophozoite (first on left) demonstrates the presence of two neighboring nuclei within a cell and arrangement of a set of eight flagella. The others represent the result of aberrant karyokinesis after 7 hours of albendazole treatment – cells with zero, one, or two nuclei. Note that the organization of flagella is not affected. Scale bar represents 10 μm.

(B) Control mitotic trophozoite with two mitotic spindles (left) and corresponding trophozoite treated for 7 hours with albendazole, which clearly lacks a mitotic spindle. Cells are stained with DAPI and tubulin antibody. Scale bar represents 10 μm.

(C) The control trophozoite population separates into two sub-populations by DNA content, represented here by a dominant G2 and minor G1 peak (first plot). Rapid redistribution of the G1 and G2 peaks was observed after 7 hours of albendazole treatment in addition to the formation of a third peak corresponding to double DNA

content (second plot). Three distinct sub-populations based on DNA content are present after 24 hours of albendazole treatment.

(D) Mitotic spreads showing multiplication of chromosomes after 24 hours treatment with albendazole. The picture on the left shows the two nuclei of a single control G2 trophozoite with 10 and 11 chromosomes.

(E) In control *Giardia* trophozoites DNA synthesis usually occurs in both nuclei simultaneously (arrow), but one of the nuclei may precede the other (arrowhead). Albendazole-treated cells lack properly segregated chromosomes, were positive for DNA synthesis and the nuclei were enlarged. DNA synthesis occurred in both trophozoites with two nuclei (arrow) and one nucleus (arrowhead). Bar represents 10 µm.

Fig. 2 The effect of epoxomicin and albendazole on *Giardia*

(A) The exponentially growing culture of *Giardia* exposed to epoxomicin for 12 hours exhibited aberrant karyokinesis resulting in cells with multiple nuclei or fragments of nuclei (arrows). Control trophozoite contains two symmetrically positioned nuclei (upper left picture). Flagella are stained green to visualize the entire cell. (B) Western blott analysis with anti-ubiquitin antibody visualized accumulation of ubiquitinylated proteins in epoxomicin treated cells. Three bands in each group correspond to specific times of cultivation/incubation (6, 8 and 12 hours) with drug. Note that albendazole treated cell lysates are comparable to control cell lysates.

Fig. 3 Cyclin-B and ubiquitinylated proteins in albendazole or epoxomicin treated *Giardia* cells

(A) The comparison of control (upper pictures) and albendazole treated *Giardia*
trophozoites (bottom) showed comparable signals of cyclin B-like proteins. Cyclin-B
co-localized in *Giardia* with basal bodies throughout the cell cycle. The signal was
enhanced in mitotic cells where basal bodies form spindle poles and move to
opposite sites according to cell division (middle upper picture). (B) Active form of
aurora kinase is localized identically in both control and albendazole treated mitotic
trophozoites.

(C) Comparative cyclin-B immunoblot analysis of lysates of *Giardia* cells exposed to
albendazole (alb) or epoxomicin (epo) for 6, 12 or 24 hours (three bands from left to
right). Three minor bands may correspond to additional cyclin-like proteins encoded
by *Giardia* genome. Note, the similar trend of the dominant band in lysates from
both control and albendazole treated cells. Interestingly, the decrease of cyclin-B
after 24 hours was pronounced in epoxomicin treated cells where the accumulation
due to the arrest of cyclin degradation in mitotic cells was proposed. Surprisingly, the
trends of additional bands were similar for control and albendazole treated cells
(accumulation), but differed when compared to epoxomicin cells (decrease). This
reflects that the senescing population (G2 trophozoites mostly) may resemble
albendazole cells, which are virtually G2 cells, since they did not perform mitosis but
did replicate their genome.

(D) The expression of mad-2, cdc-14 and cyclin-B decreased in albendazole treated
cells compared to control cells suggesting that these genes were not utilized during
treatment. Plot performs the ratio of transcripts normalized to glutamate
dehydrogenase (GDH) as endogenous control. The maximum decrease (5×) was
achieved by mad-2 and cyclin-B (up to 4×). (D) Semiquantitative PCR visualized the
differences in expression as validated by real time PCR (above). 0 stands for an

untreated sample while <u>A</u> represents albendazole treated cells. Glycyl-tRNA synthetase was used as endogenous control.

Fig. 4 Mad-2 overexpression did not influence *Giardia* trophozoites

(A) Mad-2 was localized along caudal flagella (along the anterior-posterior axis) in the majority of transfected *Giardia* trophozoites. Mitotic cells produced an identical pattern of Mad-2 expression as interphase cells (see the cutouts), or missed any detectable expression. (B) The expression of Mad-2 fused to the HA tag was confirmed by immunoblott where monomeric and dimeric Mad-2 were observed. (C) Transfectants responded to albendazole treatment in the same way as control cells. Despite the defective distribution of nuclei, proper flagella and basal body organization were maintained. (D) Cyclin-B localization in interphase and during mitosis was not affected by Mad-2 overexpression.
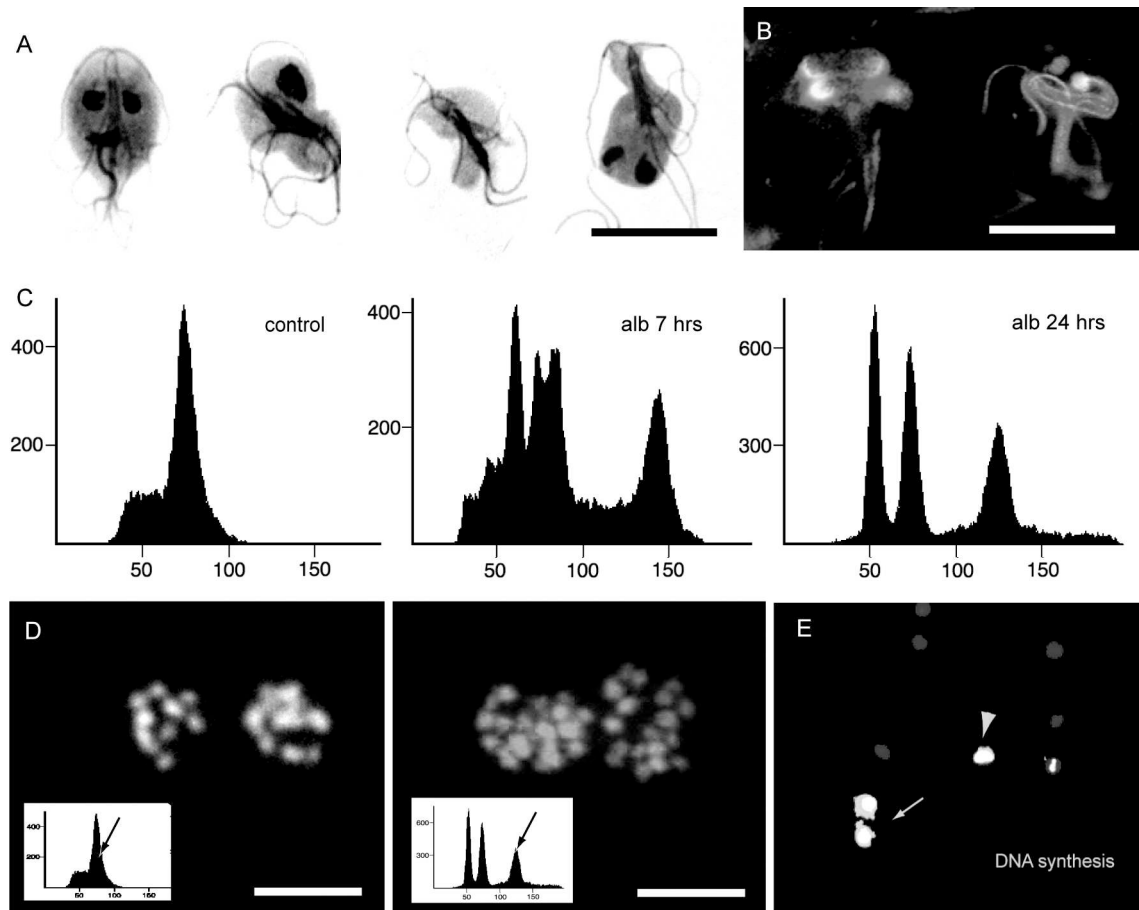
Fig. 1 Albendazole-treated Giardia cells re-replicate DNA without preceding proper chromosome segregation

(A) A control trophozoite (first on left) demonstrates the presence of two neighboring nuclei within a cell and a set of eight flagella. The others represent the result of aberrant karyokinesis after 7 hours of albendazole treatment – cells with one, zero or two nuclei. Note that the organization of flagella is not affected. Scale bar represents 10 μm.

(B) Control mitotic trophozoite with two mitotic spindles (left) and corresponding trophozoite treated for 7 hours with albendazole, which clearly lacks a mitotic spindle. Cells are stained with DAPI and tubulin antibody. Scale bar represents 10 μm.

(C) The control trophozoite population separates into two sub-populations by DNA content, represented here by a dominant G2 and minor G1 peak (first plot). Rapid redistribution of the G1 and G2 peaks was observed after 7 hours of albendazole treatment in addition to the formation of a third peak corresponding to double DNA content (second plot). Three distinct sub-populations based on DNA content are present after 24 hours of albendazole treatment.

(D) Mitotic spreads showing multiplication of chromosomes after 24 hours treatment with albendazole. The picture on the left shows the two nuclei of a single control G2 trophozoite with 10 and 11 chromosomes. Bar represents 5 μm.

(E) Albendazole-treated cells were positive for DNA synthesis and the nuclei were enlarged. DNA synthesis occurred in both trophozoites with two nuclei (arrow) and one nucleus (arrowhead).
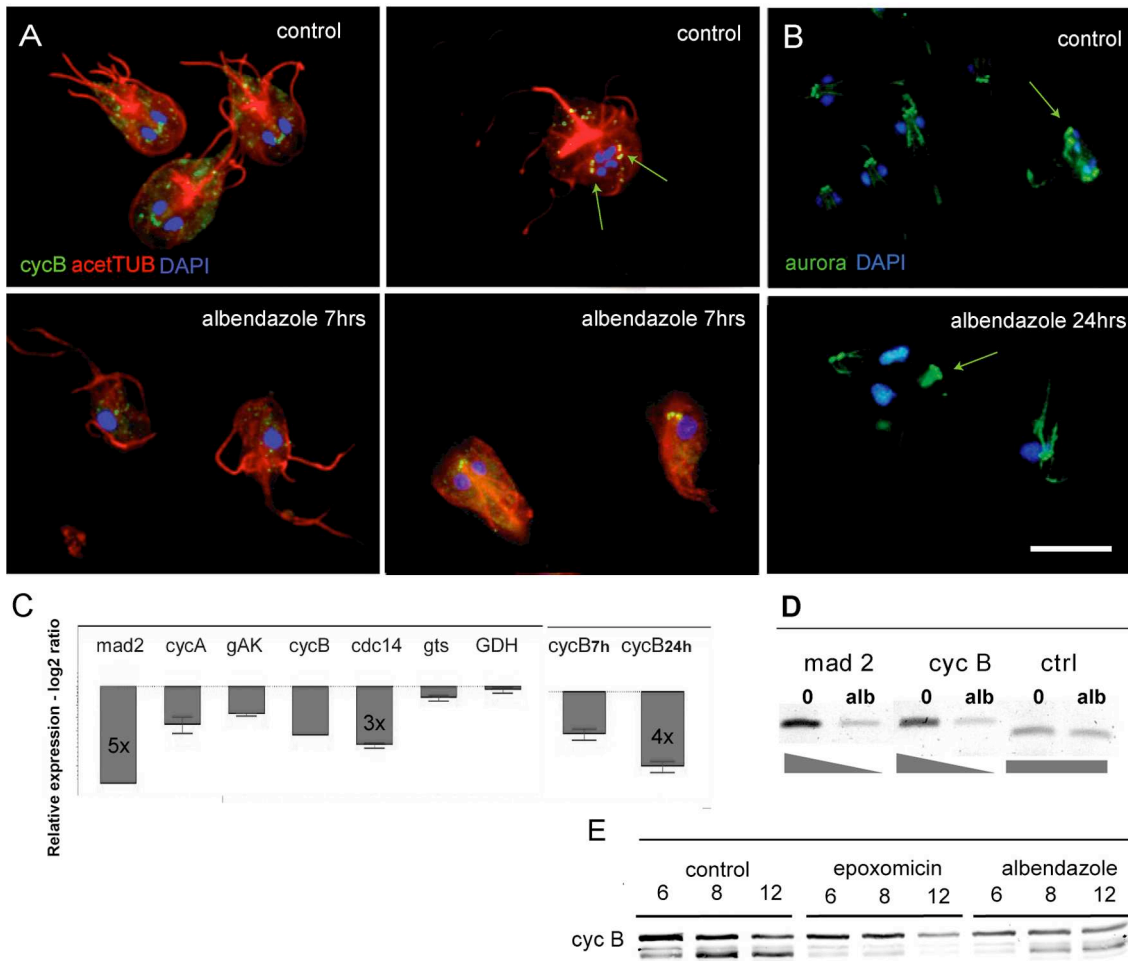
Fig. 2 Cyclin-B in albendazole or epoxomicin treated Giardia cells

(A) The comparison of control and albendazole treated Giardia trophozoites showed comparable signals of cyclin B-like proteins. Cyclin-B co-localized in Giardia with basal bodies throughout the cell cycle. The signal was enhanced in mitotic cells (green arrows) where basal bodies form spindle poles and move to opposite sites according to cell division. (B) Active form of aurora kinase is localized identically in both control and albendazole treated mitotic trophozoites. (C) qRT-PCR analysis of genes of interest. The expression of mad-2, cdc-14 and cyclin-B decreased in albendazole treated cells compared to control cells suggesting that these genes were not utilized during treatment. The results were normalized to glutamate dehydrogenase mRNA level (endogenous control) and shown relative (ratio) to untreated proliferating cells at time zero. The maximum decrease (5×) was achieved by mad-2 and cyclin-B (up to 4×). (D) Semiquantitative PCR visualized the differences in expression as validated by real time PCR (above). 0 stands for an untreated sample while alb represents albendazole treated cells. Glycyl-tRNA synthetase was used as endogenous control. (E) Comparative cyclin-B immunoblot analysis of lysates of Giardia cells exposed to albendazole or epoxomicin for 6, 8 or 12 hours. Three minor bands may correspond to additional cyclin-like proteins encoded by Giardia genome. Note, the similar trend of the dominant band in lysates from both control and albendazole treated cells. Interestingly, the decrease of cyclin-B after 12 hours was pronounced in epoxomicin treated cells where the accumulation due to the arrest of cyclin degradation in mitotic cells was proposed. Surprisingly, the trends of additional bands were similar for control and albendazole treated cells (accumulation), but differed when compared to epoxomicin cells (decrease). This reflects possibly that the senescing population (G2 trophozoites mostly) may resemble albendazole cells, which are virtually G2 cells, since they did not perform mitosis but did replicate their genome.
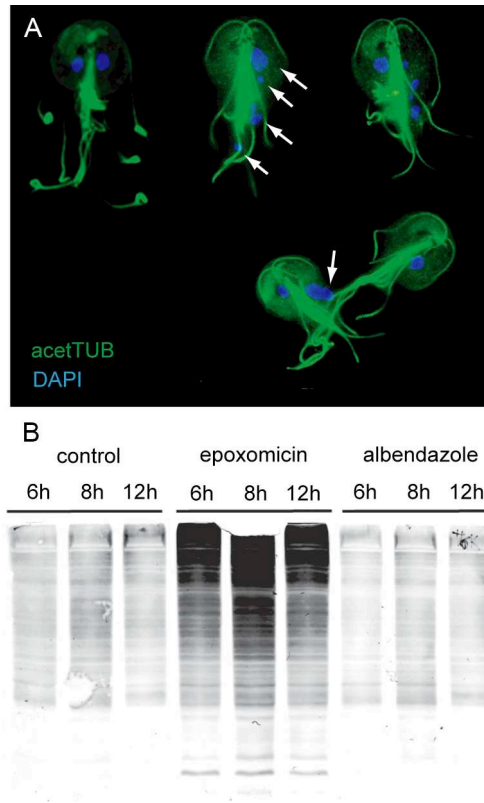
Fig. 3 The effect of epoxomicin and albendazole on Giardia

(A) The exponentially growing culture of Giardia exposed to epoxomicin for 12 hours exhibited aberrant karyokinesis resulting in cells with multiple nuclei or fragments of nuclei (arrows). Control trophozoite contains two symmetrically positioned nuclei (upper left picture). Flagella are stained green to visualize the entire cell. (B) Western blott analysis with anti-ubiquitin antibody visualized accumulation of ubiquitinylated proteins in epoxomicin treated cells. Three bands in each group correspond to specific times of cultivation/incubation (6, 8 and 12 hours) with drug. Note that albendazole treated cells lysates are comparable to control cells lysates.
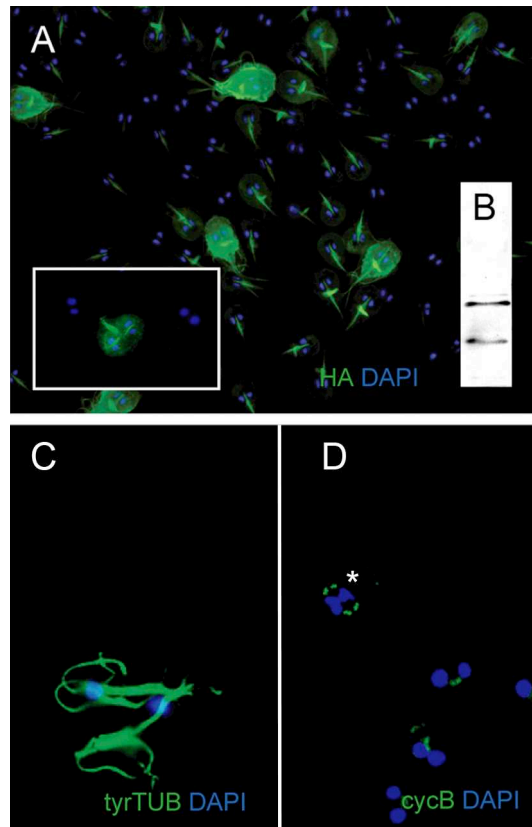
Fig. 4 Mad-2 overexpression did not influence Giardia trophozoites

(A) Mad-2 was localized along caudal flagella (along the anterior-posterior axis) in the majority of transfected Giardia trophozoites. Mitotic cells produced an identical pattern of Mad-2 expression as interphase cells (see the cutout), or missed any detectable expression. (B) The expression of Mad-2 fused to the HA tag was confirmed by immunoblott where monomeric and possibly dimeric Mad-2 were observed. (C) Transfectants responded to albendazole treatment in the same way as control cells. A typical doublet of cells interconnected in caudal flagella is displayed. Note the presence of only two nuclei. Despite the defective distribution of nuclei, proper flagella and basal body organization were maintained. TyrTUB stands for tyrosylated tubulin. (D) Cyclin-B localization in interphase and during mitosis was not affected by Mad-2 overexpression. An asterisk denotes a signal from a mitotic cell.